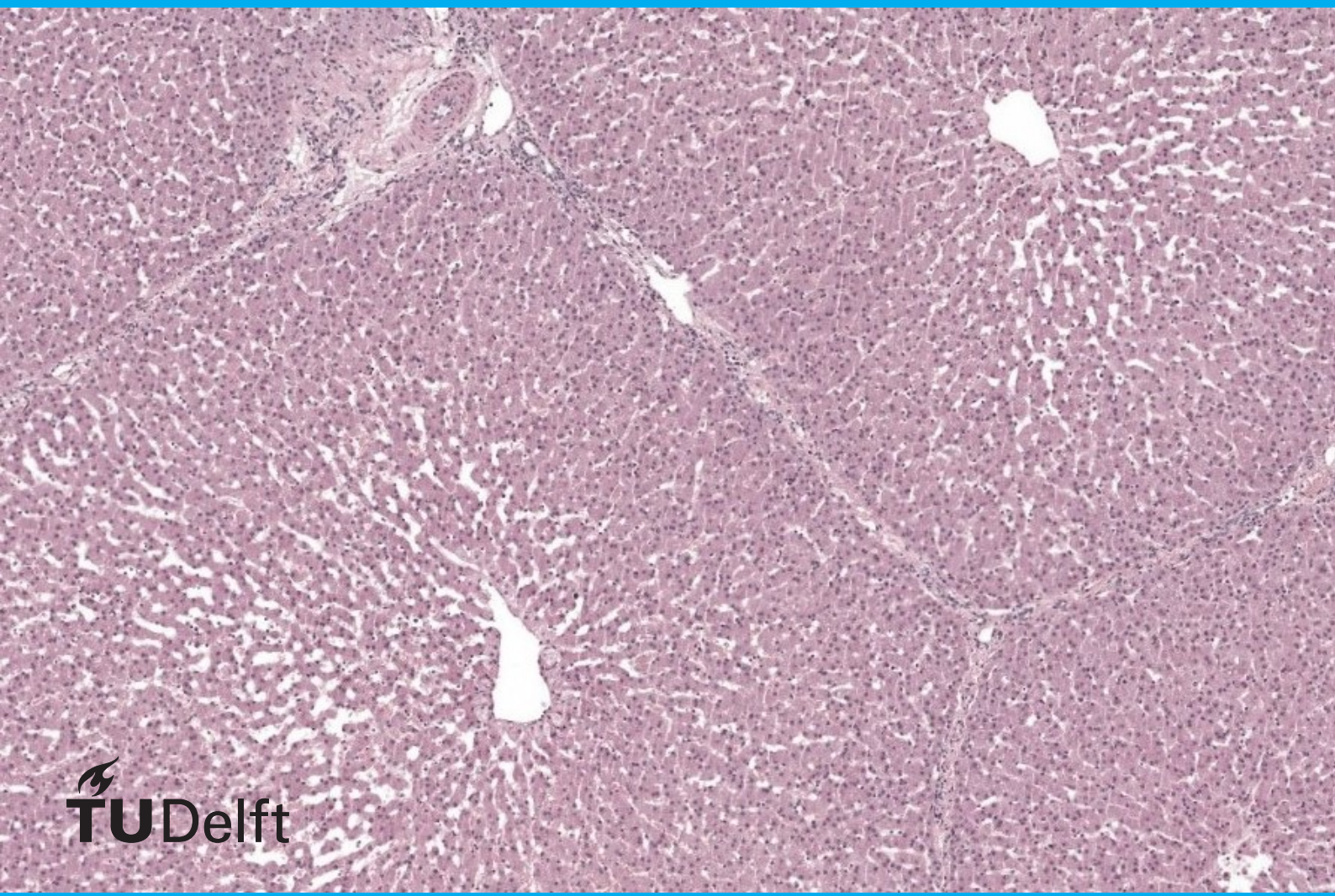
MSc thesis in Biomedical Engineering

The Effect of Liver Movement During Porcine Normothermic Machine Perfusion on Function and Tissue Integrity

Sophie van de Gevel



TU Delft

MSc thesis in Biomedical Engineering

The Effect of Liver Movement During Porcine Normothermic Machine Perfusion on Function and Tissue Integrity

by

S.E.T.M. van de Gevel (4550145)

in partial fulfillment of the requirements of the degree of Master of Science
at the Delft University of Technology,
to be defended publicly on Friday 22 September 2023 at 9:00 AM.



Student:	Sophie Emilie Thérèse Maria van de Gevel
Student number:	4550145
Project duration:	January 30, 2023 – September 22, 2023
Place:	Faculty of Mechanical Engineering, Delft

Thesis Committee:			
	Prof. dr. ir. A.A. Zadpoor	TU Delft	Chair
	Assist. Prof. dr. ir. E.L. Fratila-Apachitei	TU Delft	Supervisor
	L.J. Stevens	TNO	Daily Supervisor
	Dr. E. van de Steeg	TNO	Committee member
	Assist. Prof. dr. R.P. Tas	TU Delft	Committee member
	Assoc. Prof. dr. M.M.A. Verstegen	Erasmus MC	Committee member

An electronic version of this thesis is available at http://repository.tudelft.nl/.

TU Delft

Preface

This thesis stands as the culmination of my MSc in Biomedical Engineering, specializing in the Medical Devices track with a focus on Biomaterials and Implants. It marks the conclusion of a seven-year academic journey at Delft University of Technology. Building on my background in Nanobiology, I have been fascinated by the intersection of cell biology and biomedical technological advancements, encompassing domains such as the tissue-implant interface, organ-on-chip technology, and regenerative medicine. Consequently, my immersion in the field of normothermic machine perfusion (NMP) was met with profound gratitude and enthusiasm. This novel area of research offers abundant opportunities for optimization and research.

Embarking on the journey of conducting this thesis project has been an incredible adventure, one filled with learning, challenges, and growth. As I present the culmination of my efforts, I find myself indebted to a multitude of individuals who have stood by me, directly or indirectly, during this remarkable academic endeavor.

Foremost, my appreciation goes to my circle of friends and family who have been my pillars of support by patiently listening to my constant stream of thought. Their enthusiasm for my topic and our discussions around the dinner table have been a constant source of inspiration and kept my motivation alive.

To my fellow students, who have traversed the same path of thesis projects and writing, your camaraderie and shared experiences have been invaluable. The insights gained from our conversations, whether celebrating successes or navigating challenges, have provided me with a broader perspective on this academic voyage.

A special note of gratitude goes out to the incredible team *Humane Cel Biologie* at TNO. The biweekly journal clubs and scientific data discussions have been eye-opening, exposing me to a plethora of captivating research areas. Your engagement, thought-provoking questions, and collaborative spirit have expanded my horizons, shaping the way I approach academic discourse. Furthermore, I wish to acknowledge the invaluable assistance of those who contributed during the NMP experiments, underscoring the collaborative nature of research.

My heartfelt thanks extend to my daily supervisor, Lianne Stevens from TNO/LUMC, for opening the doors to this engaging project in the captivating realm of NMP. Lianne's infectious passion for the subject ignited my own excitement and determination. Her patient guidance through the NMP experiments and the time she devoted to our discussions have been instrumental in my journey. Witnessing her contributions to the field of NMP has been truly inspiring.

A debt of gratitude is owed to my TU Delft supervisor, Lidy Fratila-Apachitei, for her astute insights and constructive critiques. Her guidance has refined my work, pushing me to deliver my best.

In closing, this thesis is a tribute to the collective efforts of those who have walked this path with me. It is a testament to the connections forged, the lessons learned, and the growth achieved.

With sincere gratitude and appreciation,

Sophie van de Gevel
Delft, September 2023

Abstract

Background. Liver transplantation remains the only definite cure for end-stage liver disease, yet the demand for donor livers far surpasses their supply, resulting in substantial wait-list mortality rates. This has led to the exploration of extended criteria donor (ECD) livers, which often exhibit compromised function and susceptibility to post-transplantation complications. *Ex vivo* normothermic machine perfusion (NMP), emerges as a promising approach to assess liver quality, extend preservation duration, and therefore reduce the supply-and-demand imbalance and post-transplantation complications. Moreover, long-term (> 24 hours) NMP could enable treatment, repair, and regeneration of liver grafts and serve as a valuable platform for drug testing and disease modeling. To achieve long-term NMP, it is crucial to recreate the *in vivo* physical conditions during *ex vivo* perfusion. The aim of this thesis was to incorporate liver movement during porcine liver NMP and assess the effect of liver movement on liver function and tissue integrity.

Methods. Therefore, a new liver reservoir including liver movement was developed and subsequently used to perform porcine liver NMP experiments. Slaughterhouse procured porcine livers (n = 4), were perfused via the hepatic artery (HA) and portal vein (PV) under the established movement condition for 360 minutes. After 120 and 300 minutes of perfusion, indocyanine green (ICG), a fluorescent dye, was dosed, and samples were taken from the arterial circulation and bile to study the clearance capacity of the liver. Hourly samples of the perfusate and bile were taken for blood gas analysis and measurement of injury markers, to assess the general viability and functionality of the liver. And tissue samples were taken at the end of perfusion to study tissue integrity.

Results. Liver movement was established by alternatively inflating and deflating two balloons underneath the liver, with both inflation and deflation lasting 8 seconds. The 6-hour porcine liver NMP experiments under the established movement condition showed liver viability and functionality in terms of glucose metabolism, lactate and bilirubin clearance, stable levels of injury markers, and continuous bile production. A larger perfusate volume was necessary (2.8 ± 0.4 versus 2 L) and the portal vein (PV) flow was 60 % lower during NMP under the movement condition compared to NMP under the static condition. The ICG clearance capacity of the liver showed to be improved, although not significantly, under the movement condition, with a mean perfusate disappearance rate (PDR_{ICG}) of 30.6 ± 11.7 % per minute, compared to the static condition (11.0 ± 3.3 (Zeist) and 21.8 ± 13.8 (Leiden) % per minute), after 300 minutes of NMP. The macroscopic appearance and histological analysis of the liver revealed some non-perfused areas on the bottom of the liver, but overall, the liver tissue was intact, and no major hepatocellular damage occurred after 5−7 hours of NMP under the movement condition.

Conclusion. In this thesis, a novel liver reservoir including liver movement was established to study the sole effect of movement during NMP. During the 6-hour porcine liver NMP experiments under the established movement condition, the livers showed proper clearance capacity and tissue integrity. Although inclusion of movement did not result in a significant improvement with respect to liver function, it is hypothesized that movement will prolong the viability and functionality of livers when performing NMP for more than 24 hours. Further work is now required to improve the setup, especially making the movement simulation more automatic, facilitating the execution of prolonged NMP experiments, and enabling the assessment of the effect of liver movement over extended durations of NMP.

Keywords: *Porcine Liver Normothermic Machine Perfusion, Liver Movement Simulation, Liver Reservoir Design, Clearance Capacity, Tissue Integrity.*

Contents

Preface ii

Abstract iii

Abbreviations vi

List of Figures vii

List of Tables xi

1 Introduction 1

2 Materials & Methods 5
- 2.1 Movement Simulation and Liver Reservoir Development . . . 5
  - 2.1.1 Liver Reservoir and General Design Considerations . . . 5
  - 2.1.2 List of Materials . . . 6
  - 2.1.3 Electronic Circuit and Movement Simulation . . . 6
  - 2.1.4 Liver Reservoir Components and Assembly . . . 7
  - 2.1.5 Redesigned Liver Reservoir and Full setup . . . 9
  - 2.1.6 Validation experiments . . . 10
- 2.2 Porcine Liver NMP Experiments . . . 10
  - 2.2.1 Chemicals . . . 10
  - 2.2.2 Porcine Liver Procurement . . . 11
  - 2.2.3 Normothermic Machine Perfusion . . . 12
  - 2.2.4 Perfusion Measurements and Assays . . . 13
  - 2.2.5 Control Group and Static Reservoir . . . 15
  - 2.2.6 Data Analysis . . . 15

3 Results 16
- 3.1 Movement Simulation and Liver Reservoir Development . . . 16
  - 3.1.1 Movement simulation . . . 16
  - 3.1.2 Redesigned Liver Reservoir During Perfusion . . . 18
- 3.2 Porcine Liver NMP Experiments . . . 19
  - 3.2.1 Liver Procurement and Perfusion Performance . . . 19
  - 3.2.2 General Liver Viability and Functionality . . . 20
  - 3.2.3 Liver Injury . . . 22
  - 3.2.4 Clearance Capacity . . . 23
  - 3.2.5 Tissue Integrity . . . 24

4 Discussion 28
- 4.1 Establishment of a Liver Reservoir Including Liver Movement . . . 28
- 4.2 Porcine Liver NMP Experiments . . . 29
  - 4.2.1 General Performance of Perfusion . . . 30
  - 4.2.2 General Liver Viability and Functionality . . . 31
  - 4.2.3 Liver Injury . . . 31
  - 4.2.4 The Effect of Liver Movement on Clearance Capacity . . . 32
  - 4.2.5 The Effect of Liver Movement on Tissue Integrity . . . 33
- 4.3 Current Status and Perspective . . . 33

5 Conclusion 36

Appendix 43
A Perfusion machine setups used in previous porcine NMP experiments . . . 43
B Arduino code . . . 46
C Validation Experiments . . . 49
C.1 Setup HMP Validation experiments . . . 49
C.2 Additional Results Validation Experiments . . . 49
D Reference Values Blood Gas Analysis . . . 50
E Additional Results NMP Experiments . . . 51
E.1 Setup Alterations . . . 51
E.2 Additional Graphs of Perfusate Temperature and Hemodynamics . . . 52
E.3 Additional Graphs of Blood Gas Analysis . . . 53
E.4 Additional Graphs of Bile production . . . 56
E.5 Additional Pictures of Appearance . . . 57
E.6 Additional Results Histological Analysis . . . 62
F Additional Results Statistical Analysis . . . 63

Abbreviations

ALT	Alanine aminotransferease
AST	Aspartate aminotransferease
ATP	Adenosine triphosphate
BE	Base excess
BUN	Urea nitrogen
CIT	Cold ischemia time
Cl	Chloride
Cre	Creatinine
DBD	Donation after brain death
DCD	Donation after circulatory death
EAD	Early allograft disfunction
ECD	Extended criteria donor
Glu	Glucose
HA	Hepatic artery
Hgb	Hemoglobin
HCO_3	Bicarbonate
H & E	Hematoxylin-eosin
Hct	Hematocrit
HMP	Hypothermic machine perfusion
iCa	Ionized calcium
ICG	Indocyanine green
IRI	Ischemia-reperfusion injury
IU	International unit
IVC	Inferior vena cava
K	Potassium
MMP	Midthermic machine perfusion
MP	Machine perfusion
Na	Sodium
NMP	Normothermic machine perfusion
PCO_2	Partial pressure of carbon dioxide
PDR_{ICG}	Perfusate disappearance rate of ICG
PO_2	Partial pressure of oxygen
PNF	Primary non-function
PV	Portal vein
RBC	Red blood cell
RCF	Relative centrifugal force
RFU	Relative fluorescent unit
SCS	Static cold storage
SMP	Subnormothermic machine perfusion
sO_2	Oxygen saturation
SVC	Superior vena cava
TCO_2	Total carbon dioxide
WBC	White blood cell
WIT	Warm ischemia time

List of Figures

1.1 An overview of the different *ex vivo* liver preservation methods with their respective advantages and disadvantages [17]. Created with BioRender.com. 2
1.2 Long-term NMP can be used as a platform for multiple purposes: viability testing, treatment, repair, regeneration, drug discovery, and disease modeling. Created with BioRender.com. 2
1.3 *In vivo* the liver is influenced by physiological processes occurring in and around the liver (red) and physical conditions (blue). Created with BioRender.com. 3
1.4 **(a)** The diaphragmatic surface of a porcine liver. **(b)**. The porcine liver placed in the liver reservoir of a commercial perfusion device. **(c)** The diaphragmatic surface of the liver that was placed in the liver reservoir of a commercial perfusion machine after 24 hours. **(d)** Close-up of the liver that was placed in the liver reservoir of the commercial perfusion machine for 24 hours. The net-like structure clearly leaves an imprint on the liver. Scale bars 100 mm. 4

2.1 A schematic representation of the electronic circuit with the latex balloons. The Arduino microcontroller was connected to a laptop such that the code could be uploaded and a wall power adapter for the power supply. The sensor shield to which the electronic circuit components were attached was plugged onto the Arduino microcontroller. The different electronic components, four pumps and two 3-way valves, were connected to the depicted pins on the sensor shield. The arrows show which pumps cause inflation and which pumps cause deflation of the balloons. 7
2.2 The separate system components. **(a)** The balloons are attached in the crate, with tie wraps attaching them to one side and the silicone tubes through the crate keeping them in place on the other side. **(b)** The net is stretched over the crate above the balloons, which is slightly suspended in the box when the liver is placed on it, dividing the weight of the liver over the balloons and the net. **(c)** The net is attached to the box with velcro strips, making the tension of the net adjustable. **(d)** On top of the net the plastic mat is placed on which the liver is placed with a hole for the inferior vena cava (IVC) cannula and perfusate leaking from the liver. **(e)** The gravity bag through which the perfusate can flow from the mat and IVC cannula back to the perfusate reservoir. **(f)** The perfusate reservoir in which the perfusate flowing out of the IVC and leaking from the liver is caught and circulated through the tubing system back to the liver. Scale bars 100 mm. 8
2.3 **(a)** The experimental setup with the redesigned liver reservoir, from left to right, (1) the laptop and electronic circuit, (2) the gas mixer and (3) infusion station, (4) the redesigned liver reservoir with movement simulation, (5) the perfusate reservoir, (6) tubing, and (7) the Liver Assist device. **(b)** A schematic representation of the redesigned setup with depicted the liver reservoir with the balloons, the perfusate reservoir, tubing, and the Liver Assist system components (see subsection 2.2.3). Created with BioRender.com. 9
2.4 The setup utilized to measure the rythm and range of movement of the balloons **(a)** without the liver and **(b)** with a liver model. The ToF sensor is steadied above the balloons and model liver and measures the distance between the sensor and the balloons and model liver which are moving from and to the sensor. 10
2.5 The setup of the NMP validation experiment. **(a)** In the front, the Arduino microcontroller, connected to the laptop, wall adapter, and electronic components, is depicted. In the back, the liver reservoir, in which the balloons are moving, and on which the liver is placed, is depicted. **(b)** From left to right, the liver reservoir, tubing, and the Liver Assist device are depicted. **(c)** The perfusate reservoir with tubing to the liver and from the perfusate reservoir back to the Liver Assist system. **(d)** Tubing connected to the hepatic artery (HA) and portal vein (PV) cannulae, and underneath the liver and mat the drain from the mat and the perfusate reservoir are visible. 11

2.6 The Liver Assist device. **(a)** The trolley with the two pump units with control panels and display for controlling and continuous monitoring of the (1) hepatic artery (HA) and (2) portal vein (PV) hemodynamics and perfusate temperature, (3) the thermo unit, and (4) the table in which the disposable set, including the static liver and perfusate reservoir, tubing, and oxygenators, is held. **(b)** A schematic representation of the Liver Assist system including the static Liver Assist liver reservoir. During static perfusion experiments, the liver was placed on the net-like structure in the liver holder, above the perfusate reservoir, which is closed off by a lid. Both the HA and PV side include tubing coming from the perfusate reservoir, through which the perfusate is pumped back to the oxygenators with rotary pumps. In the oxygenator, the perfusate is warmed and supplied with oxygen and carbon dioxide is removed from the perfusate. After the perfusate passes the oxygenator, HA perfusate samples are taken, the flow, pressure, and temperature are measured, and the continuous infusion is administered, before the perfusate enters the liver. Furthermore, bile produced in the gallbladder is collected. Created with BioRender.com. 12
2.7 A schematic of the biopsies taken during the NMP experiments under the established movement condition. **(a)** A flushed liver for reference. **(b)** A schematic representation of the liver with numbered lobes and punch biospies taken during the NMP experiments. The time points at which the biopsies were taken are indicated, the biopsies were coded with the letter 'P' for punch biopsy, and numbered according to the number of biopsies taken at that time point. scale bars 100 mm. Created with BioRender.com. 14
2.8 The disposable liver reservoir of the Liver Assist device used during the control experiments **(a)** without the liver and **(b)** with the liver placed on the net. Scale bars 100 mm. 15

3.1 Graph of the movement simulated by the individual balloons. The rhythm and range of movement of balloons 1 and 2, in the absence of the liver's weight, are displayed in dark red and blue. The rhythm and range of the movement of balloons 1 and 2, with the liver's weight on top of the balloons, are displayed in light red and blue. 17
3.2 The alternating movement mode of the balloons without and with a liver model. **(a,d)** Balloon 1 at its minimum volume and balloon 2 at its maximum volume. **(b,e)** Balloons at equal volume. **(c, f)** Balloon 1 at its maximum volume and balloon 2 at its minimal volume. Scale bars 100 mm. 17
3.3 The liver during the NMP validation experiment under the established movement condition. **(a)** The liver was placed on the mat of the liver reservoir. **(b)** The liver was covered to reduce heat loss and condensation of the perfusate. **(c)** Leakage of perfusate from the liver during the experiment. **(d)** The bottom of the liver after 2 hours of NMP. Scale bars 100 mm. 18
3.4 **(a)** Hepatic artery (HA) and **(b)** portal vein (PV) flow during NMP under the established movement condition. Each of the four NMP experiments under the movement condition is depicted individually. The data from the control NMP experiments performed in Zeist (n = 3) and Leiden (n = 3) are presented as the means of the three experiments, accompanied by their respective standard deviations. 20
3.5 General liver viability and functionality markers measured during NMP under the established movement condition. **(a)** Glucose, **(b)** lactate, and **(c)** bilirubin perfusate concentrations. **(d)** pH of the perfusate. Each of the four NMP experiments under the movement condition is depicted individually. For liver 4, the bilirubin concentration in the perfusate was not measured. The data from the control NMP experiments performed in Zeist (n = 3) and Leiden (n = 3) are presented as the means of the three experiments, accompanied by their respective standard deviations. . . 21
3.6 **(a)** Cumulative bile production and **(b)** bilirubin concentration in the bile corrected for mL bile produced per hour under the established movement condition. Each of the four NMP experiments under the movement condition is depicted individually. The data from the control NMP experiments performed in Zeist (n = 3) and Leiden (n = 3) are presented as the means of the three experiments, accompanied by their respective standard deviations. Bilirubin in the bile was only measured for Experiments 1 and 3, and control NMP experiments performed in Zeist. 22
3.7 Liver injury markers measured during NMP under the established movement condition. **(a)** Alanine transaminase (ALT) and **(b)** aspartate transaminase (AST) perfusate concentrations. Each of the four NMP experiments under the movement condition is depicted individually. The data from the control NMP experiments performed in Zeist (n = 3) and Leiden (n = 3) are presented as the means of the three experiments, accompanied by their respective standard deviations. . . 23

3.8 ICG measured in the perfusate and bile for 60 minutes after administration of ICG during NMP under the established movement condition. ICG was dosed at 120 minutes (Experiments 1, 2, 3, and 4) and at 300 minutes (Experiments 1 and 4) during the experiments with liver movement. For the perfusate, the ICG data is presented as % ICG and for bile the ICG data is presented in RFU. % ICG in the perfusate after dosage at **(a)** t = 120 min and **(b)** 300 min. ICG in the bile after dosage at **(c)** t = 120 min and **(d)** t = 300 min. Each of the four NMP experiments under the movement condition is depicted individually. The data from the control NMP experiments performed in Zeist (n = 3) and Leiden (n = 3) are presented as the means of the three experiments, accompanied by their respective standard deviations. In all graphs control data of ICG administration at t = 360 and t = 300 min, for Zeist and Leiden, respectively, is presented. For Zeist, ICG in the bile was only measured during 2 experiments. 24
3.9 The macroscopic appearance of the bottom of the liver after 5-6 hours of NMP. Pictures taken of the bottom of the liver after **(a)** 6 hours (Experiment 1), **(b)** and **(c)** 5 hours (Experiments 2 and 3), and **(d)** 7 hours (Experiment 4) of NMP under the established movement condition. And pictures taken of the liver after NMP on the static reservoir of the Liver Assist device after 6 hours, **(e)** the bottom of the liver and **(f)** a magnified picture of the bottom of lobe 2. Scale bars 100 mm. 26
3.10 Histological analysis of liver biopsies taken during and after NMP under the established movement condition. Microscopic images of H&E stained liver provide insights into various cellular changes within the liver structure. Examples of observed phenomena: **(a)** A central vein with surrounding cord structure (Liver 1 at t = 360 min). **(b)** Single cell necrosis associated with hemorrhages (red blood cell infiltration)(Liver 2 at t = 300 min). **(c)** Hepatocellular vacuolation (Liver 3 at t = 300 min). **(d)** Hepatocellular hypertrophy, characterized by pale, swollen, and round hepatocytes and loss of cord structure (Liver 4 at t = 360 min). **(a)** Scale bar 200 μm (200x magnification), **(b-d)** scale bars 100 μm (400x magnification). 27

C1 The setup of the HMP validation experiments. **(a)** From left to right the Liver Assist device, the liver reservoir, and the electronic system with the laptop. **(b)** Measurement of inferior vena cava (IVC) flow. During these experiments, the perfusate reservoir of the Liver Assist device was used, which is depicted in the lower right corner. 49
C2 The different net configurations used. **(a)** The configuration during the validation experiments. **(b)** The configuration after the validation experiments, during Experiment 1. **(c)** The configuration of the net during Experiments 2, 3, and 4. Scale bars 50 mm. 49
E1 Setup alterations after the first NMP experiment under the established movement condition. **(a)** The net configuration was changed and the distance between the balloons was reduced, to give the liver more support between the balloons. **(b)** The volume of the perfusate reservoir was reduced. Scale bars 100 mm. 51
E2 Perfusate temperature and hemodynamics to assess the stability of the NMP experiments under the established movement condition. **(a)** Perfusate temperature. **(b)** Hepatic artery (HA) and **(c)** portal vein (PV) pressure. Each of the four NMP experiments under the movement condition is depicted individually. **(d)** HA and **(e)** PV resistance. Additionally, the data from the control NMP experiments performed in Zeist (n = 3) and Leiden (n = 3) are presented as the means of the three experiments, accompanied by their respective standard deviations. 52
E3 Measurement of electrolytes in the perfusate to assess the overall performance of the NMP experiments under the established movement condition. **(a)** Sodium, **(b)** potassium (2 = < 2, 9 = > 9, out of measurable range), **(c)** chloride, **(d)** ionized calcium, **(e)** urea nitrogen (BUN), and **(f)** creatinine perfusate concentrations. Each of the four NMP experiments under the movement condition is depicted individually. 53
E4 Measurements of blood gasses in the perfusate to assess the overall performance of the NMP experiments under the established movement condition. **(a)** PO_2, **(b)** PCO_2 (5 = < 5, out of measurable range), **(c)** TCO_2, **(d)** HCO_3, **(e)** base excess, and **(f)** sO_2. Each of the four NMP experiments under the movement condition is depicted individually. 54
E5 Measurement of **(a)** Hematocrit and **(b)** hemoglobin concentrations in the perfusate during NMP under the established movement condition. Each of the four NMP experiments under the movement condition is depicted individually. 55

E6 **(a)** Hourly bile production and **(b)** bile bilirubin concentration during NMP under the established movement condition. With these measurements the bilirubin concentration in the bile corrected by the hourly bile production was calculated. Each of the four NMP experiments under the movement condition is depicted individually. The data from the control NMP experiments performed in Zeist (n = 3) and Leiden (n = 3) are presented as the means of the three experiments, accompanied by their respective standard deviations. Bilirubin in the bile was only measured for Experiments 1 and 3, and control NMP experiments performed in Zeist. . . . 56
E7 The damaged liver before the start of NMP for which the experiment was terminated. The liver had multiple cuts and tears in different areas **(a-e)**. Scale bars 100 mm. 57
E8 Appearance of the liver during NMP Experiment 1 under the established movement condition. The top of the liver at **(a)** t = 120 min, **(b)** 240 min, and **(c)** 360 min. The bottom of lobe 1 at **(d)** t = 120 min, **(e)** 240 min, and **(f)** 360 min. The bottom of lobe 4 at **(g)** t = 120 min, **(h)** 240 min, and **(i)** 360 min. The top of the liver at **(j)** t = 0 and **(k)** the top and **(l)** bottom of the liver at t = 360 min. Scale bars 100 mm. 58
E9 Appearance of the liver during NMP Experiment 2 under the established movement condition. The top of the liver at **(a)** t = 120 min and **(b)** 240 min. The bottom of lobe 1 at **(c)** t = 120 min and **(d)** 240 min. The bottom of lobe 4 at **(e)** t = 120 min and **(f)** 240 min. The top of the liver at **(g)** t = 0 and **(h)** the top and **(i)** bottom of the liver at t = 300 min. Scale bars 100 mm. 59
E10 Appearance of the liver during NMP Experiment 3 under the established movement condition. The top of the liver at **(a)** t = 120 min and **(b)** 240 min. The bottom of lobe 1 at **(c)** t = 120 min and **(d)** 240 min. The bottom of lobe 4 at **(e)** t = 120 min and **(f)** 240 min. The top of the liver at **(g)** t = 0 and the **(h)** top and **(i)** bottom of the liver at t = 300 min. Scale bars 100 mm. 60
E11 Injuries of Liver 4 before the start of NMP Experiment 4. Torn tissue at the bottom of **(a)** lobe 1 and **(b)** lobe 4. Scale bars 50 mm. 61
E12 Appearance of the liver during NMP Experiment 4 under the established movement condition. The top of the liver at **(a)** t = 120 min, **(b)** 240 min, **(c)** 360 min, and **(d)** 420 min. The bottom of lobe 1 at **(e)** t = 120 min, **(f)** 240 min, **(g)** 360 min, and **(h)** 420 min. The bottom of lobe 4 at **(i)** t = 120 min, **(j)** 240 min, **(k)** 360 min, and **(l)** 420 min. The top of the liver at **(m)** t = 0 min and **(n)** t = 420 min. The bottom of the liver at **(o)** t = 0 min and **(p)** t = 420 min. Scale bars 100 mm. . . . 61

List of Tables

2.1 Composition of the perfusate. 13
2.2 Composition of the additional perfusate. 13
2.3 Composition of the continuous infusion. 13
2.4 Bolus injections. 13

3.1 The warm and cold ischemic time (WIT and CIT), duration of NMP, and liver weight before and after the NMP experiments performed under the established movement condition. 19

A1 Schematic representations and pictures of NMP setups described by porcine NMP studies with their main principle. 43
D1 Reference values blood gas analysis used during the NMP experiments. Based on physiological human and porcine arterial blood gas analysis [93]. 50
E1 Sodium bicarbonate (HCO_3) administration in mL at different time points during NMP under the established movement condition to keep the pH in the physiological range (7.35−7.45). . . . 54
E2 Observations and scores of the H&E stained liver sections from the biopsies obtained during and after NMP under the established movement condition. According to the observations done, a blinded pathologist scored the liver sections from good tissue quality (dark green) to poor tissue quality (red). 62
F1 Descriptive statistics and *t* test results comparing the mean of various measurements between the NMP experiments under the established movement condition (n = 4) and the control NMP experiments performed in Zeist (n =3), without liver movement. Two-sided unpaired *t* tests were performed. No test was performed when there was only one data point for the group, there was no data for one group, or data was idential between groups. Mean (M), standard deviation (SD), t(df)= *t* statistic, *p* value, and significance at a 0.05 level are reported. 63
F2 Descriptive statistics and *t* test results comparing the mean of various measurements between the NMP experiments under the established movement condition (n = 4) and the control NMP experiments performed in Leiden (n =3), without liver movement. Two-sided unpaired *t* tests were performed. No test was performed when there was only one data point for the group, there was no data for one group, or data was idential between groups. Mean (M), standard deviation (SD), t(df)= *t* statistic, *p* value, and significance at a 0.05 level are reported. 65
F3 Descriptive statistics and *t* test results comparing the mean PDR_{ICG} and % of ICG cleared from the perfusate after 60 minutes between the t = 120 min (n = 2) and t = 300 min (n = 2) administration of ICG during NMP under the established movement condition. Two-sided unpaired *t* tests were performed. Mean (M), standard deviation (SD), t(df)= *t* statistic, *p* value, and significance at a 0.05 level are reported. 66

1

Introduction

Currently, the only definite cure for end-stage liver disease is liver transplantation [1]. However, the demand for donor livers outweighs the supply, resulting in worldwide wait-list mortality rates, of approximately 10 to 20 % [2–5]. The increasing prevalence of chronic liver disease due to factors such as unhealthy lifestyles and alcohol and drug abuse, and the decline in the quality of available donor livers due to the aging donor population has further exacerbated the supply-demand imbalance [1, 6–8]. This imbalance has led to the use of extended criteria donor (ECD) livers for liver transplantation, including those from elderly donors, donors with abnormal liver function, steatosis, a history of alcohol or drug abuse, or from donation after circulatory death (DCD) [9]. However, ECD livers often exhibit impaired metabolic function, compromised cellular regeneration, obstructed microvasculature, cellular injury, and increased susceptibility to ischemia-reperfusion injury (IRI), leading to significant postoperative complications such as biliary necrosis, ischemic cholangiopathy, early allograft dysfunction (EAD), and primary non-function (PNF) [10–13]. Static cold storage (SCS) is the prevailing method of liver preservation employed in liver transplantation; however, its effectiveness in preserving ECD livers is limited, consequently restricting the utilization of ECD livers in transplantation procedures. DCD livers, particularly due to their extended warm ischemic time (WIT), are highly sensitive to cold storage, rendering them more susceptible to cold-induced injury and prolonged hypoxia compared to donation after brain death (DBD) livers [14].

Ex vivo liver machine perfusion has emerged as a promising technique for organ preservation, offering the potential to supply oxygen-and nutrient-rich blood to the liver [15–17]. Different temperature ranges, including hypothermic (HMP) (4−12 ° C), midthermic (MMP) (13−24 ° C), subnormothermic (SMP) (25−34 ° C), and normothermic (NMP) (35−38 ° C), have been explored in ex vivo liver machine perfusion to flush out metabolites, maintain vascular circulation, and optimize oxygen and nutrient supply [18]. Several studies have investigated the various modes of ex vivo liver machine perfusion [19]. While hypothermic machine perfusion (HMP) is primarily used to mitigate the damage caused by extended WIT in DCD livers. Continuous perfusion with warm oxygenated perfusion solutions during normothermic machine perfusion (NMP) has demonstrated significant promise as a method for assessing liver quality prior to transplantation and provides the possibility to extend the duration of preservation [17, 18, 20–22]. Therefore, NMP holds the potential to reduce post-transplantation complications and increase transplantation success rates compared to SCS and HMP (Figure 1.1) [23–32].

Furthermore, long-term (≥ 24 h) NMP could improve the quality of DCD livers, by enabling treatment, repair, and regeneration, thereby potentially increasing the number of viable livers available for transplantation and reducing the gap between supply and demand (Figure 1.2) [20, 33–36]. For instance, patients undergoing hepatectomy experience nearly complete liver mass regeneration and normalized biochemistry within 10 days [37]. Thus, realizing *ex vivo* liver regeneration for damaged or split livers necessitates an extended duration of NMP [36]. Furthermore, NMP may emerge as a therapeutic option for acute liver failure patients, with the possibility of extended perfusion for detoxification in an *ex vivo* setting [35]. Prolonged NMP is also crucial for treating steatotic livers using defatting agents, which require extensive perfusion for effective defatting and metabolic conditioning [38].

Additionally, NMP of the liver has been proposed as a valuable preclinical model for predicting drug pharmacokinetics and dynamics [29, 38]. Current drug discovery models, such as hepatocyte cultures and rodent liver perfusion models, have limitations in terms of functionality and inter-species differences in pharma-

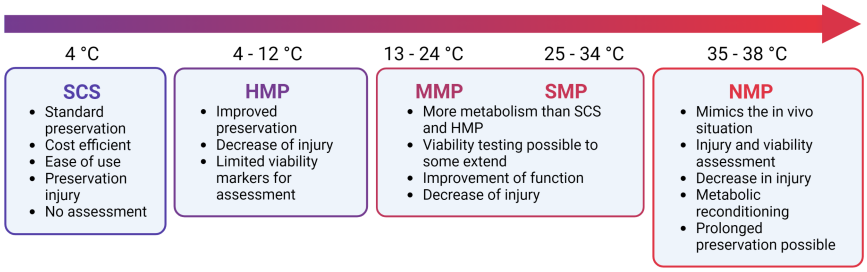


Figure 1.1: An overview of the different *ex vivo* liver preservation methods with their respective advantages and disadvantages [17]. Created with BioRender.com.

cokinetics [39–41]. The use of whole *ex vivo* livers, provides a more physiologically relevant model for studying drug metabolism, given the presence of the complex liver architecture including the biliary excretion pathway. Livers perfused at normothermic temperature are metabolically functional, allowing for the assessment of drug uptake, metabolism, and biliary clearance [42, 43]. While healthy human livers cannot be used for this end because they are meant for transplantation, human livers declined for transplantation affected by specific diseases can be utilized to study the impact of diseases on drug metabolism or the effectiveness of disease-specific drug interventions. For example, the study by Tingle *et al.* [33] examines drug pharmacokinetics and the effect of therapeutics on *ex vivo* steatotic livers during NMP. Several studies have demonstrated the potential of porcine liver NMP as a model for drug discovery and disease modeling [42, 44, 45]. The use of porcine livers compared to rodent livers additionally allows for better translation to humans due to anatomical, physiological, and biochemical similarities, facilitating direct comparison with human values [29, 36, 44, 46]. Moreover, the use of porcine slaughterhouse livers or discarded human livers can partially replace preclinical animal trials, offering faster and better translation to human pharmacokinetics and reducing ethical concerns. To study drug efficacy during NMP, it is crucial that the *ex vivo* liver is viable and functional for extended periods of time, considering that the half-life of drugs varies from hours to several days or even weeks.

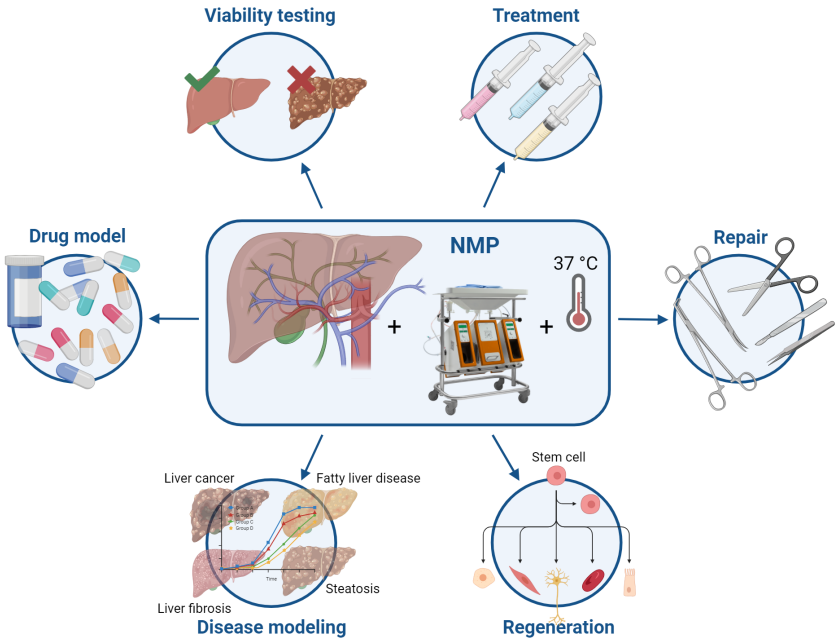


Figure 1.2: Long-term NMP can be used as a platform for multiple purposes: viability testing, treatment, repair, regeneration, drug discovery, and disease modeling. Created with BioRender.com.

To achieve long-term NMP of the liver, it is important to mimic the *in vivo* physiological processes occurring in and around the liver as closely as possible. Numerous strategies have been explored to enhance liver viability and functionality during NMP by adding substances or system components believed to make NMP more physiological [24, 25, 28–30, 32, 36, 38, 47–58]. However, some physiological conditions which could be beneficial for long-term perfusion are often overlooked. *In vivo*, the liver is located in the upper right-hand side of the abdominal cavity beneath the diaphragm and surrounded by the intestines, stomach, spleen, and right kidney [59, 60]. During respiration, the diaphragm contracts and relaxes, moving up and down respectively, producing a pressure difference in the abdominal cavity [38, 60]. The intra-abdominal pressure leads to expansion and compression of the vasculature of the liver. Furthermore, because the liver is suspended underneath the diaphragm the liver moves up and down with the rhythm of respiration, which for humans is in the range of 10−26 mm with on average 15−20 breaths per minute [61–63]. Other abdominal organs in contact with the liver also induce movement of the liver, exert pressure on the liver, and create a soft surrounding for the liver. Additionally, because the abdominal cavity is hermetically closed it also provides a sterile and humid environment with a constant temperature. These factors collectively contribute to the liver's *in vivo* physical conditions: temperature, sterility, humidity, orientation, contact with other organs, intra-abdominal pressure differences, and movement (Figure 1.3).

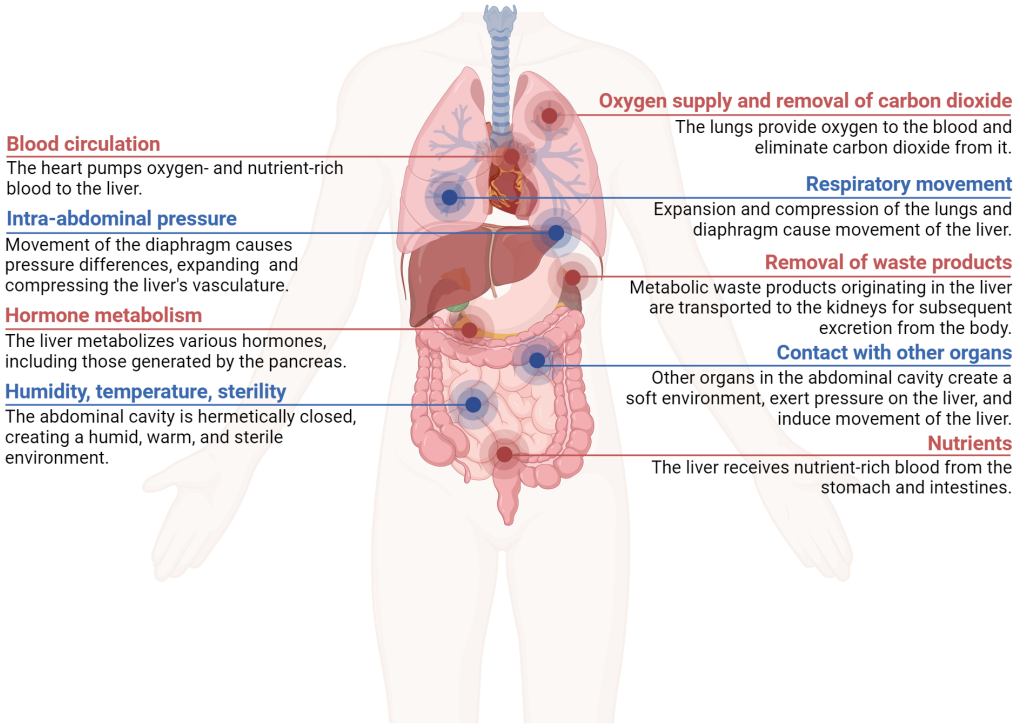
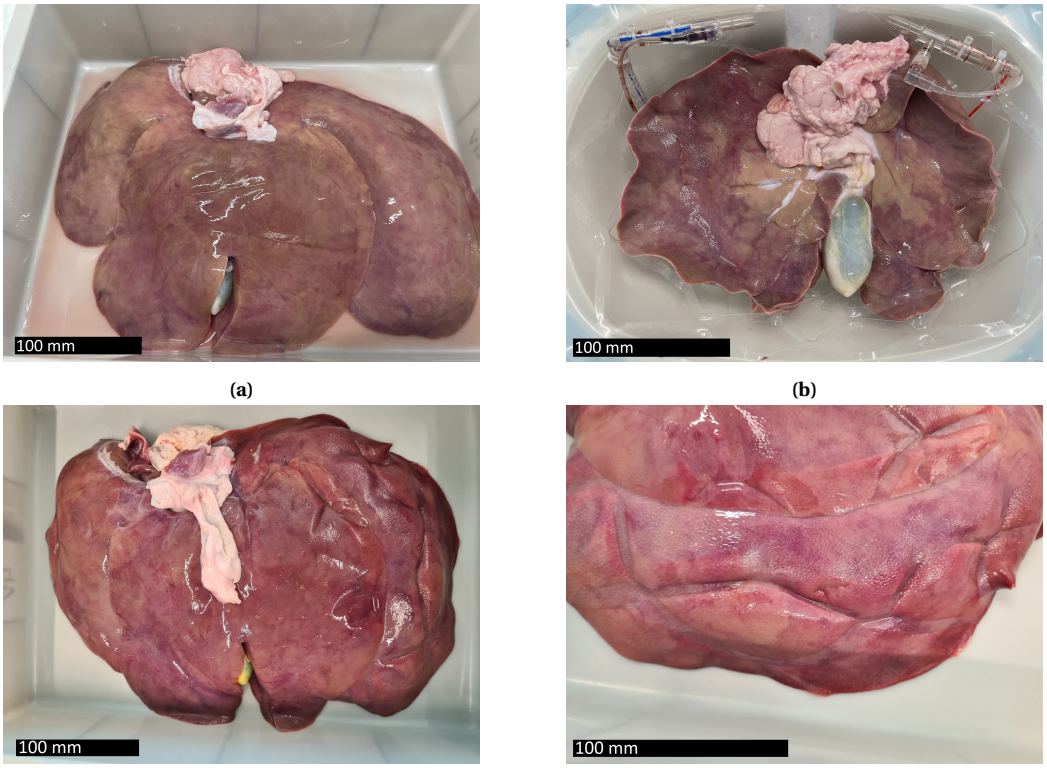


Figure 1.3: *In vivo* the liver is influenced by physiological processes occurring in and around the liver (red) and physical conditions (blue). Created with BioRender.com.

During *ex vivo* liver NMP, the liver is placed in a so-called liver reservoir, often devoid of several *in vivo* physical conditions. Notably, the use of a commercial machine, often involving liver placement on a net-like structure suspended over the perfusate reservoir, inadequately supports the liver (Figure 1.4b). Furthermore, after 24 hours, imprints of the net structure are apparent (Figure 1.4c and 1.4d). Additionally, studies reveal that placing the liver in a static liver reservoir leads to compression of liver tissue and heterogeneous distribution of the perfusate resulting in subsequent hepatocellular necrosis and deterioration in liver function after 3 to 6 hours of NMP [36, 47, 48, 52, 64–66]. These studies emphasize the necessity of improving the liver reservoir, considering the *in vivo* physical conditions, to facilitate long-term NMP.



(a) **(b)** **(c)** **(d)**

Figure 1.4: **(a)** The diaphragmatic surface of a porcine liver. **(b)**. The porcine liver placed in the liver reservoir of a commercial perfusion device. **(c)** The diaphragmatic surface of the liver that was placed in the liver reservoir of a commercial perfusion machine after 24 hours. **(d)** Close-up of the liver that was placed in the liver reservoir of the commercial perfusion machine for 24 hours. The net-like structure clearly leaves an imprint on the liver. Scale bars 100 mm.

Therefore, the aim of this thesis was to incorporate liver movement during porcine liver NMP and assess the effect of liver movement on liver function and tissue integrity. By enhancing the physiological resemblance of porcine liver NMP, the goal is to minimize pressure induced tissue necrosis and ensure homogeneous perfusion of the whole liver in an *ex vivo* setting, enabling long-term viability and functionality of the liver during NMP experiments.

In pursuit of this aim, in this thesis a suitable setup was developed and validated, which was then used to perform 6-hour porcine liver NMP experiments. This thesis is structured as follows. Chapter 2 is divided into two main sections. The first section covers the development and validation process of the liver reservoir including liver movement. The second section covers the porcine liver NMP experiments performed with the final setup during which the effect of liver movement on liver function and tissue integrity was evaluated. Chapter 3, first presents the results of the validation experiments of the movement simulation, the liver reservoir, and the full setup, and second the results of the porcine liver NMP experiments. Chapter 4 provides a comprehensive discussion of the results, addresses study limitations, and outlines potential directions for future research. Lastly, Chapter 5 offers a summary of the main findings of this thesis project and the impact of these findings on the field of NMP.

2

Materials & Methods

This chapter provides a comprehensive description of the materials and methods employed in the course of this research. The chapter is divided in two main sections dedicated to the simulation of liver movement and the development of the liver reservoir and the porcine liver NMP experiments, respectively (section 2.1 and section 2.2). The first section of this chapter starts by providing the design considerations and an inventory of the materials employed for the simulation of liver movement and the construction of the liver reservoir. Following this, the methodology for simulating the movement is described. Subsequently, a breakdown of the individual components constituting the liver reservoir is presented, along with the step-by-step assembly and validation process of the final setup. The second section of this chapter starts with an inventory of chemicals utilized during the NMP experiments, followed by an outline of the procedures for obtaining porcine livers and conducting the porcine liver NMP experiments. This is followed by a detailed description of the assays and measurements performed during the NMP experiments. Furthermore, the static reservoir used during the control experiments is described. Finally, the data analysis methods applied to the NMP results are elucidated.

2.1. Movement Simulation and Liver Reservoir Development

2.1.1. Liver Reservoir and General Design Considerations

During the design process of the liver reservoir, several requirements and considerations were carefully evaluated. To lay the groundwork for this thesis, a comprehensive literature study was conducted to explore the impact of mimicking the *in vivo* physical conditions the liver is subjected to on NMP of porcine livers. The findings from this literature study not only served as the motivation for this project but also played a crucial role in shaping the design of the liver reservoir. In this literature study the *in vivo* physical conditions the liver is subjected to, including temperature, sterility, orientation, humidity, contact with other organs, intra-abdominal pressure differences, and movement, are discussed, and how studies took these conditions into account during porcine liver NMP. These *in vivo* physical conditions were considered while choosing materials and components for the development and assembly of the final design, even though it was not possible to take all conditions into account. Additionally, different liver reservoir designs, highlighting their main principle, as employed by prior studies in this field are presented in Appendix A Table A1. These liver reservoir designs were studied for inspiration on materials, components, and methods used in designing a liver reservoir for NMP.

Furthermore, during the whole process, some general considerations were kept in mind. As this study aimed to be a proof-of-concept study, the design of the liver reservoir with movement simulation was intended to be straightforward, controllable, adaptable, easy-to-use, cost-effective, and reproducible. The goal was to utilize readily available, inexpensive, and adaptable materials and components as much as possible. Furthermore, compatibility of the liver reservoir with commercial perfusion machines, particularly the Liver Assist device used at TNO, was crucial.

2.1.2. List of Materials

- Arduino UNO (SOS Solutions.nl, Eindhoven, The Netherlands)
- Air and vacuum pump x4 (4.5V, 500 mA) (SOS Solutions.nl, Eindhoven, The Netherlands)
- 3-Way air valve (6V, 240 mA) x2 (SOS Solutions.nl, Eindhoven, The Netherlands)
- Sensor shield v5 (SOS Solutions.nl, Eindhoven, The Netherlands)
- JST PH male and female 2 pin 2.54 mm x6 (SOS Solutions.nl, Eindhoven, The Netherlands)
- Dupont female 3 pin x6 (SOS Solutions.nl, Eindhoven, The Netherlands)
- Pulse Width Modulation (PWM) electronic switch x6 (SOS Solutions.nl, Eindhoven, The Netherlands)
- USB-A - USB-B Cable (own possession)
- DC power cable female (own possession)
- Power adapter/bank (5V, 1A) (own possession)
- Kopp heat shrink tubing (Intergamma BV, Leusden, The Netherlands)
- Silicone tubes (inner-outer diameter 3-5mm) (SOS Solutions.nl, Eindhoven, The Netherlands)
- Latex punch balloons (diameter 52 cm) (Intro International BV, Woudenburg, The Netherlands)
- Foldable crate with holes 34 L (475 x 345 x 240 mm) (Curver, Zaragoza, Spain)
- Dry goods storage box 2.1 L (200 x 100 x 142 mm) (Blokker BV, Amsterdam-Duivendrecht, The Netherlands)
- Bubble wrap (Intergamma BV, Leusden, The Netherlands)
- Tie wraps (Intergamma BV, Leusden, The Netherlands)
- Elastics (own possession)
- Self-adhesive velcro (Fetim Group, Amsterdam, The Netherlands)
- Polyester wire mesh (Fetim Group, Amsterdam, The Netherlands)
- Polypropylene bags (VWR International BV, Amsterdam, The Netherlands)
- Cardboard (own possession)
- Enteral feeding bag gravity set 1000 mL
- Soft and hard plastic glue (Bison International BV, Goes, The Netherlands)
- Super silicone sanitair sealant (Bison International BV, Goes, The Netherlands)

2.1.3. Electronic Circuit and Movement Simulation

The method adopted to simulate movement was inspired by the study conducted by Eshmuminov *et al.* [36], where the liver was placed on a silicone mat with underneath a balloon that was inflated and deflated with an air oscillator. Additionally, surgical phantom studies, in which liver movement was simulated *ex vivo* for training and preoperative planning of liver interventions and surgery, and the field of soft robotics, were explored [67–69]. After carefully considering the different components and mechanisms used in these studies, the decision was made to use two balloons, with inflation and deflation controlled by pumps through an Arduino microcontroller. The Arduino microcontroller served as the central control unit, capable of programming and controlling various electronic components. The microcontroller was powered by a 5V wall adapter and connected to a laptop such that the code to control the electronic components could be uploaded. The sensor shield, attached to the Arduino microcontroller, facilitated easy connection to the sensors and actuators. The microcontroller was programmed to send signals to 3-way valves and air pumps to regulate the airflow into and out of two balloons. Two modes of movement were considered: the alternating mode and the simultaneous mode.

For the alternating mode, four air pumps and two 3-way valves were used to control the alternative inflation and deflation of two balloons (Figure 2.1). All electronic components were connected to the sensor shield using PWM switches to control the power supplied to the pumps and valves. The outflow of pump 1 was connected to the normally open interface of 3-way valve 1 with a silicone tube. The inflow of pump 2 was connected to the normally closed interface of 3-way valve 1 with a silicone tube. The outflow of pump 3 was connected to the normally open interface of 3-way valve 2 with a silicone tube. The inflow of pump 4 was connected to the normally closed interface of 3-way valve 2 with a silicone tube. The common interface of valve 1 was connected to balloon 1 and the common interface of valve 2 to balloon 2 via silicone tubes secured with elastics. The movement was initiated by inflating the balloons to a total volume by turning on pumps 1 and 3 and turning off the rest of the electronic components. Subsequently, pumps 1 and 4 and 3-way valve 2 were turned on, and pumps 2 and 3 and 3-way valve 1 were turned off, allowing air to flow into balloon 1 and out of balloon 2. Next pumps 1 and 4 and 3-way valve 2 were turned off, and pumps 2 and 3 and 3-way valve 1 were turned on, allowing air to flow out of balloon 1 and into balloon 2. This inflation and deflation cycle was repeated continuously, with one balloon undergoing inflation while the other balloon was deflated, and

vice versa.

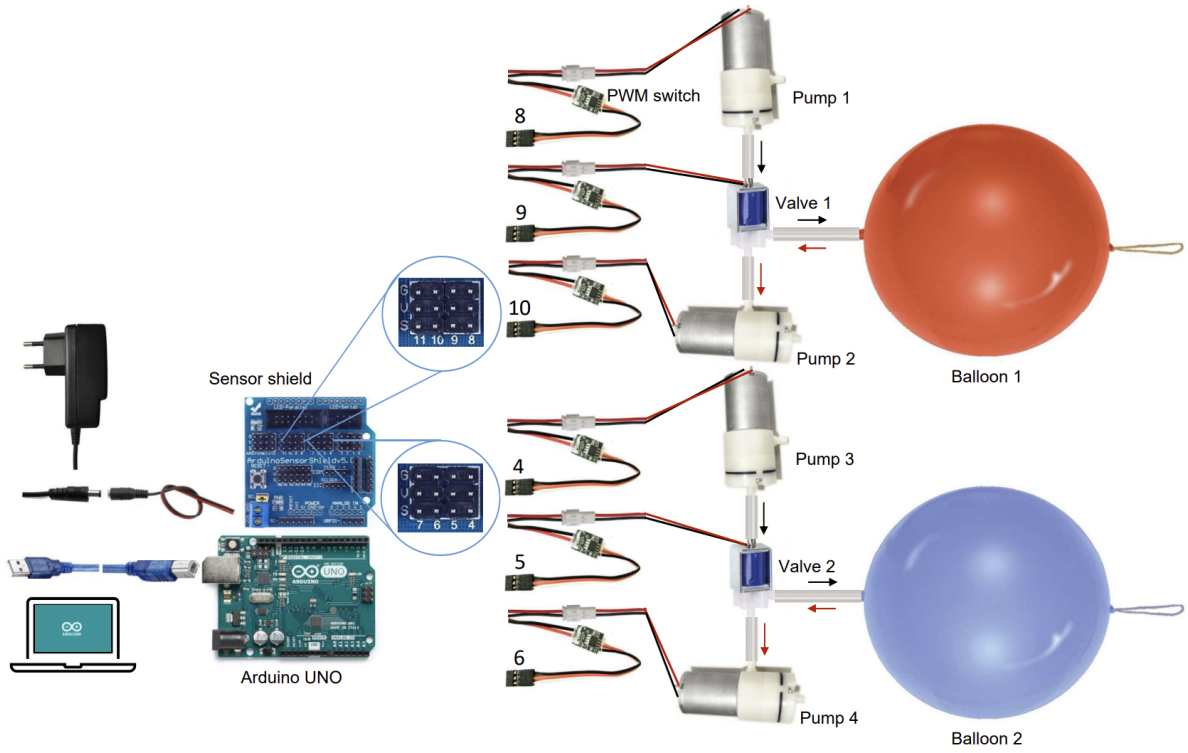


Figure 2.1: A schematic representation of the electronic circuit with the latex balloons. The Arduino microcontroller was connected to a laptop such that the code could be uploaded and a wall power adapter for the power supply. The sensor shield to which the electronic circuit components were attached was plugged onto the Arduino microcontroller. The different electronic components, four pumps and two 3-way valves, were connected to the depicted pins on the sensor shield. The arrows show which pumps cause inflation and which pumps cause deflation of the balloons.

For the simultaneous mode, four air pumps and two 3-way valves were used to control the simultaneous inflation and deflation of two balloons. The outflow interfaces of pumps 1 and 3 were connected to the normally open interfaces of 3-way valves 1 and 2, respectively, and the inflow interfaces of pumps 2 and 4 were connected to the normally closed interfaces of 3-way valves 1 and 2, respectively. The common interface of 3-way valve 1 was connected to balloon 1 and the common interface of 3-way valve 2 was connected to balloon 2. Again the balloons were inflated to their total volume. Subsequently, pumps 1 and 3 were simultaneously turned on, while pumps 2 and 4 and the 3-way valves were turned off, allowing air to flow into balloons 1 and 2. While pumps 1 and 3 were turned off 3-way valves 1 and 2 and air pumps 2 and 4 were turned on, allowing the air to flow out of the balloons. This inflation and deflation cycle was repeated continuously, with both balloons inflating and deflating simultaneously.

Using an Arduino microcontroller, the rhythm or range of movement could be controlled by adjusting the duration of inflation and deflation. Additionally, the air pressure could be regulated by turning the servos' positions from 0 to 180 degrees, corresponding to minimal and maximal power supply and air pressure, respectively.

2.1.4. Liver Reservoir Components and Assembly

Integrating liver movement into NMP necessitated addressing both the simulation of movement and its incorporation into the liver reservoir. The subsequent section outlines the various components of the liver reservoir.

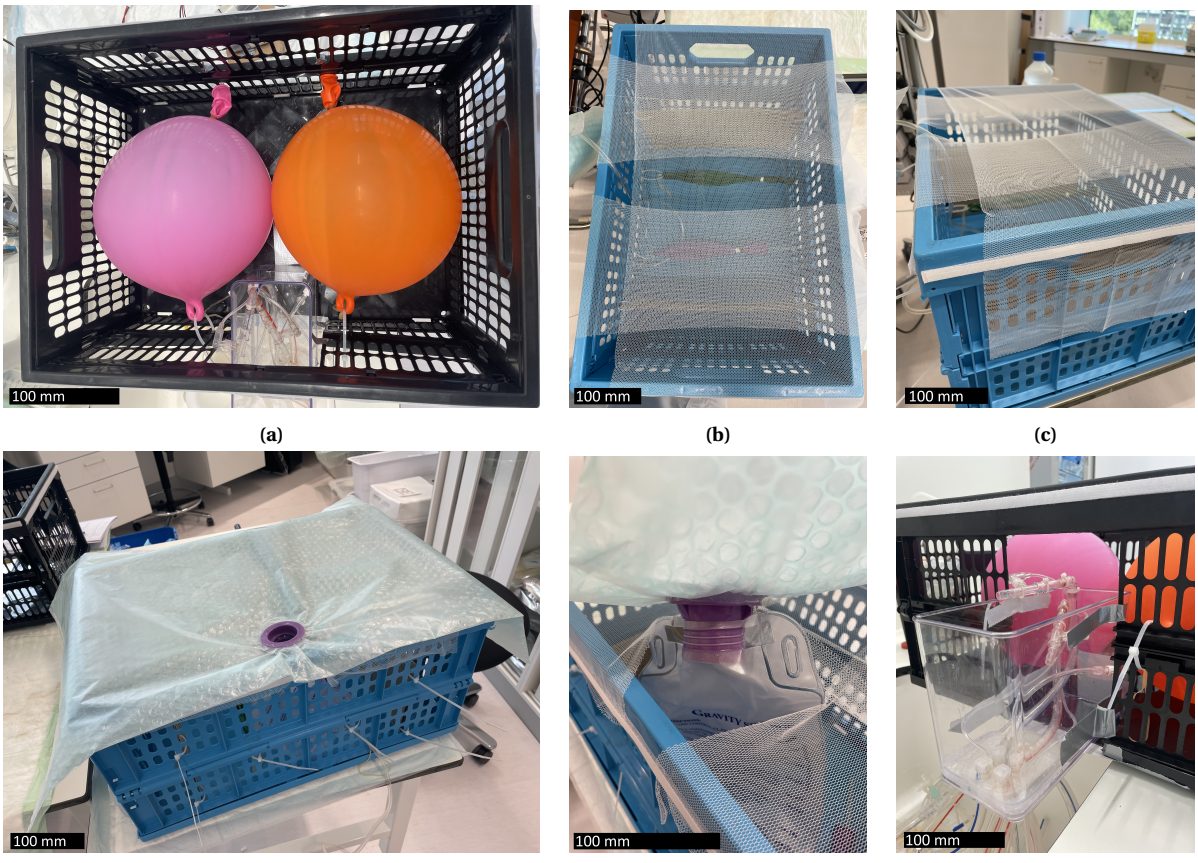
The balloons utilized in the study were made of flexible latex material and had a maximum diameter of 52 cm. These balloons were equipped with loops on the opposite side of the opening of the balloon, facilitating their attachment to other objects. This feature allowed the balloons to be securely positioned underneath

the liver. A crate, with holes, enabled easy attachment of the balloons to its walls using tie wraps, thus enabling precise positioning of the balloons at the desired height and width to provide full support to the liver (Figure 2.2a).

To support the liver atop the moving balloons, a flexible net made of polyester wire gauze was suspended over the crate (Figure 2.2b). Fixation of the net to the crate's sides was achieved using self-adhesive velcro (Figure 2.2c). The net's tension could be adjusted in accordance with the liver's weight, ensuring that the liver's weight was distributed between the balloons and the net without restricting the range of liver movement. A soft, thin, flexible, watertight, and biocompatible mat, constructed from recycled bubble wrap sandwiched between two layers of polypropylene, was then placed atop the net (Figure 2.2d). A drain, made of a gravity set, was incorporated into the mat, allowing perfusate to flow out of the inferior vena cava (IVC) of the liver and any perfusate leaking from the liver to be channeled back to the perfusate reservoir (Figure 2.2e). The plastic sheets and gravity set were securely attached to each other using soft and hard plastic glue, as well as silicone sealant.

A new perfusate reservoir was also crafted to be placed underneath the drain to facilitate recirculation of the perfusate. The perfusate reservoir was constructed from food-safe hard plastic and featured tubing from the Liver Assist disposable set securely attached to its base using silicone sealant (Figure 2.2f).

During the perfusion experiments, the liver should be positioned on the mat with its diaphragmatic surface facing down, and the IVC cannula should be suspended above the drain for efficient drainage. Furthermore, to minimize heat loss and condensation, the liver should be covered with a polypropylene sheet.



(a) **(b)** **(c)**

(d) **(e)** **(f)**

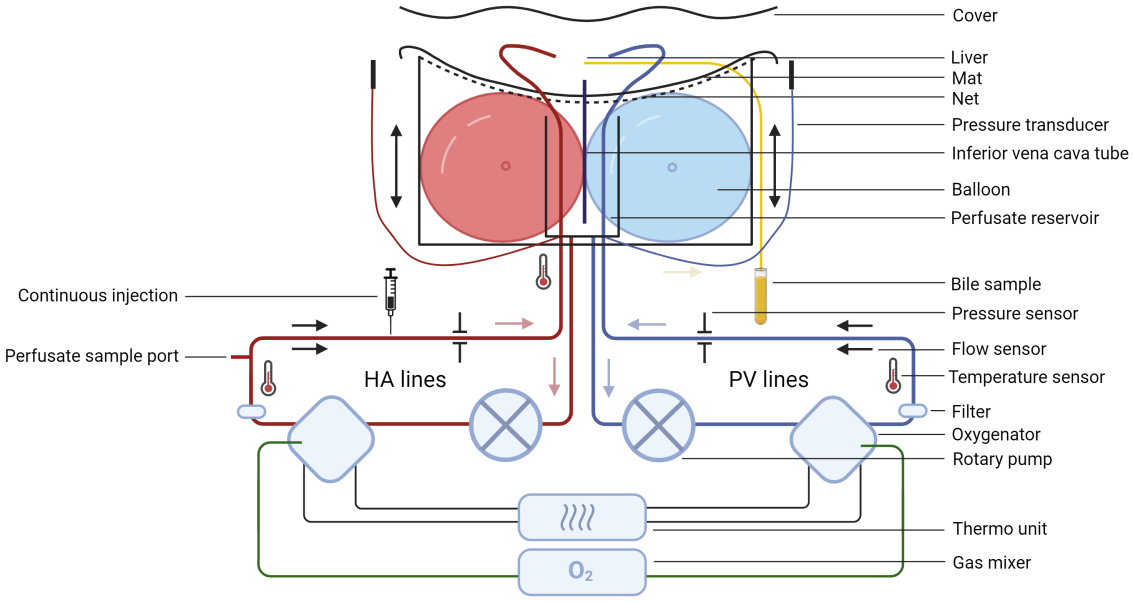
Figure 2.2: The separate system components. **(a)** The balloons are attached in the crate, with tie wraps attaching them to one side and the silicone tubes through the crate keeping them in place on the other side. **(b)** The net is stretched over the crate above the balloons, which is slightly suspended in the box when the liver is placed on it, dividing the weight of the liver over the balloons and the net. **(c)** The net is attached to the box with velcro strips, making the tension of the net adjustable. **(d)** On top of the net the plastic mat is placed on which the liver is placed with a hole for the inferior vena cava (IVC) cannula and perfusate leaking from the liver. **(e)** The gravity bag through which the perfusate can flow from the mat and IVC cannula back to the perfusate reservoir. **(f)** The perfusate reservoir in which the perfusate flowing out of the IVC and leaking from the liver is caught and circulated through the tubing system back to the liver. Scale bars 100 mm.

2.1.5. Redesigned Liver Reservoir and Full setup

During an iterative process, the electronic system simulating movement and the components described above were assembled and according to observations altered to obtain the final liver reservoir. Furthermore, the liver reservoir was combined with the other system components necessary to perform NMP experiments. The liver reservoir including the moving balloons, the perfusate reservoir with tubing, and the Liver Assist device including the gas mixer and continuous injection holder were interconnected as shown in Figure 2.3a. The Liver Assist device is described in detail in subsection 2.2.3 and shown in Figure 2.6. In Figure 2.3b a schematic representation of the system is depicted for further clarification.



(a)



(b)

Figure 2.3: (a) The experimental setup with the redesigned liver reservoir, from left to right, (1) the laptop and electronic circuit, (2) the gas mixer and (3) infusion station, (4) the redesigned liver reservoir with movement simulation, (5) the perfusate reservoir, (6) tubing, and (7) the Liver Assist device. **(b)** A schematic representation of the redesigned setup with depicted the liver reservoir with the balloons, the perfusate reservoir, tubing, and the Liver Assist system components (see subsection 2.2.3). Created with BioRender.com.

2.1.6. Validation experiments

2.1.6.1. Movement Simulation Validation

Both the alternative and simultaneous modes of movement, described above, were tested and observed. Furthermore, various durations of inflation and deflation were explored, encompassing slow to fast rhythms of movement, with small to large ranges of movement, respectively. This encompassed slow rhythms of 12 seconds in and 12 seconds out, to fast rhythms of 2 seconds in and 2 seconds out, with increments of 2 seconds. Based on observation and intuition, a specific mode of movement was chosen.

Subsequently, the range and rhythm of movement of the balloons, with and without the weight of the liver, were quantified using a Time-of-Flight (ToF) sensor (Seeed Studio, Shenzhen, China) (Figure 2.4). A ToF sensor calculates the distance to an object by the observed phase difference between the illumination and reflection of a light source. In this experiment, a laptop sleeve, with the approximate weight of the liver, was used to simulate the liver. Additionally, the Arduino system responsible for simulating movement was evaluated for its automated operation and the stability of the rythm and range of movement over extended periods of time, as the goal was to perform NMP experiments lasting beyond 6 hours.



(a) **(b)**

Figure 2.4: The setup utilized to measure the rythm and range of movement of the balloons **(a)** without the liver and **(b)** with a liver model. The ToF sensor is steadied above the balloons and model liver and measures the distance between the sensor and the balloons and model liver which are moving from and to the sensor.

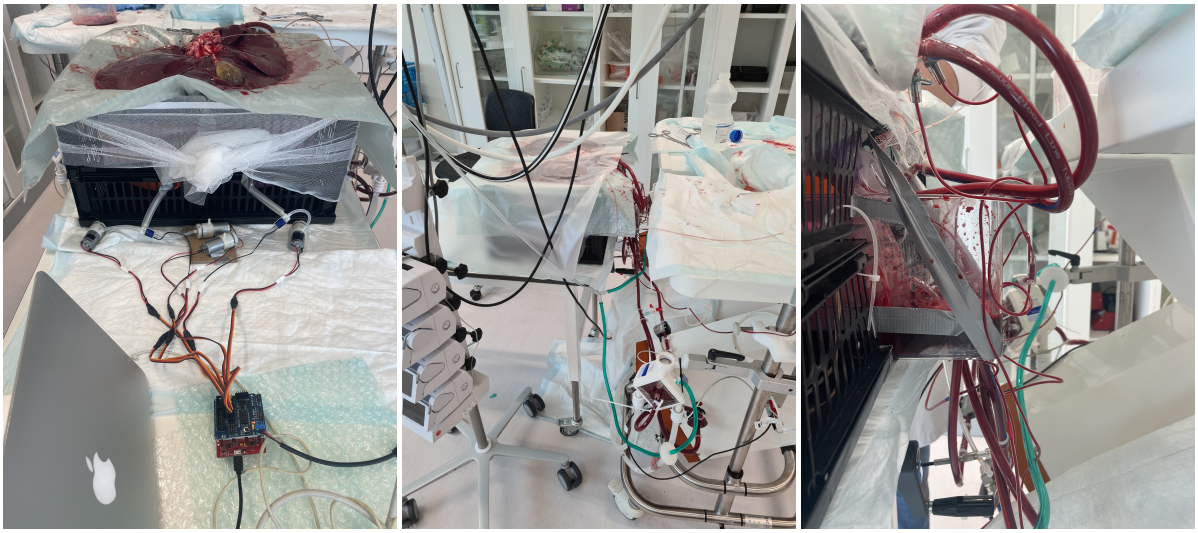
2.1.6.2. Liver Reservoir and Final NMP Setup Validation

The compatibility of the redesigned reservoir with a commercial perfusion machine, the Liver Assist device, was investigated through HMP (15 °C) (n = 3) and NMP (38 °C) (n = 1) experiments lasting 1 to 2 hours using 3 L of saline and 2 L of porcine blood, respectively (Figure 2.5 and Appendix C.1 Figure C1). During these experiments the focus was on observing hemodynamic stability under different rhythms and ranges of movement, the effective integration of all system components, fluid flow from the liver through the IVC cannula, the maintenance of a watertight system, and the ability of the setup to adequately support the liver. During these experiments, the setup was iteratively optimized according to observations and experienced challenges. The results of these experiments are based on observations, no measurements were done.

2.2. Porcine Liver NMP Experiments

2.2.1. Chemicals

The chemicals used in the NMP experiments were purchased from different suppliers. Indocyanine green (ICG), heparin, taurocholic acid (TCA), glycocholic acid (GCA), insulin, sodium bicarbonate (HCO_3), D-Glucose, and bovine serum albumin (BSA) were purchased from Sigma-Aldrich Chemie BV (Zwijndrecht, The Netherlands). Epoprostenol was purchased from Tocris (Bristol, UK), calcium gluconate 10 % was purchased from B. Braun (Melsungen, Germany), saline (NaCl 0.9 %) was purchased from Baxter BV (Utrecht, The Netherlands), and penicillin and streptomycin (Pen-Strep) was purchased from Fisher Scientific (Landsmeer, The Netherlands).



(a) (b) (c)



(d)

Figure 2.5: The setup of the NMP validation experiment. **(a)** In the front, the Arduino microcontroller, connected to the laptop, wall adapter, and electronic components, is depicted. In the back, the liver reservoir, in which the balloons are moving, and on which the liver is placed, is depicted. **(b)** From left to right, the liver reservoir, tubing, and the Liver Assist device are depicted. **(c)** The perfusate reservoir with tubing to the liver and from the perfusate reservoir back to the Liver Assist system. **(d)** Tubing connected to the hepatic artery (HA) and portal vein (PV) cannulae, and underneath the liver and mat the drain from the mat and the perfusate reservoir are visible.

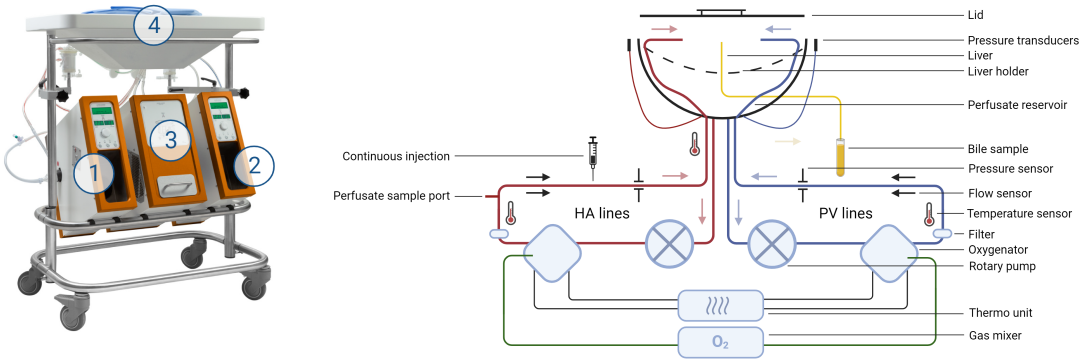
2.2.2. Porcine Liver Procurement

Five porcine livers (Sus scrofa domesticus) were obtained from a slaughterhouse (Visser BV, Lunteren, The Netherlands) from female or male pigs at approximately 6 months of age, with a body weight ranging from 100 to 120 kg. The pigs were sacrificed using a standardized electrocution procedure, followed by exsanguination. Subsequently, 3 L of blood was collected in a container supplemented with 25,000 IU of heparin. Following termination and exsanguination, all abdominal organs were dissected outside the animal and collected. The portal vein (PV) was cannulated and flushed by gravity with 3 L of cold saline, per liter supplemented with 5000 IU of heparin. During excision from the other abdominal organs, care was taken to ensure sufficient length of the PV, hepatic artery (HA), and inferior vena cava (IVC) to facilitate cannulation during perfusion. After excision from the other abdominal organs, the liver was placed in a plastic bag on ice and flushed by gravity with 1 L of cold saline and 1 L of PumpProtect (Carnamedica, Warsaw, Poland), both supplemented with 5000 IU of heparin. Or alternatively, with 2 L of Histidine-Trypotphan-Ketoglutarate (HTK) solution (Carnamedica, Warsaw, Poland), per liter supplemented with 5000 IU of heparin. During transportation to the laboratory, the liver was immersed in these preservation fluids within a coolbox filled with ice. Upon arrival at the laboratory, the PV, HA, IVC, and common bile duct were cannulated and side branches, including the *ductus cysticus*, derived from the gall bladder, and the superior vena cava (SVC) were ligated. Following the

preparation of the liver and the NMP device, the liver was placed on the redesigned liver reservoir including liver movement.

2.2.3. Normothermic Machine Perfusion

NMP experiments of 6 hours were performed using the Liver Assist^{TM} device (XVIVO, Groningen, The Netherlands) (Figure 2.6). The Liver Assist device is a pressure-driven dual perfusion machine primarily designed for human livers. It comprises two rotary pumps providing a pulsatile flow to the HA and a continuous flow to the PV, two oxygenators for perfusate oxygenation and removal of carbon dioxide (CO_2), a thermo unit to maintain the desired perfusate temperature, as well as temperature, flow, and pressure sensors to monitor hemodynamics. The system was primed with approximately 2 L of perfusion fluid, mainly consisting of red blood cells (RBCs) and plasma obtained from autologous blood (Table 2.1). The autologous blood was centrifuged to separate RBCs, white blood cells (WBCs), and plasma, thus allowing for the removal of WBCs. Furthermore, the perfusate contained 10 % calcium gluconate, pen-strep, heparin, and 8.4 % sodium bicarbonate. During the final experiment, an additional perfusate, mainly consisting of saline and BSA, was kept at hand in case more perfusate volume was needed (Table 2.2). A continuous infusion of insulin, heparin, taurocholate, and epoprostenol was provided in the HA by the UNIQUEDOC infusion station (Acromed AG Medical Systems, Zürich, Swiss) at a rate of 10 IU h^{-1}, 1041 IU h^{-1}, 10 mL h^{-1} (2 % w/v), and 8 μg h^{-1}, respectively, to maintain liver function, including bile flow (Table 2.3). Gas delivery to both the oxygenators consisted of 40 % oxygen (O_2) and 60 % compressed air, regulated at a rate of 1.5 L min^{-1} using the Air-Oxygen Blender (Medicare Uitgeest, Uitgeest, The Netherlands). The temperature was set at 38 °C (body temperature for pigs). The livers were perfused with a portal pressure of 9−11 mmHg and a mean arterial pressure of 50−60 mmHg. Following priming, de-airing, zeroing, and warming of the circuit, the liver was removed from the ice and placed on the liver reservoir including liver movement. Furthermore, the height of the liver reservoir was adjusted such that the HA and PV cannulae were aligned with the pressure transducers of the Liver Assist device. Perfusion was initiated by sequentially setting the desired pressure for the PV and connecting the tubing to the PV cannula, followed by a similar procedure for the HA. During perfusion, additional boluses of sodium bicarbonate and D-glucose were administered depending on the perfusate pH (range 7.35–7.45) and glucose concentration (<5 mmol L^{-1}), respectively, to maintain physiological levels (Table 2.4).



(a) **(b)**

Figure 2.6: The Liver Assist device. **(a)** The trolley with the two pump units with control panels and display for controlling and continuous monitoring of the (1) hepatic artery (HA) and (2) portal vein (PV) hemodynamics and perfusate temperature, (3) the thermo unit, and (4) the table in which the disposable set, including the static liver and perfusate reservoir, tubing, and oxygenators, is held. **(b)** A schematic representation of the Liver Assist system including the static Liver Assist liver reservoir. During static perfusion experiments, the liver was placed on the net-like structure in the liver holder, above the perfusate reservoir, which is closed off by a lid. Both the HA and PV side include tubing coming from the perfusate reservoir, through which the perfusate is pumped back to the oxygenators with rotary pumps. In the oxygenator, the perfusate is warmed and supplied with oxygen and carbon dioxide is removed from the perfusate. After the perfusate passes the oxygenator, HA perfusate samples are taken, the flow, pressure, and temperature are measured, and the continuous infusion is administered, before the perfusate enters the liver. Furthermore, bile produced in the gallbladder is collected. Created with BioRender.com.

Table 2.1: Composition of the perfusate.

Compound	Amount
Erythrocytes	1000 mL
Plasma	1000 mL
10 % calcium gluconate solution	10 mL
8.4 % sodium bicarbonate solution	Depending on the pH of the perfusate at the start of perfusion
Penicillin and streptomycin	10 mL
Heparin	2 mL

Table 2.2: Composition of the additional perfusate.

Compound	Amount
Saline (NaCl 0.9 %)	1000 mL
Bovine serum albumin (BSA)	40 g
10 % calcium gluconate solution	5 mL
8.4 % sodium bicarbonate solution	Depending on the pH
Penicillin and streptomycin	5 mL
Heparin	1 mL

Table 2.3: Composition of the continuous infusion.

Compound	Dosis	Stock	Duration infusion	Final amount
Heparine	1041 IU h^{-1}	5000 IU mL^{-1}	7	1.45 mL
Insuline	10 IU h^{-1}	135 IU mL^{-1}	7	0.518 mL
Epoprostenol	8 μg h^{-1}	0.8 mg mL^{-1}	7	70 μL
Taurocholic acid (TCA)*	0.2 g h^{-1}		7	1.4 g
Saline (NaCl 0.9 %)			7	28 mL

*Experiment 3: 0.69 g TCA + 0.71 g glycocholic acid (GCA)

Table 2.4: Bolus injections.

Compound	When	What
8.4 %(w/v) sodium bicarbonate	pH outside 7.35 - 7.45	Add 10-15 mL per 0.1 pH too low
40 % (w/v) glucose	glucose < 5 mmol L^{-1}	Add 10-15 mL

2.2.4. Perfusion Measurements and Assays

Various measurements and assays were conducted prior to, during, and after the NMP experiments to assess the overall performance of the NMP experiments, liver viability and functionality, clearance capacity, and tissue integrity. In this section, the different assays and measurements are described.

2.2.4.1. Liver Viability and Functionality

To evaluate the performance of the NMP experiment, the HA and PV temperature, pressure, flow, and resistance were reported from the Liver Assist device every 30 minutes. Additionally, before and after the experiments the weight of the liver was registered. Arterial perfusate and bile samples were collected every 30 minutes. To assess the general viability and functionality of the liver during perfusion blood gas analysis was performed every hour, including measurement of pH, partial pressure of carbon dioxide (PCO_2), partial pressure of oxygen (PO_2), total carbon dioxide (TCO_2), bicarbonate (HCO_3), base excess (BE), oxygen saturation (sO_2), sodium (Na), potassium (K), chloride (Cl), ionized calcium (iCa), urea nitrogen (BUN), creatinine (Crea), glucose, lactate, hematocrit (Hct), and hemoglobin (Hgb), using the i-STAT alinity clinical analyzer (Abbott Point of Care Inc., Princeton, NJ, USA). After collection of the samples, the perfusate samples were centrifuged at 21100 RCF for 10 minutes at 4 °C and stored at ≤ -70 °C along with the bile samples until further handling. The hourly perfusate samples, were used to measure the concentration of injury markers, including the total alanine transaminase (ALT) and aspartate transaminase (AST) concentrations, using a Reflotron Plus Analyzer (Roche Diagnostics, Basel, Switzerland). Additionally, total bilirubin concentrations in hourly

perfusate samples and 1, 3, and 5-hour bile samples were measured using the Reflotron Plus Analyzer.

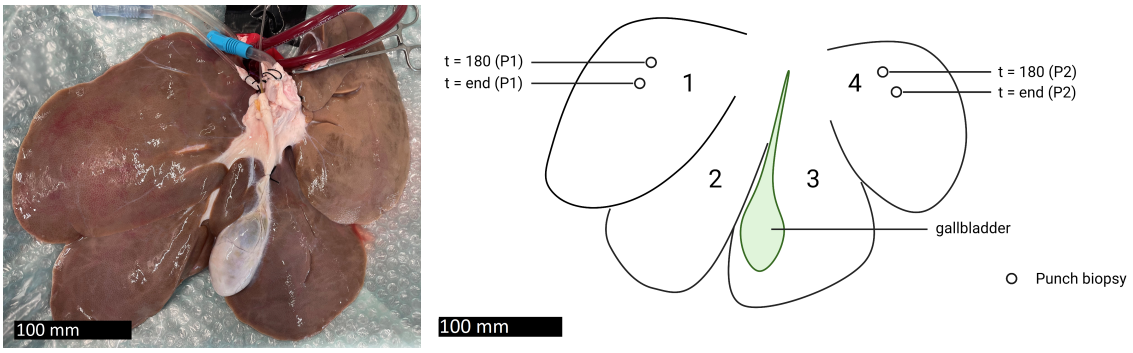
2.2.4.2. Clearance Capacity

Indocyanine green (ICG), a fluorescent dye, was administered to the liver at two time points to study its clearance from the perfusate and biliary excretion, providing insight into the clearance capacity of the *ex vivo* porcine liver. ICG was administered in a bolus of 3 mg to the HA and PV after 120 minutes and after 300 minutes of NMP. Subsequently, arterial blood samples were taken at t = 0, 2, 4, 6, 8, 10, 15, 20, 30, 40, 50, 60 minutes and bile samples were collected in 10-minute fractions after ICG administration. The collected blood samples were immediately centrifuged at 21100 RCF for 10 minutes at 4 °C, and 100 μL of the perfusate and bile samples was pipetted into a 96-wells plate (Costar 96 Flat Bottom White Polystyrene) and stored in the dark at -20 °C until further processing. The perfusate and biliary concentrations of ICG were determined by measuring the fluorescence in relative fluorescence units (RFUs) at 788 nm wavelength emission and 813 nm wavelength excitation using a microplate reader (Tecan Infinite m200 Pro, Männedorf, Switzerland). Subsequently, the ICG perfusate disappearance rate (PDR_{ICG}) was calculated by backward extrapolation to time point zero (100 %) and fitting the perfusate concentration curve over time to a mono-exponential distribution ($C_{ICG} = C_0 \times e^{-kt}$) using GraphPad Prism version 9.1.2 for Windows (GraphPad Software, Boston, Massachusetts, USA). After which the half-life was obtained and the PDR_{ICG} was calculated using the formula: PDR_{ICG} (% per minute) = $\ln 2 / t_{1/2} \times 100$ [70]. Additionally, the percentage of the total ICG cleared from the perfusate after 60 minutes was calculated.

2.2.4.3. Tissue integrity

Continuous physiological assessment of the liver was conducted during perfusion, involving manual evaluation and macroscopic examination of the liver's appearance at regular intervals, with photographs taken of the liver's top and bottom surfaces every 2 hours.

Furthermore, a histological analysis was performed to assess the cellular integrity of the liver. At t = 180 min (n = 2) and post-perfusion (n = 2) punch biopsies were taken at the bottom of the liver, where the liver was in contact with the balloons. The exact locations of the punch biopsies can be found in Figure 2.7. The biopsies were immediately fixed in 10 % formalin, stored in 70 % ethanol, and subsequently embedded in paraffin. The 4-μm thick paraffin-embedded liver sections were cut and stained with hematoxylin and eosin (H&E) for examination under light microscopy. Images acquired were analyzed and scored by a pathologist who was blinded to the experimental conditions. For each liver section, specific observations were recorded, and a color-coded system was implemented to indicate the severity (minimal, mild, moderate, severe) and extent (focal, multifocal, diffuse) of tissue degeneration. This degeneration was characterized by a set of features including single cell necrosis (pyknosis, karyolysis, and karyorrhexis), hepatocellular vacuolation, hemorrhages, and hepatocellular hypertrophy indicated by pale, swollen, and rounded hepatocytes and the loss of the hepatocellular cord structure.



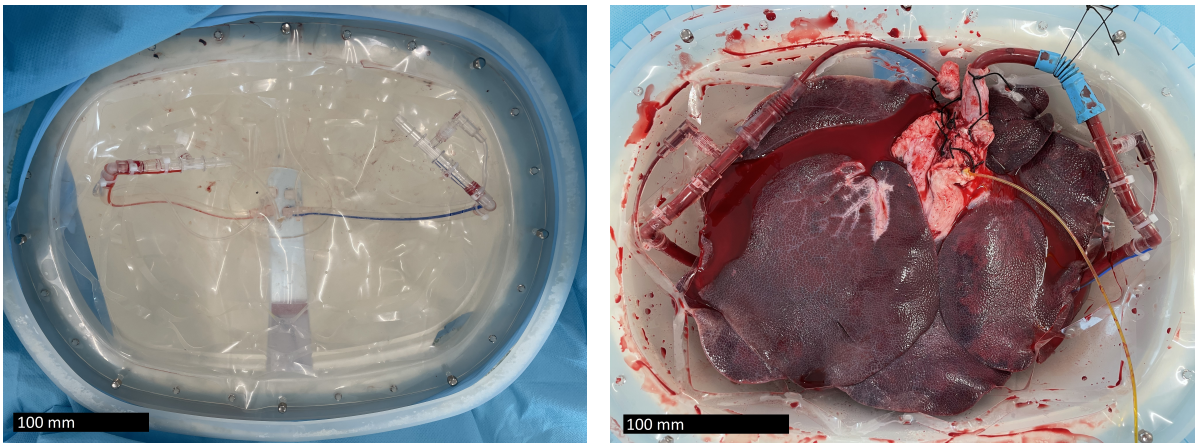
(a) **(b)**

Figure 2.7: A schematic of the biopsies taken during the NMP experiments under the established movement condition. **(a)** A flushed liver for reference. **(b)** A schematic representation of the liver with numbered lobes and punch biospies taken during the NMP experiments. The time points at which the biopsies were taken are indicated, the biopsies were coded with the letter 'P' for punch biopsy, and numbered according to the number of biopsies taken at that time point. scale bars 100 mm. Created with BioRender.com.

2.2.5. Control Group and Static Reservoir

Two control groups were established to provide reference data for this study. Both control groups consist of data obtained during NMP experiments performed on the Liver Assist device without any additional interventions, following the same protocol as performed in this study, except for the utilization of liver movement and the new liver reservoir. In both control groups, the static liver reservoir of the Liver Assist device was utilized, as illustrated in Figure 2.6b and further depicted in Figure 2.8. The liver reservoir, possessing dimensions of 340 x 240 mm, comprised a plastic net with perforations and larger holes. On the liver reservoir, the liver was positioned on its diaphragmatic surface, suspended above a soft, flexible perfusate reservoir, allowing for free leakage of perfusate from the IVC. Additionally, the liver reservoir could be covered with a lid to facilitate easy access while reducing thermal dissipation to the environment.

These experiments served as a basis for comparison with standard measurements of hemodynamics, blood gasses, bile production, ICG clearance capacity, as well as AST, ALT, and bilirubin concentrations. The historical data was collected from prior NMP experiments conducted by TNO at two separate locations: Zeist (n = 3) and Leiden (n = 3). The only variation between these experiments was the gas supply; carbogen (95 % O_2 and 5 % CO_2) was delivered at a rate of 0.5 L min^{-1} in Zeist, while in Leiden, a gas mixer supplied 40−60 % O_2 mixed with compressed air at a rate of 2.0 L min^{-1}. For this reason, the data of Zeist and Leiden are presented as two separate control groups. Measurements during these experiments were not always performed at the same time points as during the experiments with liver movement, especially, during the control experiments, ICG was only administered at t = 360 min and t = 300 min, for Zeist and Leiden, respectively.



(a) **(b)**

Figure 2.8: The disposable liver reservoir of the Liver Assist device used during the control experiments **(a)** without the liver and **(b)** with the liver placed on the net. Scale bars 100 mm.

2.2.6. Data Analysis

Data analysis and graphical visualization were performed using GraphPad Prism version 9.1.2 for Windows (GraphPad Software, Boston, Massachusetts, USA). For the statistical analysis, the data points from the experiments performed under the established movement condition (n = 4), the control experiments performed under the static condition in Zeist (n = 3), and the control experiments performed under the static condition in Leiden (n = 3) were organized into three separate data sets. For each data set, the mean and standard deviation (M ± SD) at each time point were calculated. In the figures in section 3.2 the replicates of the experiments performed under the movement condition are displayed separately to illustrate the variability between the experiments. When applicable, the control data from Zeist and Leiden are represented as means with SD at each measured time point. To compare the means of various measurements of the experiments performed under the movement condition to both control groups performed under the static condition, unpaired two-tailed Student's t tests were employed. The t tests were employed on the widely accepted viability markers, e.g. blood flow, bile production, glucose, lactate, and bilirubin concentration, and additionally ALT and AST level and the PDR_{ICG} and % of ICG cleared from the perfusate after 60 minutes.

3

Results

In this chapter, first, the results of the movement simulation and the redesigned liver reservoir validation experiments are described (section 3.1). Subsequently, the results of the 6-hour NMP experiments with liver movement are presented, categorized by liver characteristics and perfusion parameters, general liver viability and functionality markers, injury markers, metabolic function, and tissue integrity (section 3.2).

3.1. Movement Simulation and Liver Reservoir Development

3.1.1. Movement simulation

During one of the HMP validation experiments, it was observed that the different modes of movement, the alternating and simultaneous balloon movement, as well as varying rhythms of movement, did not influence the HA and PV flow. Ultimately, the alternating mode with an intermediate rhythm and range of movement (8 seconds in 8 seconds out) was chosen for the subsequent porcine liver NMP experiments. Moreover, an inflation duration of 120 seconds was determined as necessary to reach the initial volume of the balloons. This volume was chosen such that the liver model laying on top of the net was supported and movement of the liver was induced once the alternating movement was started. The corresponding Arduino code sent to the Arduino microcontroller for this mode can be found in Appendix B. In Figure 3.1, a repetition of the rhythm and range of movement measured for one inflation-deflation cycle is shown. In the absence of the liver's weight atop the balloons, this mode yielded a range of approximately 14 mm for a single balloon at a frequency of 4 inflation-deflation cycles per minute (Figure 3.1). With the liver's weight on top of the balloons, this mode resulted in a range of 6 mm for a single balloon at a frequency of 4 inflation-deflation cycles per minute (Figure 3.1). The central points of the balloons were placed at an approximate distance of 200 mm from each other. When one balloon was at its maximum volume and one balloon at its minimal volume, there was a slope between the top of the balloons of approximately 4° and 1.72°, without and with the weight of the liver, respectively (Figure 3.2).

To validate the stability of the movement simulation, the working of the individual pumps was evaluated and the system was run for an extended period of time. During this evaluation, it was observed that inflating the balloons using different pumps for a specific duration resulted in varying final volumes of the balloons. Additionally, when using a single pump to inflate and deflate a single balloon, the final volume deviated from the initial volume, indicating an imbalance in the volume of air entering and exiting the balloon for that particular pump. When the alternating mode of movement was employed, with all pumps configured for equal inflation and deflation durations, the balloon volumes exhibited gradual changes over a duration of 2-hours.

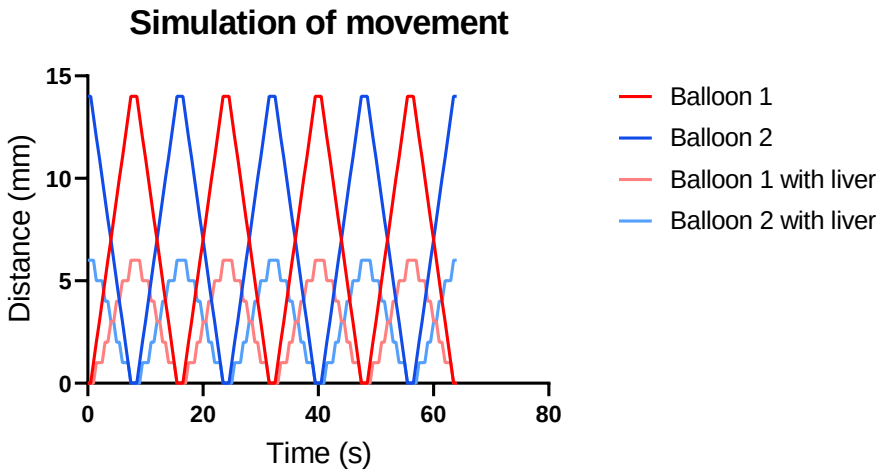


Figure 3.1: Graph of the movement simulated by the individual balloons. The rhythm and range of movement of balloons 1 and 2, in the absence of the liver's weight, are displayed in dark red and blue. The rhythm and range of the movement of balloons 1 and 2, with the liver's weight on top of the balloons, are displayed in light red and blue.

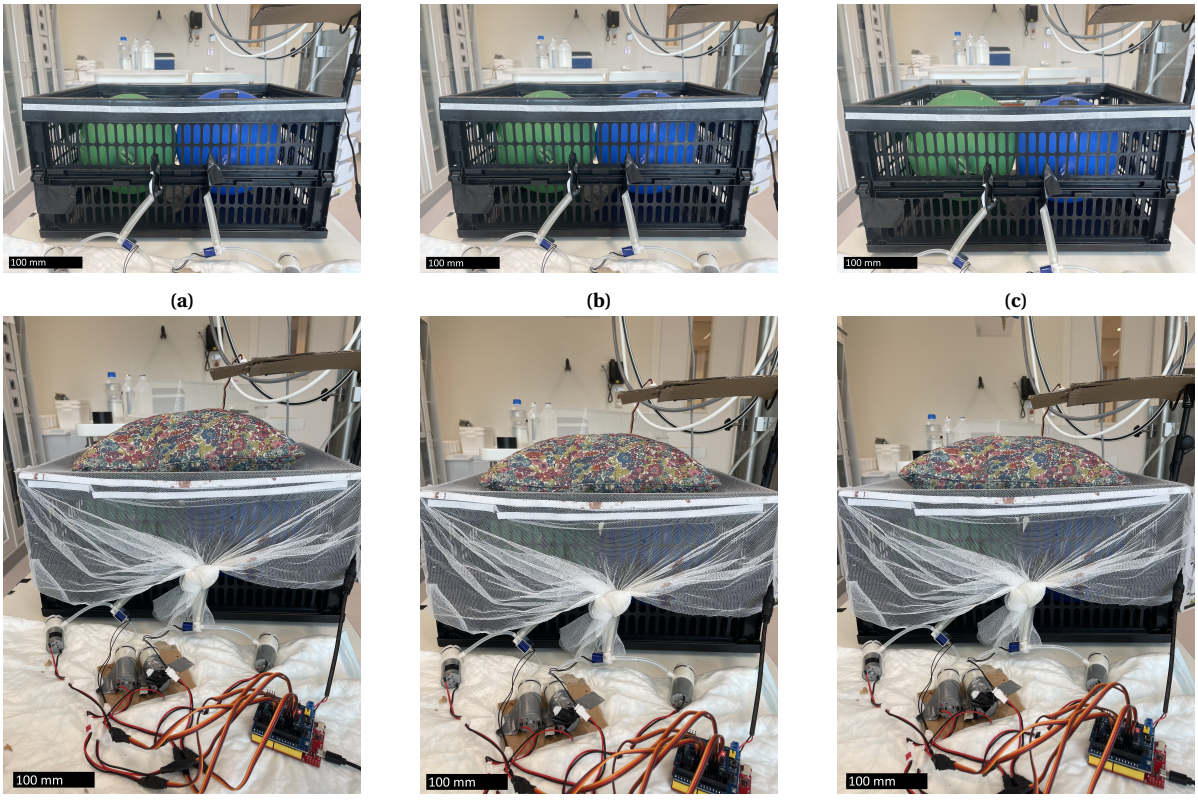


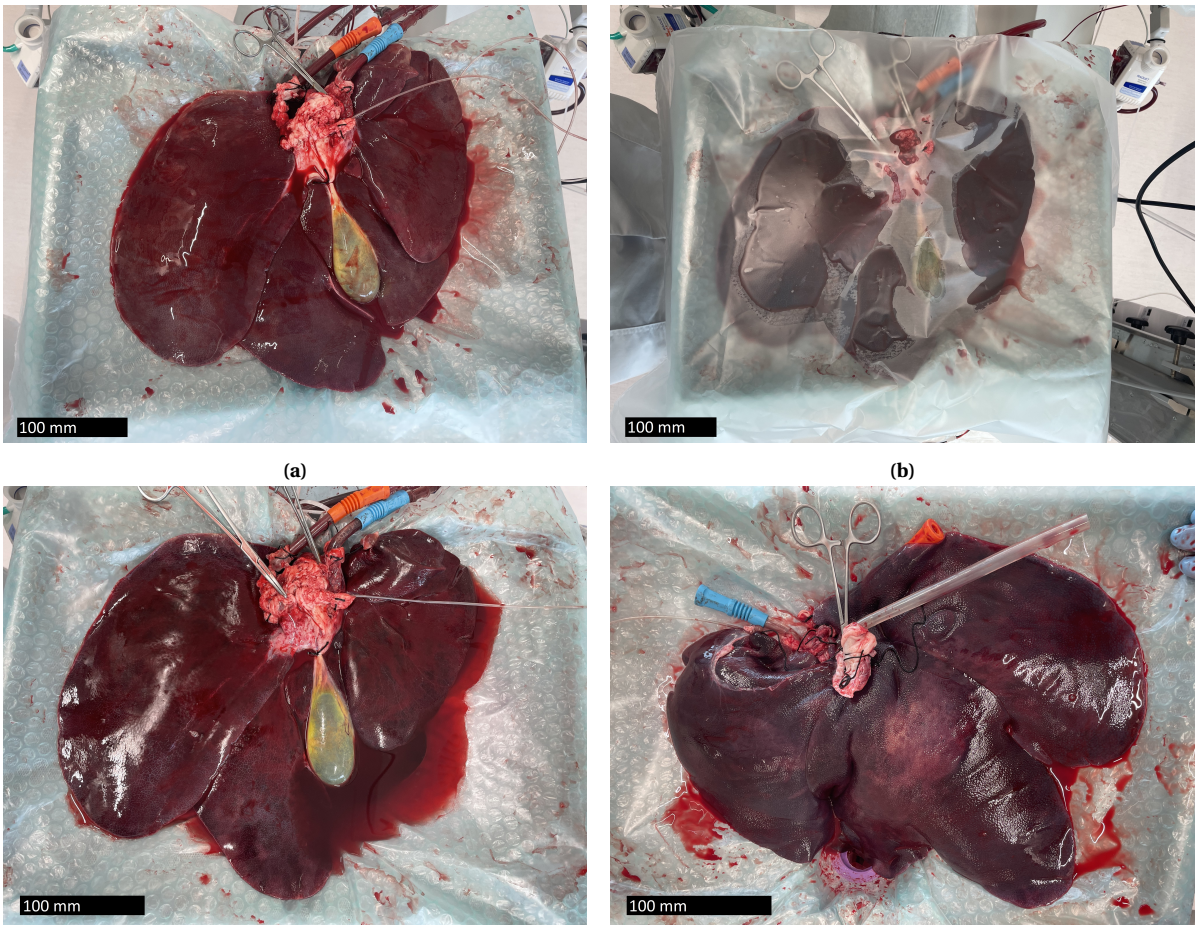
Figure 3.2: The alternating movement mode of the balloons without and with a liver model. **(a,d)** Balloon 1 at its minimum volume and balloon 2 at its maximum volume. **(b,e)** Balloons at equal volume. **(c, f)** Balloon 1 at its maximum volume and balloon 2 at its minimal volume. Scale bars 100 mm.

3.1.2. Redesigned Liver Reservoir During Perfusion

To validate the individual components of the liver reservoir and their integration with the Liver Assist device, HMP (n = 3) and NMP (n = 1) experiments were performed.

The first HMP perfusion experiment was performed with a liver previously subjected to 22 hours of NMP during which biopsies were taken and which was terminated due to loss of function. Despite establishing PV and HA flow, no fluid flow out of the cannulated and non-cannulated IVC was observed. Subsequently, a second HMP perfusion experiment was performed using a healthy liver. During this experiment, IVC flow was established through the cannula. However, fluid leaking from the liver was noted, particularly around cuts in the liver. A third HMP experiment revealed that different movement modes, rhythms, and ranges did not influence the HA and PV flow. Throughout all HMP experiments, the adequacy of liver support by the net, mat, and balloons, as well as the absence of leaks in the components, were continuously assessed and iteratively adjusted. The findings of these HMP experiments were incorporated into the setup before the NMP validation experiment was performed.

The validation NMP experiment demonstrated stable hemodynamics. The liver positioned within the liver reservoir was observed to have ample space, was supported by the net, mat, and balloons, and movement of the liver was induced by the moving balloons (Figure 3.3a). Moreover, the plastic cover helped to maintain moisture (Figure 3.3b). However, a recurring observation was that some fluid leaking from the liver was not effectively drained from the liver reservoir to the perfusate reservoir (Figure 3.3c). Additionally, after 2 hours of perfusion, a non-perfused area underneath the liver was observed (Figure 3.3d).



(a) **(b)** **(c)** **(d)**

Figure 3.3: The liver during the NMP validation experiment under the established movement condition. **(a)** The liver was placed on the mat of the liver reservoir. **(b)** The liver was covered to reduce heat loss and condensation of the perfusate. **(c)** Leakage of perfusate from the liver during the experiment. **(d)** The bottom of the liver after 2 hours of NMP. Scale bars 100 mm.

3.2. Porcine Liver NMP Experiments

Five 6-hour NMP experiments were conducted utilizing the validated liver reservoir with the established movement condition, involving alternative inflation and deflation of two balloons with both inflation and deflation lasting 8 seconds. One experiment was terminated within one hour of NMP due to severe liver injury obtained prior to NMP and extensive leakage of perfusate from the liver (Appendix E.5 Figure E7). The results of the remaining four experiments, labeled as Liver 1, Liver 2, Liver 3, and Liver 4, are presented below.

3.2.1. Liver Procurement and Perfusion Performance

The slaughterhouse procured livers had a mean warm ischemic time (WIT) of 15.3 (± 4.1) min and a mean CIT of 255.5 (± 25.7) min. The mean weight of the liver before the start of NMP was 2498 (± 87.4) g. The mean weight of the liver after NMP was 2814 (± 49.9) (Table 3.1). Under the movement condition, all livers gained weight during NMP with a mean weight gain of 12.8 (± 4.2) %, which is in line with control data (8.9 ± 11.0 %). The duration of Experiment 1 was 6 hours, the duration of Experiments 2 and 3 was 5 hours, and the duration of Experiment 4 was 7 hours.

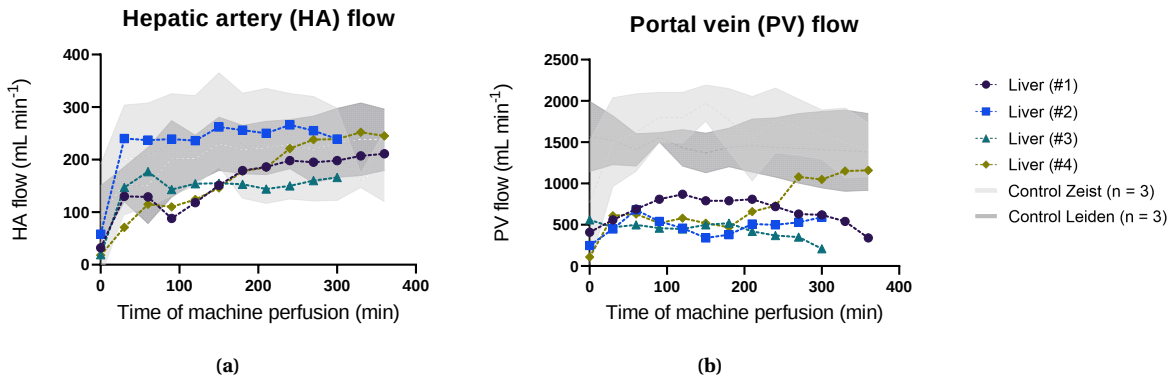
Table 3.1: The warm and cold ischemic time (WIT and CIT), duration of NMP, and liver weight before and after the NMP experiments performed under the established movement condition.

	Liver 1	Liver 2	Liver 3	Liver 4
Warm ischemic time (WIT)	15 min	16 min	10 min	20 min
Cold ischemic time (CIT)	233 min	292 min	244 min	253 min
Duration of NMP	6 h	5 h	5 h	7h*
Weight before NMP	2513 g	2418 g	2614 g	2445 g
Weight after NMP	2818 g	2753 g	2811 g	2875 g
Weight gain over 6 h	12.14 %	13.85 %	7.54 %	17.58 %

*At 6 hours the IVC cannula was removed

The perfusate volume, temperature, and hemodynamics were monitored during NMP to assess the overall performance of the NMP experiments performed under the movement condition (Figure 3.4 and Appendix E.2 Figure E2). The total perfusate volume used was 2.2 L, 3.2 L, 3 L, and 2.6 L (2.8 ± 0.4 L), during Experiments 1, 2, 3, and 4, respectively. The total perfusate volume used during the NMP experiments under the movement condition was larger than the perfusate volume used under the static condition, which was 2 L. During Experiments 2 and 3, more perfusate volume was added towards the end of NMP, because the perfusate volume in the perfusate reservoir ran low. Due to the same reason, these experiments were prematurely terminated at t = 300 min. The mean HA flow over the whole duration of NMP under the movement condition was 176.6 (± 52.2) mL min^{-1}. The mean HA flow during the control experiments performed in Zeist and Leiden were 206.7 (± 46.0) and 202.3 (± 43.2) mL min^{-1}, respectively. The mean HA flow of the NMP experiments under the movement condition was not significantly different from both the control experiments performed in Zeist ($p = 0.13$) and Leiden ($p = 0.18$). The mean PV flow over the whole duration of NMP under the movement condition was 597.7 (± 119.6) mL min^{-1}. Compared to the mean PV flow during the control experiments performed in Zeist and Leiden, 1593 (± 293.5) and 1447 (± 64.7) mL min^{-1}, respectively, the mean PV flow during the experiments under the movement condition was lower. The mean PV flow of the NMP experiments under the movement condition was significantly different from both the control experiments performed in Zeist ($p = <0.0001$) and Leiden ($p = <0.0001$).

During Experiments 2 and 3, the HA flow was stable over time, at t = 60 min the HA flows were 237 and 177 mL min^{-1}, respectively, and at t = 300 min the HA flows were 239 and 166 mL min^{-1}, respectively. During Experiments 1 and 4 the HA flow increased over time, at t = 60 min the HA flows were 129 and 115 mL min^{-1}, respectively, and at t = 300 min the HA flows were 198 and 239 mL min^{-1}, respectively. During Experiment 1 the PV flow increased from 690 mL min^{-1} at t = 60 min to 870 mL min^{-1} at t = 120 min, and decreased to 620 mL min^{-1} at t = 300 min. During Experiment 2 the PV flow decreased from 680 mL min^{-1} at t = 60 min to 340 mL min^{-1} at t = 150 min, and increased to 590 mL min^{-1} at t = 300 min. During Experiment 3 the PV flow continuously decreased, from 500 mL min^{-1} at t = 60 min to 210 mL min^{-1} at t = 300 min. During Experiment 4 the PV continuously increased, from 630 mL min^{-1} at t = 60 min to 1050 mL min^{-1} at t = 300 min.



(a) **(b)**

Figure 3.4: (a) Hepatic artery (HA) and **(b)** portal vein (PV) flow during NMP under the established movement condition. Each of the four NMP experiments under the movement condition is depicted individually. The data from the control NMP experiments performed in Zeist (n = 3) and Leiden (n = 3) are presented as the means of the three experiments, accompanied by their respective standard deviations.

3.2.2. General Liver Viability and Functionality

Blood and bile samples were taken during NMP to assess the general viability and functionality of the liver. Blood gas analysis was performed during NMP and values were compared to physiological human and porcine arterial blood gas analysis reference values (Appendix D Table D1). Most measurements were used to evaluate the overall performance of the experiments and identify the need for any interventions, and were not primarily analyzed to investigate the effect of liver movement (Appendix E.3 Figure E4, E3, and E5).

The glucose concentration was initially low at t = 0 min (3.9 ± 0.6 mmol L^{-1}) followed by a peak at t = 60 min (34.5 ± 8.8 mmol L^{-1}) during all experiments under the movement condition (Figure 3.5a). This was also observed during both the control experiments performed in Zeist and Leiden, with at t = 0 min mean glucose concentrations of 4.0 (± 0.2) and 4.1 (± 0.7) mmol L^{-1}, respectively, and at t = 60 min mean glucose concentrations of 30.3 (± 14.8) and 33.9 (± 8.6) mmol L^{-1}, respectively. Note that values higher than 38.9 mmol L^{-1} could not be measured. In Experiments 2 and 4, the glucose concentration started to decrease after 180 minutes of NMP, similar to the trends observed in the control groups. In Experiments 1 and 3, the glucose concentration started to decrease after 240 minutes of NMP. Experiment 4 showed a less pronounced initial glucose peak at t = 60 min (21.4 versus 38.9 (± 0.0) mmol L^{-1}), which decreased more slowly compared to the other experiments under the movement condition. Overall, the glucose concentration decreased towards the end of NMP to a mean glucose concentration of 20.7 (± 5.7) mmol L^{-1} at t = 300 min for the experiments under the movement condition (Appendix E.3 Figure 3.5a). During the control experiments performed in Zeist and Leiden the mean glucose concentrations at t = 300 min were lower, 13.5 (± 9.4) and 12.1 (± 8.4) mmol L^{-1}, respectively. No significant difference in mean glucose concentration was observed between the NMP experiments under the movement condition and the control experiments performed in Zeist and Leiden at all measured time points. Exact *p* values are provided in Appendix F Table F1 and F2.

In Experiment 1, the lactate concentration in the perfusate increased from 5.7 mmol L^{-1} at t = 0 min to 7.4 mmol L^{-1} at t = 120 min, after which it decreased to 6.5 mmol L^{-1} at t = 300 min (Figure 3.5b). In Experiment 2, the lactate concentration increased from 8.3 mmol L^{-1} at t = 0 min to 12.2 mmol L^{-1} at t = 180 min, after which it stayed stable until the end of NMP, at which a concentration of 11.8 mmol L^{-1} was measured. Experiment 3 showed a continuous decrease in lactate concentration, from 8.0 mmol L^{-1} at t = 0 min to 6.1 mmol L^{-1} at t = 300 min. In Experiment 4, the lactate concentration decreased rapidly from 5.2 mmol L^{-1} at t = 0 min to 1.2 mmol L^{-1} at t = 60 min after which the lactate concentration stayed low, at t = 300 min a concentration of 1.0 mmol L^{-1} was measured. During both the control experiments performed in Zeist and Leiden a similar trend as observed during Experiment 4 was observed. At t = 0 min, the mean lactate concentrations of the experiments under the movement condition, control experiments performed in Zeist, and control experiments performed in Leiden were 6.8 (± 1.6), 5.6 (± 2.9), and 6.4 (± 2.8) mmol L^{-1}, respectively. And at t = 300 min, 6.4 (± 4.4), 2.4 (± 2.0), and 1.9 (± 1.0) mmol L^{-1}, respectively. No significant difference in mean lactate concentration was observed between the NMP experiments performed under the movement condition and the control experiments performed in Zeist and Leiden at all measured time points. Exact *p* values are provided in Appendix F Table F1 and F2.

The bilirubin concentration in the perfusate was low and constant during Experiments 1 and 3, for both

experiments at both t = 60 min and t = 300 min a bilirubin concentration lower than 8.6 μmol L^{-1} was measured (Figure 3.5c). Note that values below 8.6 μmol L^{-1} could not be measured. In Experiment 2, the bilirubin concentration at t = 60 min was 8.6 μmol L^{-1} and increased to a concentration of 17.1 μmol L^{-1} at t = 240 min, after which the concentration decreased to 13.6 μmol L^{-1} at t = 300 min. For Experiment 4, the bilirubin concentration in the perfusate was not measured. The mean bilirubin concentration of the NMP experiments under the movement condition at t = 60 min and t = 300 min were 8.5 (± 0) and 10.2 (± 2.9) μmol L^{-1}, respectively. The mean bilirubin concentration of the control experiments performed in Zeist at t = 60 min and t = 300 min were 10.2 (± 2.9) and 12.9 (± 5.5) μmol L^{-1}, respectively. The mean bilirubin concentration of the control experiments performed in Leiden at t = 60 min and t = 360 min (t = 300 min was not measured) were 8.6 (± 0) and 10.7 (± 3.0) μmol L^{-1}, respectively. No significant difference in mean bilirubin concentration was observed between the NMP experiments under the movement condition and the control experiments performed in Zeist and Leiden at all measured time points. Exact p values are provided in Appendix F Table F1 and F2. For the control experiments performed in Leiden, no test could be performed at t = 180 and t = 300 min because control data at these time points did not exist, and at t = 60 and t = 120 because the data was identical.

During all experiments, sodium bicarbonate administration was necessary to keep the perfusate pH in the physiological range (7.35-7.45) (Figure 3.5d and Appendix E.3 Table E1).

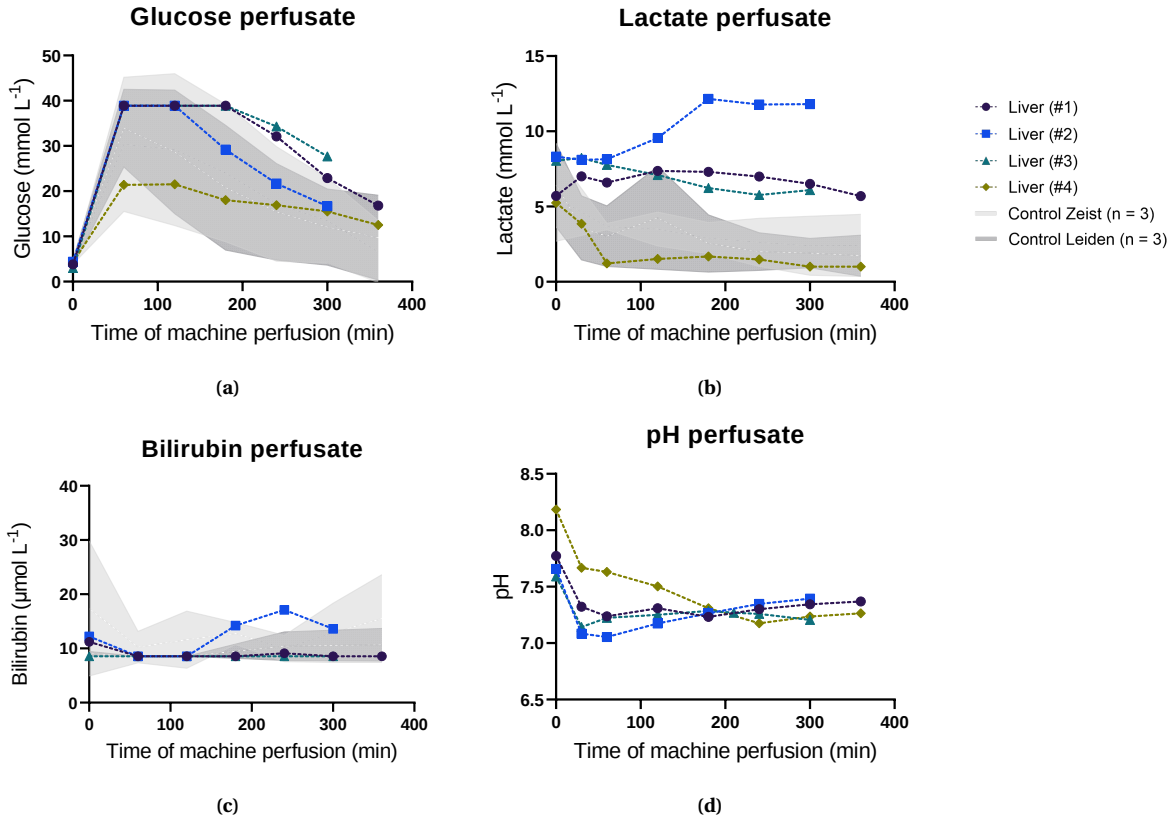
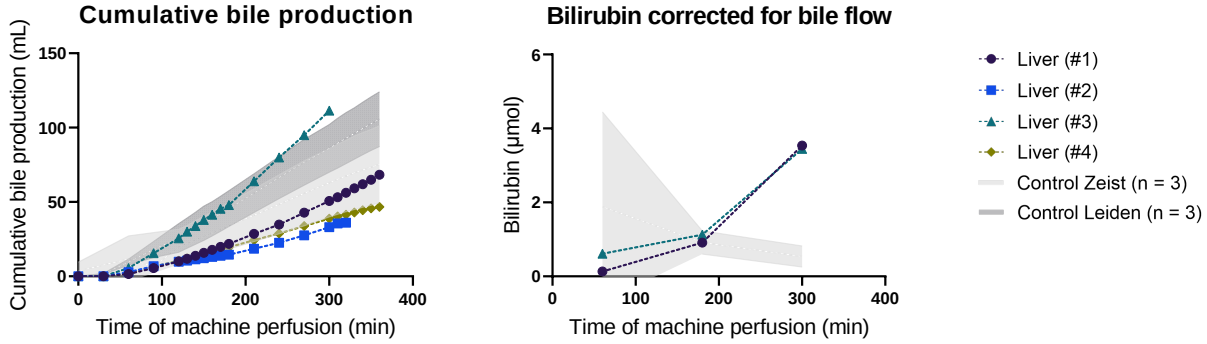


Figure 3.5: General liver viability and functionality markers measured during NMP under the established movement condition. **(a)** Glucose, **(b)** lactate, and **(c)** bilirubin perfusate concentrations. **(d)** pH of the perfusate. Each of the four NMP experiments under the movement condition is depicted individually. For liver 4, the bilirubin concentration in the perfusate was not measured. The data from the control NMP experiments performed in Zeist (n = 3) and Leiden (n = 3) are presented as the means of the three experiments, accompanied by their respective standard deviations.

The cumulative bile production at t = 300 min was 50.7, 33.1, 111.5, and 38.8 mL for Experiments 1, 2, 3, and 4, respectively (Figure 3.6a). The mean cumulative bile production for the experiments under the movement condition, control experiments performed in Zeist, and control experiments performed in Leiden was 58.5 (± 36.1), 62.9 (± 23.1), and 86.0 (± 27.9), respectively. No significant difference in mean cumulative bile production at t = 300 was observed between the experiments under the movement condition and the control experiments performed in Zeist (p = 0.86) and Leiden (p = 0.28).

The bilirubin concentration in the bile corrected for the corresponding hourly bile production, shows an upward trend throughout the duration of NMP for both Experiments 1 and 3, from t = 60 min (0.4 ± 0.3 μmol) to t = 300 min (3.5 ± 0.06 μmol) (Figure 3.6b and Appendix E.4 Figure E6). While for the control experiments performed in Zeist the bilirubin concentration in the bile decreases throughout the duration of NMP, from t = 60 min (1.9 ± 2.6 μmol) to t = 300 min (0.5 ± 0.3 μmol). No significant difference in mean bilirubin concentration in the bile was observed between experiments under the movement condition and the control experiments performed in Zeist at t = 60 min (p = 0.49) and t = 180 min (p = 0.70), while a significant difference at a 0.05 level was observed at t = 180 min (p = 0.0009). Bilirubin concentration was not measured in the bile for the control experiments performed in Leiden, and Experiments 2 and 4.



(a) **(b)**

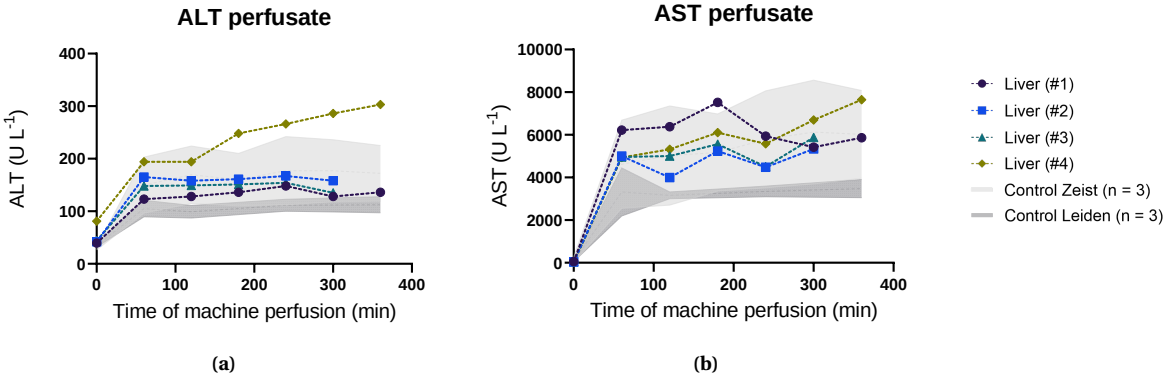
Figure 3.6: **(a)** Cumulative bile production and **(b)** bilirubin concentration in the bile corrected for mL bile produced per hour under the established movement condition. Each of the four NMP experiments under the movement condition is depicted individually. The data from the control NMP experiments performed in Zeist (n = 3) and Leiden (n = 3) are presented as the means of the three experiments, accompanied by their respective standard deviations. Bilirubin in the bile was only measured for Experiments 1 and 3, and control NMP experiments performed in Zeist.

3.2.3. Liver Injury

The concentrations of ALT and AST in the perfusate were measured every hour to assess liver injury (Figure 3.7a and 3.7b). During the experiments under the movement condition the mean ALT concentration increased from t = 0 min (51.6 ± 19.7 U L^{-1}) until t = 60 min (157.5 ± 29.8 U L^{-1}) after which it slightly increased towards t = 300 min (176.8 ± 74.0 U L^{-1}). For Experiments 1,2 and 3, the concentration stayed constant from t = 60 min (145.3 ± 21.1 U L^{-1}) until t = 300 min (140.3 ± 15.7 U L^{-1}), while for Experiment 4, the concentration increased from t = 60 min (194 U L^{-1}) until t = 300 min (286 U L^{-1}). During the control experiments performed in Zeist, similar mean ALT concentrations were observed at t = 0 min (29.6 ± 2.0 U L^{-1}), t = 60 min (149.7 ± 53.6 U L^{-1}), and t = 300 min (177.0 ± 59.1 U L^{-1}). No significant differences in mean ALT concentration were observed between the experiments under the movement condition and the control experiments performed in Zeist for all time points. Moreover, during the control experiments performed in Leiden the mean ALT concentrations, except for t = 0 min (34.9 ± 2.8 U L^{-1}), were lower at t = 60 (105.3 ± 15.7 U L^{-1}) and t = 360 min (112.6 ± 15.4 U L^{-1}) (only one data point available at t = 300) compared to the experiments under the movement condition, a significant difference at a 0.05 level was observed at t = 60 and 120 min. Test results could not be obtained for the control experiments performed in Leiden at t = 180 and t = 300 min due to the lack of available data. Exact p values are provided in Appendix F Table F1 and F2.

Similarly, for all experiments under the movement condition, the AST concentration increased form t = 0 min (43.4 ± 12.6 U L^{-1}) until t = 60 min (5280 ± 627.2 U L^{-1}). At t = 60 min, Experiment 1 showed a higher AST concentration (6220 U L^{-1}) compared to Experiments 2, 3, and 4 (4967 ± 30.6 U L^{-1}). After t = 60 min, the AST concentration remained more or less constant for Experiments 1, 2, and 3, from 5393 (± 716.2) U L^{-1} at t = 60 min to 5547 (± 291.4) U L^{-1} at t = 300 min, while in Experiment 4, the AST concentration slightly increased during the entire NMP experiment, from 4940 U L^{-1} at t = 60 min to 5880 U L^{-1} at t = 300 min. The mean AST concentrations during the experiments performed in Zeist at t = 0, t = 60, and t = 300 min were 148.9 (± 140.1) U L^{-1}, 4620 (± 2070) U L^{-1}, and 6127 (± 2438) U L^{-1}, respectively. No significant differences in mean AST concentration were observed between the experiments under the movement condition and the control experiments performed in Zeist for all time points. During the control experiments performed in Leiden,

except for t = 0 min (83.9 ± 27.9 U L^{-1}), lower AST concentrations were measured at t = 60 (3320 ± 1123 U L^{-1}) and t = 360 min (3480 ± 423.3 U L^{-1}) (only one data point available at t = 300), compared to the experiments under the movement condition, significant differences at a 0.05 level were observed at all time points. Test results could not be obtained for the control experiments performed in Leiden at t = 180 and t = 300 min due to the lack of available data. Exact *p* values are provided in Appendix F Table F1 and F2.



(a) **(b)**

Figure 3.7: Liver injury markers measured during NMP under the established movement condition. **(a)** Alanine transaminase (ALT) and **(b)** aspartate transaminase (AST) perfusate concentrations. Each of the four NMP experiments under the movement condition is depicted individually. The data from the control NMP experiments performed in Zeist (n = 3) and Leiden (n = 3) are presented as the means of the three experiments, accompanied by their respective standard deviations.

3.2.4. Clearance Capacity

To assess the clearance capacity of the liver, ICG was administered at t = 120 min and t = 300 min during NMP. The ICG level in the perfusate was measured over a period of 60 minutes after dosing and presented as % ICG, where the highest relative fluorescent unit (RFU) was set to 100 %, and the other RFU measurements were expressed as percentage change with respect to the highest value (Figure 3.8a and 3.8b). The biliary excretion of ICG was measured and expressed in RFU (Figure 3.8c and 3.8d). Additionally, the perfusate disappearance rate (PDR_{ICG}), indicating the rate at which ICG is cleared from the perfusate, and the percentage of total ICG cleared from the perfusate after 60 minutes were calculated for each experiment.

As control data for ICG administration at t = 120 minutes was unavailable, the graphs depicting ICG perfusate clearance and bile excretion for both t = 120 and t = 300 minutes administration feature the control data from t = 360 minutes and t = 300 minutes administration of experiments performed in Zeist and Leiden, respectively.

Analyzing the results of the t = 120 min administration of ICG, it was observed that ICG appeared in the perfusate 1 to 2 minutes after dosing during the experiments under the movement condition (Figure 3.8a). Subsequently, the ICG levels gradually decreased for Experiments 1, 2, 3, and 4, with half-lives of 4.9, 2.8, 1.6, and 5.3 minutes, respectively (Figure 3.8a). Correspondingly, the PDR_{ICG} values were 14.1, 25.0, 44.2, and 13.1% per minute (24.1 ± 14.5 % per minute). At the end of the 60-minute measurement period, a constant ICG level was reached, representing 85.0, 84.3, 95.7, and 88.2 % of the total ICG that appeared in the perfusate being cleared from the perfusate (88.3 ± 5.2 %). The control experiments performed in Zeist showed a mean PDR_{ICG} of 11.0 (± 3.3) % per minute, with 93.9 (± 5.8) % of ICG cleared from the perfusate after 60 minutes. The control experiments performed in Leiden displayed a mean PDR_{ICG} of 21.9 (± 13.8) % per minute, with 95.2 (± 1.3) % ICG cleared from the perfusate after 60 minutes. No significant difference in mean PDR_{ICG} and % of ICG cleared from the perfusate after 60 minutes was observed between the experiments under the movement condition and the control experiments performed in Zeist (p = 0.19 and p = 0.24, respectively) and Leiden (p = 0.85 and p = 0.08, respectively). Regarding biliary excretion, ICG was detected in the bile 10 minutes after administration for all experiments under the movement condition (Figure 3.8c). Furthermore, the total level of ICG appearing in the bile was higher for Experiments 1, 3, and 4 (7309 ± 289.0 RFU) compared to Experiment 2 (3438 RFU). The total level of ICG appearing in the bile for the control experiments performed in Zeist and Leiden was 3169 (± 3733) and 6363 (± 203.9) RFU, respectively.

For the t = 300 min administration, results were only obtained during Experiments 1 and 4, as the other two experiments were terminated at t = 300 min. As shown in Figure 3.8b, the ICG level was highest 1 minute

after administration, after which it gradually decreased, with half-lives of 1.8 and 3.1 minutes for Experiments 1 and 4, respectively, reaching a constant level. The corresponding PDR_{ICG} values were 39.0 and 22.4 % per minute (30.7 ± 11.7 % per minute), and the % of ICG cleared from the perfusate after 60 minutes were 91.4 % and 84.7% (88.0 ± 4.7 %). While the PDR_{ICG} was higher and the % of ICG cleared from the perfusate was lower compared to the control experiments performed in Zeist and Leiden, no significant difference in mean PDR_{ICG} and % of ICG cleared from the perfusate after 60 minutes was observed between the experiments under the movement condition and the control experiments performed in Zeist (p = 0.06 and p = 0.33, respectively) and Leiden (p = 0.52 and p = 0.07, respectively). Regarding biliary excretion, the ICG level in bile for Experiment 1 slightly increased from t = 0 (6733 RFU) to t = 60 min (7752 RFU), while for Experiment 4, the ICG level remained more or less constant after dosing (Figure 3.8d). While during both the control experiments performed in Zeist and Leiden a clear increase in ICG level in the bile was observed.

Finally, comparing the t = 120 min and t = 300 min administration of ICG for Experiments 1 and 4, both the PDR_{ICG} and % of ICG cleared from the perfusate after 60 minutes were higher at t = 300 min (30.7 ± 11.7 % per minute and 88.1 ± 4.7 %, respectively) than at t = 120 min (13.6 ± 0.7 % per minute and 86.6 ± 2.2 %, respectively). However, no significant difference in the mean PDR_{ICG} (p = 0.18) and % of ICG cleared from the perfusate after 60 minutes (p = 0.73) was observed between the t = 120 min and t = 300 min administration under the movement condition.

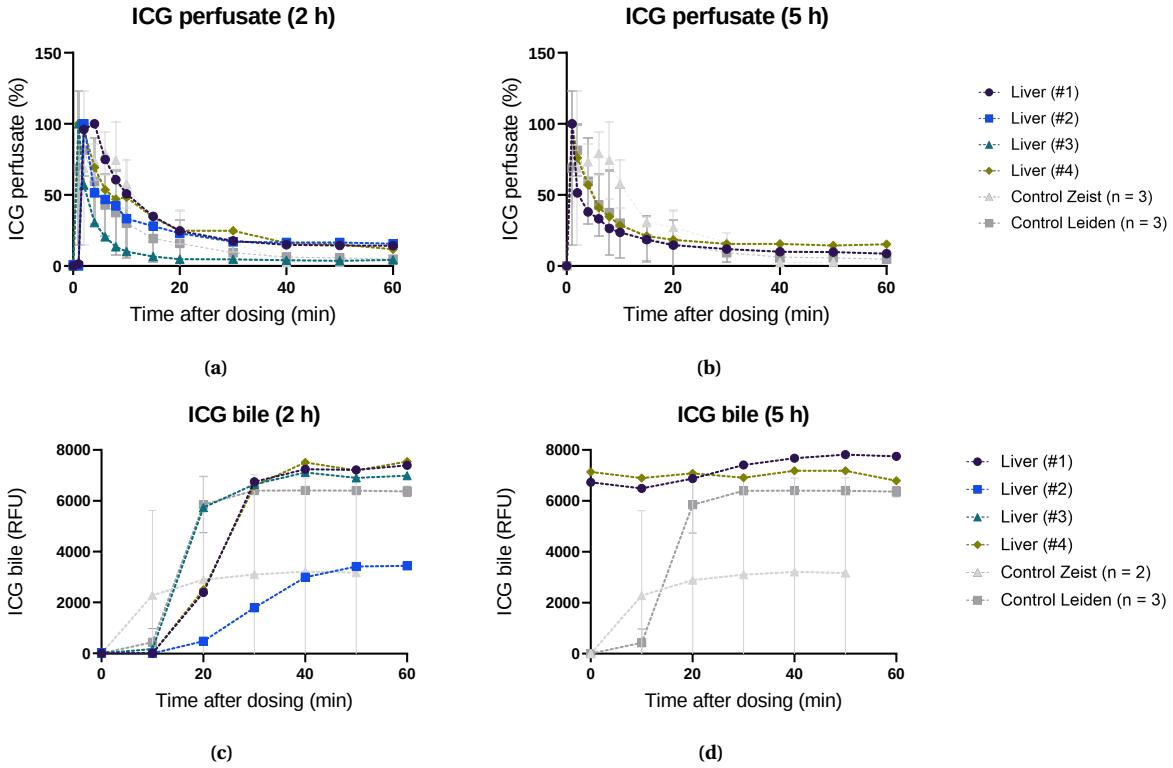


Figure 3.8: ICG measured in the perfusate and bile for 60 minutes after administration of ICG during NMP under the established movement condition. ICG was dosed at 120 minutes (Experiments 1, 2, 3, and 4) and at 300 minutes (Experiments 1 and 4) during the experiments with liver movement. For the perfusate, the ICG data is presented as % ICG and for bile the ICG data is presented in RFU. % ICG in the perfusate after dosage at **(a)** t = 120 min and **(b)** 300 min. ICG in the bile after dosage at **(c)** t = 120 min and **(d)** t = 300 min. Each of the four NMP experiments under the movement condition is depicted individually. The data from the control NMP experiments performed in Zeist (n = 3) and Leiden (n = 3) are presented as the means of the three experiments, accompanied by their respective standard deviations. In all graphs control data of ICG administration at t = 360 and t = 300 min, for Zeist and Leiden, respectively, is presented. For Zeist, ICG in the bile was only measured during 2 experiments.

3.2.5. Tissue Integrity

The tissue integrity of the livers was evaluated through the examination of both the macroscopic and microscopic appearance of the liver.

3.2.5.1. Macroscopic Appearance

Throughout the NMP experiments, images were captured of the liver's top and bottom before, during, and after the experiments. These images are accessible in Appendix E.5 Figure E8, E9, E10, and E12. To assess the effect of liver movement on tissue integrity, the bottom of the livers at the end of the NMP experiments are depicted in Figure 3.9. Figure 3.9a displays the bottom of Liver 1 after 360 minutes of NMP, revealing a non-perfused region in the central area, corresponding to lobes 2 and 3. Subsequently, adjustments were implemented in the net configuration, and the spacing between the balloons was reduced to provide better support to this specific region during NMP (Appendix C.1 Figure E1). Figure 3.9b and Figure 3.9c display the bottom of Livers 2 and 3 after NMP experiments of 300 minutes. Both livers exhibited a more homogeneous brown-reddish-purple color. As for the bottom of Liver 4, after 420 minutes of NMP, patchy liver tissue was observed (Figure 3.9d). Additionally, Figure 3.9e displays the bottom of one of the control experiments performed in Leiden after 360 minutes of NMP. A magnified view of the bottom of lobe 2 can be observed in Figure 3.9f. The liver exhibits a patchy brown-reddish color with non-perfused regions where the imprint of the Liver Assist reservoir net can be observed. During the other control experiments, pictures of the liver were not taken.

During Experiment 1, it was observed that the liver still felt supple and showed no signs of congestion at t = 240 and 300 min. During Experiments 2, 3, and 4, it was noted that the liver became enlarged and sturdier towards the end of NMP.

3.2.5.2. Histological Analysis

In Figure 3.10, examples of observations done during the histological analysis are displayed, and in Appendix E.6 Table E2 liver section specific observations and scores are displayed. After 300 to 420 minutes of NMP under the established movement condition, preserved tissue architecture could be observed (Figure 3.10a). After 300 minutes of NMP, Experiments 2 and 3, only minimal or mild (multi)focal single cell necrosis associated with mild hemorrhages (Experiment 2, Figure 3.10b), or hepatocellular hypertrophy and hepatocellular vacuolation (Experiment 3, Figure 3.10c) was observed. After 360 minutes of NMP, Experiment 1 and 4, only minimal focal single cell necrosis and mild hypertrophy was observed (Figure 3.10d). for Experiment 4, the single cell necrosis was associated with minimal hemorrhages and hepatocellular vacuolation. After 420 minutes, Experiment 4, mild multifocal single cell necrosis associated with mild hemorrhages, mild hypertrophy, and mild multifocal vacuolation was observed.

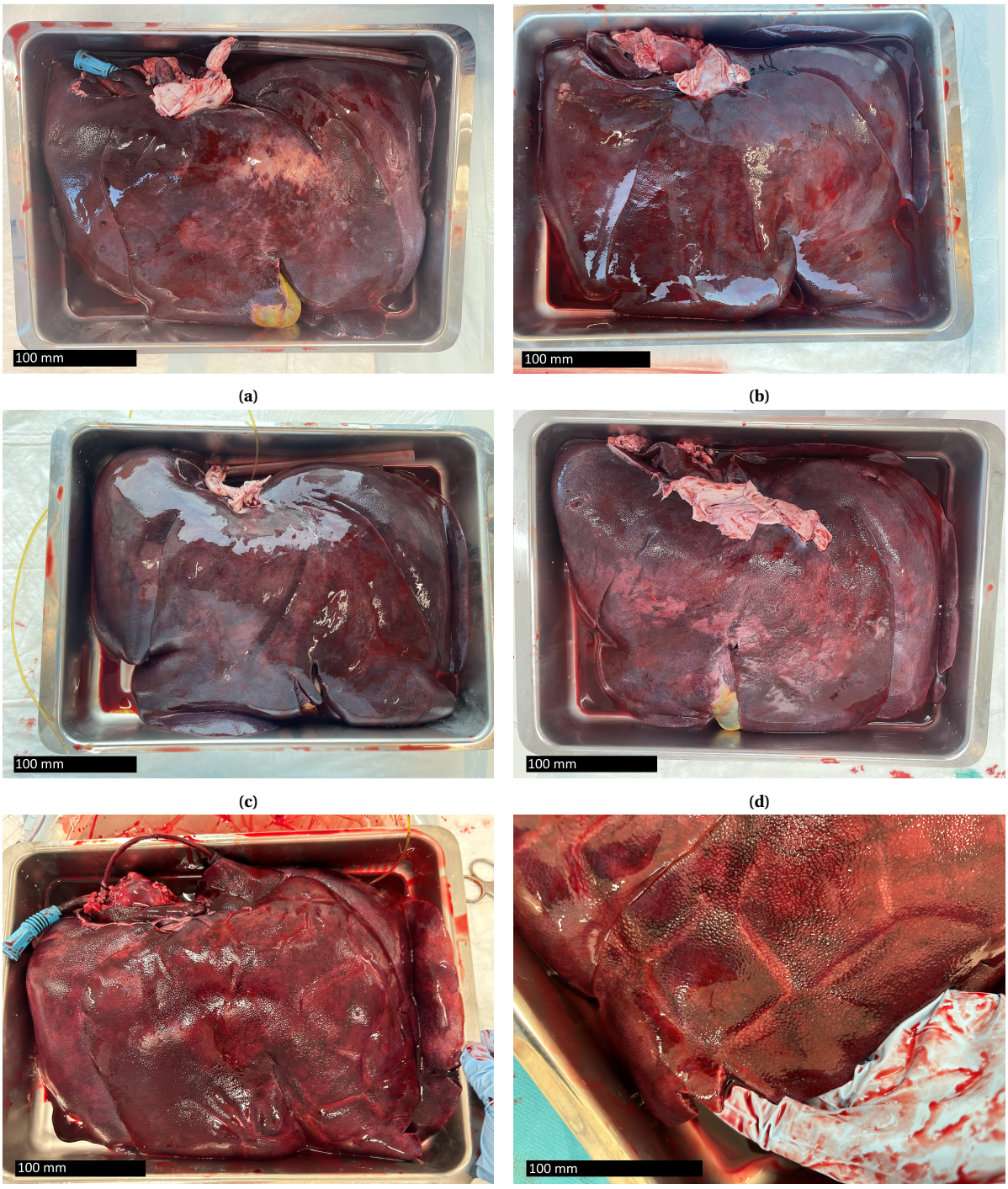


Figure 3.9: The macroscopic appearance of the bottom of the liver after 5-6 hours of NMP. Pictures taken of the bottom of the liver after **(a)** 6 hours (Experiment 1), **(b)** and **(c)** 5 hours (Experiments 2 and 3), and **(d)** 7 hours (Experiment 4) of NMP under the established movement condition. And pictures taken of the liver after NMP on the static reservoir of the Liver Assist device after 6 hours, **(e)** the bottom of the liver and **(f)** a magnified picture of the bottom of lobe 2. Scale bars 100 mm.

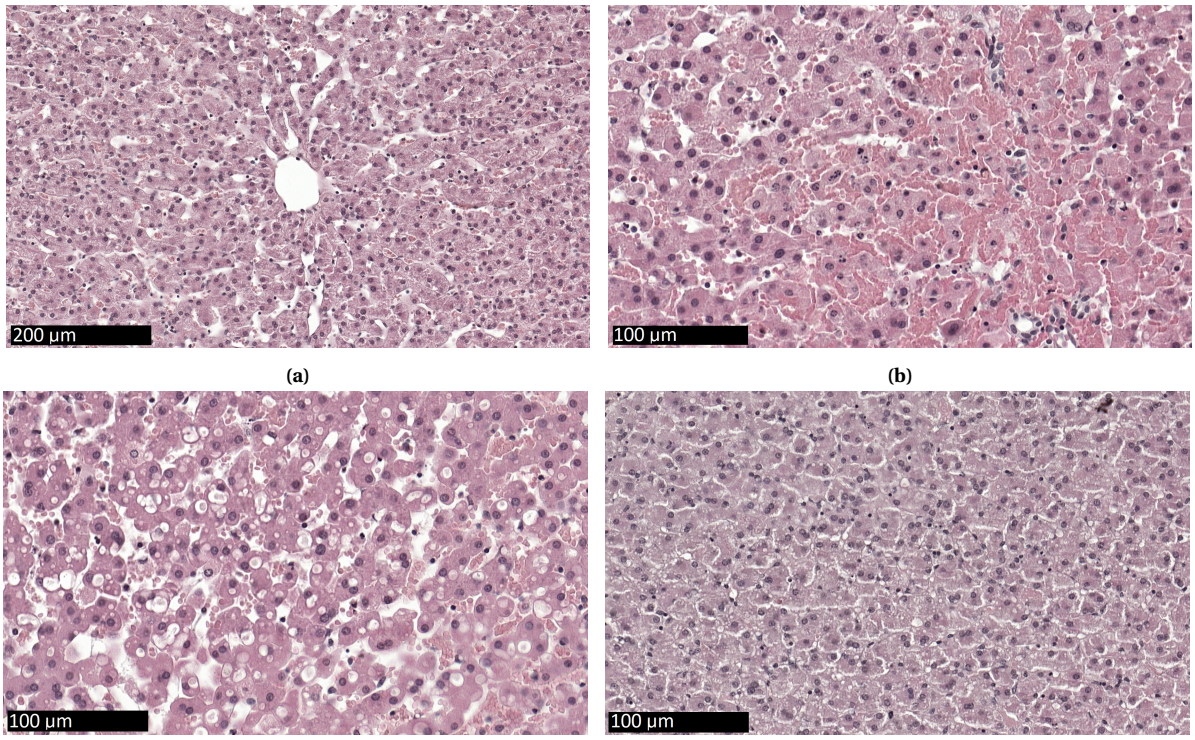


Figure 3.10: Histological analysis of liver biopsies taken during and after NMP under the established movement condition. Microscopic images of H&E stained liver provide insights into various cellular changes within the liver structure. Examples of observed phenomena: **(a)** A central vein with surrounding cord structure (Liver 1 at t = 360 min). **(b)** Single cell necrosis associated with hemorrhages (red blood cell infiltration)(Liver 2 at t = 300 min). **(c)** Hepatocellular vacuolation (Liver 3 at t = 300 min). **(d)** Hepatocellular hypertrophy, characterized by pale, swollen, and round hepatocytes and loss of cord structure (Liver 4 at t = 360 min). **(a)** Scale bar 200 μm (200x magnification), **(b-d)** scale bars 100 μm (400x magnification).

4

Discussion

The aim of this thesis was to incorporate liver movement during porcine liver NMP and assess the effect of liver movement on liver function and tissue integrity. The first phase of this thesis project focused on establishing a method to simulate liver movement, incorporating this movement into the liver reservoir, and integrating the liver reservoir with the Liver Assist device, a commercial NMP device. Following the assembly and integration, the setup underwent testing and iterative adjustments through a series of validation perfusion experiments. The aim was to ensure the stability and operational efficacy of the setup throughout the course of the porcine liver NMP experiments. The subsequent phase involved the execution of 6-hour porcine liver NMP experiments. These experiments aimed to assess the impact of liver movement on both liver function and tissue integrity. The results of both phases are discussed separately below.

4.1. Establishment of a Liver Reservoir Including Liver Movement

The first aim of this thesis was to incorporate liver movement in the liver reservoir during porcine liver NMP. To achieve this, movement was simulated through the utilization of air pumps and valves connected to an Arduino microcontroller, allowing controlled inflation and deflation of two balloons. The adoption of Arduino aimed to offer a cost-effective, adjustable, and reproducible approach to simulate movement. However, due to constraints in the pumps' maximum pressure capacity (55 kPa, with a approximate flow rate of 2.5 liters per minute (LPM)), precise control of both the rhythm and range of movement presented challenges in attaining a movement pattern closely resembling physiological liver motion. Attempts to replicate the physiological rhythm led to a minimal range of movement, whereas attempting to replicate the physiological range led to a slow rhythm of movement. Additionally, the Arduino microcontroller was powered by a 5 V wall adapter, which may not have been the most optimal method for supplying power to all individual electronic components of the electronic system.

Ultimately, an alternating mode of movement with an intermediate rhythm and range of movement (8 seconds in, 8 seconds out) was chosen for the NMP experiments. This mode encompassed both tilting and massaging motion, hypothesized to enhance perfusate flow and distribution across the liver compared to the simultaneous mode. Furthermore, by alternatively inflating and deflating multiple balloons, the system would act as a sort of anti-decubitus cushion, by alternatively changing the contact area between the balloons and the liver [71]. Unfortunately, due to resource limitations, a comprehensive comparison between simultaneous and alternating modes, as well as slower and faster rhythms of movement, was unfeasible during the NMP experiments. Therefore, the decision to select the alternating mode was founded on intuitive judgment and observations made during the assembly and validation of the setup. Previous studies used imaging and modeling techniques to estimate *in vivo* liver motion induced by respiration, which reported a rhythm of 15–20 breaths per minute and a range of 10–26 mm in cranio-caudal direction [61–63]. In this study, the movement simulated by a single balloon deviated from this motion in terms of the rhythm (4 inflation-deflation cycles per minute) and range (6 mm), due to the system's limitations described above, and this deviation was further pronounced by choosing the alternating balloon movement. Moreover, the choice of flexible latex balloons could have introduced a reduction in range of movement due to the weight of the liver, suggesting that sturdier, thicker latex might mitigate this influence. Despite these deviations from near-physiological liver movement, it was hypothesized that liver movement, irrespective if the rhythm and range of movement, dur-

ing NMP, would ensure homogeneous distribution of the perfusate throughout the whole liver and mitigate pressure induced tissue necrosis.

One requirement for the movement simulation was to ensure automatic and stable motion, over a minimum duration of 6 hours, to facilitate 6-hour NMP experiments. The validation experiments revealed disparities in balloon inflation and deflation volumes when driven by individual pumps, indicating discrepancies in pump performance. Adjustments in inflation and deflation durations, in the range of a few hundred milliseconds, were implemented to maintain consistent total balloon volumes over time. However, changing pump behaviors over time necessitated ongoing intervention to sustain the desired movement pattern, making the movement simulation less automatic. Consequently, the movement simulation system required supervision, precluding the execution of long-term perfusion experiments.

Therefore, for future advancements in systems simulating liver movement during perfusion, the establishment of automatic and stable motion over extended durations is essential. This becomes particularly crucial for conducting extended perfusion experiments lasting more than 24 hours. One approach to enhance the durability and reliability of the movement simulation system is to focus on optimizing the electronic system and to invest in high-quality components. While this study adopted a cost-effective approach, the utilization of medical-grade pumps, ventilation machines, or similar apparatus, previously used in other studies, could provide more physiological and stable liver movement [36, 67].

The incorporation of liver movement during NMP necessitated a comprehensive redesign of the liver reservoir. Given the pilot nature of this study, the aim was to employ readily available, affordable materials and components, and design flexibility to accommodate adjustments based on observations done during the validation experiments.

Observations indicated that the redesigned liver reservoir offered a stable environment for the liver. Moreover, this reservoir, in combination with the Liver Assist device, facilitated stable hemodynamics during both validation HMP and NMP experiments. During both the HMP and NMP experiments, fluid was leaking from the biopsies or incomplete ligation of the side branches of the hepatic artery. Some fluid in the liver reservoir is seen as beneficial and could provide the liver with a more soft and moist environment, but excessive fluid could interfere with the simulated liver movement [26, 30, 32, 58, 65, 72, 73]. To prevent excessive leakage during the actual NMP experiments, ways to prevent leakage and potentially drain the liver reservoir of excess fluid were considered. Three potential solutions were considered to prevent excessive fluid in the liver reservoir: using a pressure-driven pump to pump fluid back to the perfusate reservoir, applying a load to the drain to allow easier flow out of the reservoir, or creating channels in the mat to guide fluid to the drain or perfusate reservoir. However, each solution introduced potential risks or challenges, and because the amount and location of fluid leaking from the liver varied between the livers, the decision was made to assess the situation during the actual NMP experiments and, if necessary, manually pump fluid leaking from the liver back to the perfusate reservoir. Additionally, modifications were made to improve liver support, including adjusting the net configuration and balloon placement to address the non-perfused area observed underneath the liver (Appendix C.1 Figure C2). Overall, the setup was tested for its functionality and water tightness, ensuring the stability of hemodynamics during the NMP experiments. Modifications and adjustments were made as necessary to address potential issues and improve the performance of the setup.

For future development of the liver reservoir, several considerations deserve attention. First, material selection should prioritize biocompatibility with liver tissue and blood. Second, contemplating the reutilization of system components, along with their material attributes, and the feasibility of sterilizing materials within a laboratory environment, could contribute to the enhanced sustainability and cost-efficiency of the system. Third, exploring digital design and 3D printing of components could enable a more tailored liver reservoir, reducing the need for adhesives, sealants, and tapes, thereby diminishing potential leakage risks associated with component attachments.

4.2. Porcine Liver NMP Experiments

The second aim of this thesis was to study the effect of liver movement on liver function, specifically clearance capacity, and tissue integrity. The 5-to 7-hour porcine liver NMP experiments provided valuable insights, discussed here in relation to the general performance of the perfusion experiment, liver viability and functionality, liver injury, clearance capacity, and tissue integrity.

4.2.1. General Performance of Perfusion

Throughout all the experiments under the movement condition, a noticeable reduction in perfusate volume within the perfusate reservoir was observed over time. Notably, the experiments performed under the established movement condition required a larger perfusate volume (2.8 ± 0.4 L) compared to the control experiments performed in Zeist and Leiden (2 L). Despite reducing the volume of the perfusate reservoir following Experiment 1, Experiments 2 and 3 had to be prematurely terminated. This was due to the continued depletion of the perfusate volume in the perfusate reservoir, which resulted in the introduction of air into the system. As a consequence, the PV flow was diminished, preventing the liver from receiving an adequate supply of oxygen and maintaining a normothermic temperature. Despite attempts to address this issue, such as introducing blood from another pig (Experiment 2) or supplementing the perfusate with additional saline (Experiment 3), both solutions were deemed undesirable due to their influence on measurements and physiological perturbation.

During all NMP experiments under the movement condition, some accumulation of perfusate in the liver reservoir was observed, however since this perfusate leakage was manually pumped back from the liver reservoir to the perfusate reservoir, this was ruled out as the reason for the perfusate loss. Furthermore, studies use liver weight gain as indicator for edema formation, which could also be the reason the perfusate volume reduced over time [32, 47, 55, 72, 74]. However, for all experiments the weight gain was in the same range and the mean weight gain was not significantly different from the mean weight gain observed during the control experiments, therefore this was also ruled out as a reason the perfusate volume reduced over time. Because the livers became quite sturdy and big during NMP, it was hypothesized that because the liver lobes have more space in the new liver reservoir and lays on a non-perforated surface, more perfusate is distributed throughout the whole liver compared to livers placed in the net-like structure of the Liver Assist device. Additionally, the challenge of accurately measuring the final perfusate volume after the experiment due to sampling, continuous and bolus injections, ICG administration, as well as the distribution of perfusate throughout the whole liver and tubing system, posed an obstacle in fully assessing this parameter. It is important to highlight that the reduction in perfusate volume posed a limiting factor in the duration of two of the experiments, prompting the need for further investigation as the root cause of this issue remained unclear.

Furthermore, during all experiments under the movement condition, approximately a 60 % lower mean PV flow was observed throughout the whole experiment compared to both control groups (597.7 (± 119.6) mL min^{-1} versus 1593 (± 293.5) and 1447 (± 64.7) mL min^{-1}, for Zeist and Leiden, respectively). Eshmuminov *et al.* [36] measured the physiological porcine HA and PV flow and reported them to be 250 (± 70) mL min^{-1} and 1000 (± 210) mL min^{-1}, respectively. The PV flow during the control experiments is more in line with the physiological PV flow compared to the PV flow measured during the experiments under the movement condition. However, the HA and PV flow reported by different NMP studies vary a lot ranging from 95 to 654 mL min^{-1} and 310−1600 mL min^{-1}, respectively [18]. Lower flow rates do not inherently indicate negative outcomes; NMP studies, both with and without IVC cannulation, have also documented pressures and flow rates within ranges comparable to observed in this study [25, 48, 52, 75, 76].

During Experiment 4, some hypotheses were tested that were thought to be the cause of the lower PV flows and larger necessary perfusate volume. Considering that one of the primary modifications introduced, apart from liver movement and the new liver reservoir, was the IVC cannulation in contrast to the control experiments, it was hypothesized that IVC cannulation might impede the outflow of perfusate from the liver, causing accumulation of perfusate in the liver and subsequently reduction of the PV flow. However, upon removal of the cannula from the IVC, there was a slight decrease in PV flow and the perfusate volume in the perfusate reservoir also decreased. This suggests that the IVC cannulation was not responsible for the observed reduction in PV flow and loss of perfusate volume. The study by Gilbo *et al.* [77], argues that cannulation of the IVC is crucial to prevent obstruction and ensure stable hemodynamics. Furthermore, when they used a venous multiperforated tip cannula the outflow was impaired and they observed an increase in PV resistance, a decrease in PV flow, and a compensatory increase in HA flow. It appeared that the precise positioning of the cannula was important to overcome these problems. Furthermore, the study by Eshmuminov *et al.* [36] even controlled the pressure in the IVC such that it was close to physiological levels (0−2mmHg), to prevent inadequate flow, congestion, and hepatocellular injury. On the other hand Nassar *et al.* [32] argues that an open IVC with a pressure of 2−3 mmHg, is crucial in preventing edema. Hence, when employing the setup developed in this thesis for future research, greater attention should be given to the IVC cannulation process. Additionally, it was noted that minor adjustments in the orientation of the HA and PV cannulas, as well as the process of taking biopsies, had a significant impact on the PV flow. The height of the liver reservoir with respect to the pressure transducers and the distance between the liver reservoir and the Liver Assist device

were also found to influence flow to a certain degree. Lastly, in Experiment 1, an accidental over-inflation of one of the balloons led to a decrease in PV flow. It was theorized that this occurred due to the compression of the liver tissue and vasculature, or potentially due to a change in the height of the PV cannula, to which the PV pressure sensor is attached, with respect to the pressure transducers. However, when this scenario was replicated at the end of Experiment 4, there was no observed change in PV flow. Additionally, even after fully deflating the balloons underneath the liver, there was no subsequent alteration in PV flow. As a result, it was determined that the movement itself and the balloons were unlikely to be the cause of the decreased PV flow. During the experiments, it was also observed that changes in the PV flow cause the perfusate volume in the perfusate reservoir to change. For example, during Experiment 1 at some instances the PV flow increased, coinciding with a reduction in perfusate volume in the perfusate reservoir. Furthermore, at the instance that the PV flow increased, when biopsies were taken during Experiment 2, the perfusate volume in the perfusate reservoir decreased, which could have been attributed to the higher PV flow or more leakage of perfusate in the liver reservoir. Despite a thorough examination and various tested hypotheses, the exact underlying reason for the notable reduction in PV flow and loss of perfusate volume remained elusive.

4.2.2. General Liver Viability and Functionality

The ability of the human liver to metabolize glucose is a widely accepted marker for liver viability [22, 78]. The glucose kinetics observed in all experiments aligns with the glucose metabolism pattern during NMP described in existing literature [78]. During static cold storage (SCS), glycogenolysis is activated, leading to the breakdown of glycogen into glucose upon reperfusion with warm oxygenated blood, resulting in a peak in perfusate glucose levels [79]. Elevated glucose levels stimulate gluconeogenesis, during which hepatocytes take up glucose and convert it into pyruvate and ATP or store it as glycogen [78]. Throughout all experiments, this initial peak and a consistent decline in perfusate glucose concentration was observed, indicating liver metabolic function [18, 30, 66, 80, 81]. During Experiments 1 and 3, the glucose metabolism seemed to be slower compared to the control experiments, and during Experiment 4, the overall glucose level was lower. However, the mean glucose concentration observed throughout the NMP experiments under the movement condition was not significantly different from both static control groups. Additionally, the ability of the human liver to clear lactate from the blood is an established marker of aerobic metabolic activity [22, 78]. In Experiments 1, 3, and 4, the lactate concentration in the perfusate decreased, whereas during Experiment 2, the lactate concentration increased, implying that Liver 2 had difficulty clearing lactate. Although lactate clearance is used as a marker for viability testing of human livers, for porcine livers variable lactate kinetics are reported, from steep declines to constant values, to steep inclines over the duration of perfusion, and contradictory conclusions are drawn based on these observations [28, 56, 64, 66, 82]. Effective bilirubin clearance from the perfusate and its subsequent excretion into the bile are crucial indicators of hepatocellular functionality in porcine liver studies [38, 48, 66, 82]. This phenomenon was observed in Experiments 1, 3, and 4, indicating good liver functionality. In contrast, during Experiment 2, the perfusate bilirubin level increased slightly during perfusion after which it decreased again.

Continuous bile production during NMP serves as a reliable marker of excretory hepatocellular function, as it requires the intact functionality of hepatocytes and cholangiocytes [25–27, 55, 57, 58, 74, 82, 83]. A decline in bile production over the course of perfusion can be indicative of hepatic injury or substrate deficiency [25, 30, 57, 58, 82]. Notably, bile production was consistently observed in all experiments throughout the whole duration of NMP, indicating their functional excretory capacity.

Liver 2 exhibited a diminished ability to clear both lactate and bilirubin, and, compared to the other experiments reduced bile production, pointing to potential hepatocyte damage [66].

4.2.3. Liver Injury

ALT and AST, the markers for hepatocellular injury, are released by the liver when hepatocellular damage occurs and are therefore indicative of liver damage during NMP [26, 29–31, 36, 38, 48, 49, 55, 58, 64–66, 74, 83]. Often, at the onset of perfusion, ALT and AST levels rise because transaminases released during liver procurement, cold preservation, and subsequent reperfusion are washed out of the liver [22]. After this initial rise, the levels should stabilize or even decline, indicating the liver's healing process [31, 55, 78]. A steep rise in transaminase levels during the whole NMP experiments indicates severe injury [78]. Throughout the experiments under the movement condition and the control experiments under the static condition, an elevation in ALT and AST was observed within the first 60 minutes of NMP. This rise could stem from hepatocyte injury induced upon liver procurement, cold preservation, and subsequent reperfusion. At t = 60 min, the ALT and AST levels during the experiments under the liver movement condition tended to be slightly higher compared

to the control experiments. This could be attributed to the lower PV flows observed during the experiments under the movement condition, resulting in a prolonged warm-up time of the liver and consequently increased ischemia- reperfusion injury. Beyond 60 minutes, the ALT and AST levels remained relatively stable during Experiments 1, 2, and 3, as well as in the control experiments. This suggests the absence of substantial hepatocellular injury during the course of these experiments. The mean ALT and AST levels during the experiments under the movement condition were consistent with observations in Zeist, although they significantly differed from those in Leiden at multiple time points. During Experiment 4, however, a continuous increase in ALT and AST was evident, indicating ongoing injury during perfusion. In this experiment, due to an accidental error, the gas mixer was set to 40 % O_2 at a rate of 2.5 L min^{-1}, which was corrected to a rate of 1.5 L/min after 172 minutes of perfusion. Excessive oxygen supply, known as hyperoxia, has been linked to hepatocellular reperfusion injury and could elucidate the ALT and AST elevation observed during Experiment 4 [43, 84]. Furthermore, this could also elucidate the discrepancy between the two control groups, where the sole difference was the oxygen supply. Under the movement condition, the mean ALT and AST concentrations at t = 300 were 176.8 (± 74.0) and 5835 (± 623.8) U L^{-1}, respectively. Several studies reported that ALT has a lower activity in the porcine liver and was therefore relatively insensitive to liver cell injury, which would explain the lower ALT level compared to the observed AST level [38, 48, 66, 74]. In a human liver transplantation study, it was shown that a human liver with ALT and AST levels of 5576 U L^{-1} and 4963 U L^{-1}, respectively, was successfully transplanted, while a liver with ALT and AST levels of 9490 U L^{-1} and 13349 U L^{-1}, respectively, suffered primary non-function [22]. Unfortunately, ALT and AST concentrations reported in porcine liver NMP studies vary a lot and the concentration of ALT and AST are influenced by liver weight and perfusate volume, which made it hard to compare the transaminase concentrations measured in this study with other studies [24, 25, 28–30, 32, 38, 48, 52, 78, 82, 85, 86].

4.2.4. The Effect of Liver Movement on Clearance Capacity

For healthy *in vivo* human livers, normal half-life values are typically in the range of 3−5 minutes and the PDR_{ICG} should be more than 18 %−24 % per minute [70]. The the half-lives and mean PDR_{ICG}, for the 2-hour administration during the experiments under the movement condition, as well as the 5-hour administration during the control experiments performed in Leiden, are consistent with these ranges. However, following the administration of ICG after 2 hours of NMP, Experiment 3 exhibited a higher PDR_{ICG} (44.2 % per minute) and a greater percentage of total ICG cleared from the perfusate (95.7 %) compared to Experiments 1, 2, and 4, both control experiments performed in Zeist and Leiden, and the *in vivo* human liver ICG clearance data. For the 6-hour ICG administration during the experiments performed in Zeist, the mean PDR_{ICG} appeared to be lower (11.0 ± 3.3 % per minute).

While not statistically significant, the mean PDR_{ICG} after the 5-hour ICG administration was relatively higher for Experiments 1 and 4 when compared to both control groups (30.6 ± 11.7 % per minute versus 11.0 ± 3.3 (Zeist) and 21.8 ± 13.8 (Leiden) % per minute). Interestingly, Experiments 1 and 4 demonstrated, albeit insignificantly, improved PDR_{ICG} following the 5-hour administration when compared to the 2-hour administration (30.6 ± 11.7 versus 13.6 ± 0.7 % per minute, respectively). One possible explanation for this improvement over time could be attributed to the almost doubled HA flow from t = 120 min (121.0 ± 4.2 mL min^{-1}) until t = 300 min (218.5 ± 29.0 mL min^{-1}), for both Experiments 1 and 4.

Studies indicate that ICG clearance is influenced not only by hepatocyte uptake and biliary excretion but also by blood flow and energy status [70, 87]. Research has shown that doubling the total blood flow rate during porcine liver NMP resulted in faster ICG clearance [83]. The ICG 15 ratio, which represents the ICG level at t = 15 min divided by the ICG level at t = 0 minutes, multiplied by 100, should ideally be below 10 % for healthy *in vivo* human livers. In one porcine liver NMP study, this ratio was found to be 18.9 ± 6 % for a liver perfused at a total blood flow rate of 1 mL/g liver/min (n = 8) and 7.2 ± 3 % for a liver perfused at a rate of 2 mL/g liver/min (n = 7) (25 % of flow admitted to the HA and 75 % of flow admitted to the PV, with average HA pressure of 100 mmHg and Pv pressure of 11 mmHg) [70, 83]. As substances from both the HA and PV are extracted equally by the liver, both the HA and PV flow should be taken into account when interpreting the ICG clearance from the perfusate [88]. Despite the significantly lower mean PV flow observed during the experiments under the movement condition, the ICG clearance capacity appeared to be consistent with the static control experiments performed in Leiden and occasionally even faster, while ICG clearance might be expected to be slower due to the approximately 60 % lower average PV flow. This promising ICG clearance behavior after 5 hours of perfusion aligns with the healthy *in vivo* human liver ICG clearance capacity and holds potential for studying drug pharmacokinetics.

Notably, after the 2-hour administration of ICG, Experiment 2 displayed reduced biliary excretion of ICG

compared to Experiments 1, 2, and 3 (3438 versus 7309 ± 289.0 (n = 3) RFU, respectively, 60 min after dosing), which could be an additional sign, besides its inability to clear lactate and bilirubin, that hepatocyte function was compromised. Nevertheless, the liver retained the capacity to metabolize glucose, produce bile, clear ICG from the perfusate, and ALT and AST levels indicate no major hepatocellular injury. Assessing the biliary ICG excretion following the 5-hour ICG administration during Experiments 1 and 4 revealed already elevated levels at t = 0 min. Laparoscopic cholecystectomy (LC) studies demonstrated that the bile duct was best visible 45 min to 24 hours after administration of varying doses of ICG, and therefore that ICG is present in the bile duct for extended periods of time [89, 90]. This could explain the elevated level of ICG observed in the bile 0 minutes after the 5-hour administration of ICG. This phenomenon did not occur in the control experiments, where ICG was administered only at 5 or 6 hours of NMP.

4.2.5. The Effect of Liver Movement on Tissue Integrity

After Experiment 1, a non-perfused area was observed at the bottom of the liver. Accordingly, the net configuration and the distance between the balloons was changed such that this area would receive more support. After Experiments 2 and 3, the livers exhibited a more homogeneous brown-reddish-purple color without non-perfused areas. After Experiment 4, it was observed that the liver tissue on the bottom of the liver had some patchy non-perfused areas. The alteration in net configuration following Experiment 1 could have eliminated non-perfused areas during Experiment 2 and 3. This change potentially improved liver support by the net and balloons, thus preventing the occurrence of non-perfused regions. Moreover, during Experiment 4, the self-adhesive velcro's adhesive property diminished after four experiments, causing the net to intermittently hang looser. This inconsistency was rectified with new self-adhesive velcro, but it might have caused the more patchy liver tissue observed after Experiment 4. It is also possible that slight differences in the duration of the NMP experiments played a role; Experiments 2 and 3 spanned 5 hours, while Experiments 1 and 4 extended to 6 and 7 hours, respectively. These variations in duration might have contributed to the emergence of non-perfused areas. On the contrary, when livers were placed on the static liver reservoir of the Liver Assist device, tissue compression occurred due to the limited space, resulting in non-perfused areas where the structural pattern of the net was imprinted onto the liver tissue.

Throughout the perfusion duration, the livers exhibited a noticeable increase in size and became more sturdy, likely because the perfusate was distributed throughout the whole liver. Even though a weight gain was observed during all experiments, this weight gain was in line with the control experiments. Furthermore, studies report weight gain to be related to the degree of edema formation, with a weight gain of 14−27 % indicating moderate edema formation and a weight gain of 34.3−81.7 % indicating severe edema formation [32, 47, 55, 72, 74]. The mean weight gain observed in this study was 12.78 (± 4.165) %, which does not indicate major edema formation. In contrast to livers within the net-like liver reservoir of the Liver Assist device, the placement of livers on a non-perforated surface allowed for more expansive positioning. This spatial freedom minimized overlapping lobes, hypothesized to facilitate better perfusate distribution through the liver.

The histological examination of HE-stained liver sections from Experiments 1, 2, 3, and 4 shows that the liver tissue remained intact after 300 to 420 minutes of NMP. Consequently, the motion of the balloons did not induce significant hepatocellular major during NMP.

Some challenges were encountered during biopsy collection. For instance, once biopsies were taken the PV flow increased and substantial perfusate was leaking from the liver. This raised concerns, as compromised vasculature could hinder even perfusate distribution throughout the liver. Moreover, biopsy-related leaks led to perfusate accumulation in the liver reservoir, necessitating manual intervention to pump the perfusate from the liver reservoir to the perfusate reservoir, which could be a limiting factor for long-term NMP experiments. Consequently, biopsies were not taken at t = 180 min in Experiments 3 and 4.

4.3. Current Status and Perspective

Current research into NMP, with the aim of extending the viability and functionality of the liver *ex vivo*, by enhancing the liver reservoir, is relatively limited. Several porcine liver NMP studies have customized their liver reservoirs, placing the liver on its diaphragmatic surface on a suspended net or fenestrated plastic surface that mimics the concave shape of the diaphragm (Appendix A, Table A1) [28, 47, 48, 53, 55, 56, 64]. However, it has been shown that liver viability and functionality often deteriorated after 3 to 6 hours of NMP within these setups, indicated by reduced bile production, weight gain, or tissue damage [47, 48, 53, 56, 64]. Other approaches involved placing the liver in a bag or submerging it freely in fluid, aiming to counterbalance gravity pressure with hydrostatic pressure [52, 58, 65, 72]. Following 9 hours of NMP in such a setup, the research

conducted by Terajima *et al.* [65] documented heterogeneous liver tissue, swollen livers, and patchy hemorrhages. The study published by Naruse *et al.* [52] compared a more physiological liver reservoir with a simple reservoir and a reservoir where the liver was suspended in a hot water bath during 3 hours of NMP. The livers in a simple and water bath reservoir appeared black–purple and dark red, respectively, and bile secretion ceased (2–3 mL h^{-1}) and decreased, respectively. The positive effect of the more physiological reservoir was observed by improved macroscopic and microscopic appearance, maintenance of bile production (≈ 5–10 mL h^{-1}), ammonia removal, BUN production, and lower AST levels compared to the simple and water bath reservoir. These findings were considered to be the result of good configuration of the liver, allowing expansion of the parenchyma and adequate blood supply to peripheral areas. They concluded that placing the liver in a reservoir that models the *in vivo* intra-abdominal arrangement with the IVC cannulated is essential for liver preservation. Certain studies have employed a pressure chamber to expand and compress the liver's vasculature, leading to improved blood flow through the liver [38]. However, another study suggested that even with intra-abdominal pressure simulation, the liver's position on a sling compressed by its weight could limit its viability and functionality [66]. Although early research in the field of NMP explored the influence of intra-abdominal pressure differences, this factor has not been adequately addressed in current studies and commercial machines. This raises the question of whether the technical challenges associated with this principle outweigh the beneficial perfusion results. Recent research by Eshmuminov *et al.* [36] mimics respiratory movement through the use of a balloon, which was inflated and deflated with the rhythm of breathing, underneath the liver. The study demonstrated excellent liver viability and functionality, homogeneous perfusion, and prevention of pressure necrosis compared to static liver reservoirs, based on the distribution of radioactive tracer throughout the liver, macroscopic appearance, and histological analysis. Specifically, simulating intra-abdominal pressure differences and respiratory movement proved to be beneficial compared to the more simple liver reservoirs, extending preservation duration to 24 hours and 7 days, respectively [36, 38]. However, it is challenging to determine the specific aspect of their setup that was beneficial and the precise effect that movement of the liver had on its viability and functionality, as the study by Eshmuminov *et al.* [36] also incorporated automatic control of glucose and pH levels, additional substances, and a dialysis filter. Furthermore, machine perfusion was performed at 34 ° C, which would could be regarded as subnormothermic machine perfusion (SNP) ([18]). Given the substantial differences in liver injury occurrence and metabolic activity between machine perfusion at subnormothermic and normothermic temperatures, there is a need for a more comprehensive exploration of the impact of liver movement under normothermic conditions [91, 92].

Therefore, this thesis involved the design of a novel liver reservoir incorporating liver movement during NMP, enabling the assessment of the effect of liver function and tissue integrity. Throughout the trajectory of this thesis project, several challenges, observations, and results have given rise to fundamental questions, recommendations, and future research directions. For future research most importantly long-term NMP experiments should be performed. Because the 6-hour NMP control experiments performed at TNO have generally yielded positive outcomes, any influence resulting from modifications to the liver reservoir and the incorporation of liver movement may not be immediately discernible within the context of short-term perfusion experiments. Prolonged NMP experiments are imperative to unveil subtle discrepancies and would enable a more thorough exploration of the effect of liver movement during NMP. To enable long-term NMP experiments, further enhancements in the liver reservoir design and movement simulation, and the elucidation of the statistically different perfusion parameters compared to the control experiments, as described above are prerequisites.

Due to the economic and temporal constraints associated with conducting supplementary NMP control experiments, historical data from prior porcine liver NMP studies utilizing the Liver Assist liver reservoir were used. While historical data provides some insight, conducting dedicated control experiments on the redesigned liver reservoir without balloon-induced movement could have elucidated the impact of liver movement better. Discrepancies between the movement and static liver reservoir designs, such as cannulation of the IVC, differences in support structures, and altered spatial configurations, could have inadvertently influenced the experimental outcomes. Furthermore, the lower PV flow and the larger necessary perfusate volume during the experiments under the movement condition compared to the control experiments and physiological values, could be attributed to the new liver reservoir. Employing control experiments with the redesigned liver reservoir, mirroring PV flow and perfusate volume from the experiments under the movement condition would have facilitated a more comprehensive evaluation of the effect of movement on for instance ICG clearance capacity. Additionally, no histological analysis was performed during the control experiments of t = 360 minutes. Therefore, control experiments devoid of movement, with synchronized biopsy collection around

the 300 to 420 minute mark, could have provided clearer insights into the effect of movement on liver tissue integrity.

The evaluation of the effect of the liver reservoir on liver viability and functionality remains challenging, as only a limited number of studies have addressed this aspect explicitly, and established assays for such assessments are not widely available. Additional assays could be performed during the prolonged NMP experiments to augment our understanding of the effect of liver movement and the liver reservoir. Eshmuminov *et al.* [36], utilizing positron emission tomography–computed tomography (PET-CT) with radioactive tracers, successfully visualized the perfusate distribution within the liver, providing insights into liver viability and metabolic activity. This visualization not only provides insights into viability and metabolic activity but also indicates the presence of pressure-induced necrosis. Furthermore, good metabolism and a uniform distribution of perfusate across the liver could serve as an indicator of vascular integrity, unburdened by compression, kinking, mechanical stress, or inadequate support [36]. Similarly, angiography, using X-ray with contrast medium administration, has been employed to study perfusate distribution within the hepatic vasculature, facilitating the examination of vascular occlusions or leaks [51, 55]. Additionally, the injection of casting material through the portal vein, followed by the assessment of the resulting corrosion cast, has been utilized to ascertain the homogeneity of perfusate distribution within the liver [38]. Moreover, the utilization of laser Doppler flowmetry combined with remission spectroscopy has enabled the assessment of liver microcirculation during NMP [57]. Integrating the aforementioned assays could provide valuable insights into the potential impact of the liver reservoir and balloon movement on the integrity of the perfusate distribution through the liver and liver's vascular and tissue integrity. To further explore the effect of liver movement during NMP and the relevance of liver movement in a preclinical model for predicting pharmacokinetics and dynamics, additional assays can be conducted. These assays may involve the administration of model drugs, wherein the uptake, metabolism, and biliary excretion of the administered drug are examined and subsequently compared with human *in vivo* pharmacokinetic data.

The observed inter-liver variability, which lacks a clear explanation, underscores the necessity for additional experiments to support the reliability of the findings. Discrepancies in viability and functionality across different livers may be attributed to multiple factors including the variation in liver donors, transportation, hemodynamics, and perfusate volumes. Given the multitude of variables influencing the NMP process, further experimentation is advised. Furthermore, once liver movement during extended NMP experiments is proved to be beneficial, a comprehensive assessment of alternating versus simultaneous movement patterns, slow versus rapid rhythms, and small versus large movement ranges can be undertaken during NMP experiments. However, it is acknowledged that the feasibility of investigating these aspects within the NMP research domain may be constrained by resource-intensive demands. The economic considerations attached to performing NMP experiments warrant that interventions are substantiated by discernible impacts prior to their execution.

5

Conclusion

The aim of this thesis was to incorporate liver movement during porcine liver NMP and assess the effect of liver movement on liver function and tissue integrity. This study represents an initial exploration into the sole effect of liver movement during NMP. A novel liver reservoir including liver movement was established. Additionally, the setup designed in this thesis provides an easy to control, adaptable, cost-efficient, and reproducible way to study the effect of liver movement during NMP. Although minimal improvements in general liver viability and functionality were observed compared to NMP under the static condition, we have shown that after 5-hours of NMP, the clearance capacity of the liver, although not significantly, improved, and the liver tissue was still intact without signs of major hepatocallular injury. These promising outcomes suggest the need for further investigations into the effect of liver movement during NMP, particularly during NMP experiments exceeding 24 hours. We postulate that incorporating liver movement will extend liver viability and functionality during prolonged NMP experiments. Further work is now required to refine the setup, particularly in automating the movement simulation, to facilitate the execution of long-term NMP experiments. In pursuit of achieving long-term clearance capacity and tissue integrity, thereby enabling NMP of whole porcine livers to be used as a preclinical model for predicting drug pharmacokinetics and dynamics. Furthermore, once proven to be beneficial, the principle of liver movement during NMP could be adopted in the clinical setting to achieve long-term NMP for human liver treatment, repair, and regeneration.

References

[1] Arulraj, R. and Neuberger, J., "Liver transplantation: Filling the gapbetween supply and demand," *Clinical medicine*, vol. 11, no. 2, p. 194, 2011.

[2] Lewis, A., Koukoura, A., Tsianos, G.-I., Gargavanis, A. A., Nielsen, A. A., and Vassiliadis, E., "Organ donation in the us and europe: The supply vs demand imbalance," *Transplantation Reviews*, vol. 35, no. 2, p. 100 585, 2021.

[3] Meulen, J. H. van der, Lewsey, J. D., Dawwas, M. F., Copley, L. P., *et al.*, "Adult orthotopic liver transplantation in the united kingdom and ireland between 1994 and 2005," *Transplantation*, vol. 84, no. 5, pp. 572–579, 2007.

[4] Lai, J. C., Feng, S., and Roberts, J. P., "An examination of liver offers to candidates on the liver transplant wait-list," *Gastroenterology*, vol. 143, no. 5, pp. 1261–1265, 2012.

[5] Wolfe, R. A., Roys, E., and Merion, R. M., "Trends in organ donation and transplantation in the united states, 1999-2008," *American Journal of Transplantation*, vol. 10, no. 4, pp. 961–972, 2010.

[6] Blood, N. H. S. and Transplant, "Transplant activity report 2017–2018,"

[7] Mikolasevic, I., Bozic, D., Pavić, T., Ruzic, A., Hauser, G., Radic, M., Radic-Kristo, D., Razov-Radas, M., Puljiz, Z., and Milic, S., "Liver disease in the era of covid-19: Is the worst yet to come?" *World Journal of Gastroenterology*, vol. 27, no. 36, p. 6039, 2021.

[8] Cheemerla, S. and Balakrishnan, M., "Global epidemiology of chronic liver disease," *Clinical liver disease*, vol. 17, no. 5, p. 365, 2021.

[9] Mihaylov, P., Mangus, R., Ekser, B., Cabrales, A., Timsina, L., Fridell, J., Lacerda, M., Ghabril, M., Nephew, L., Chalasani, N., *et al.*, "Expanding the donor pool with the use of extended criteria donation after circulatory death livers," *Liver Transplantation*, vol. 25, no. 8, pp. 1198–1208, 2019.

[10] Dasari, B. V., Schlegel, A., Mergental, H., and Perera, M. T. P., "The use of old donors in liver transplantation," *Best Practice & Research Clinical Gastroenterology*, vol. 31, no. 2, pp. 211–217, 2017.

[11] Zhu, Z. J., Zheng, H., Deng, Y. L., Sun, L. Y., Pan, C., Liu, Y. H., Song, H. L., Shen, Z. Y., *et al.*, "Effect of steatosis donor liver transplantation on hepatocellular carcinoma recurrence: Experience at a single institution.," *Hepato-gastroenterology*, vol. 59, no. 115, pp. 858–862, 2012.

[12] Zhang, Q.-Y., Zhang, Q.-F., and Zhang, D.-Z., "The impact of steatosis on the outcome of liver transplantation: A meta-analysis," *BioMed research international*, vol. 2019, 2019.

[13] Nemes, B., Gámán, G., Polak, W. G., Gelley, F., Hara, T., Ono, S., Baimakhanov, Z., Piros, L., and Eguchi, S., "Extended-criteria donors in liver transplantation part ii: Reviewing the impact of extended-criteria donors on the complications and outcomes of liver transplantation," *Expert review of gastroenterology & hepatology*, vol. 10, no. 7, pp. 841–859, 2016.

[14] Reddy, S., Zilvetti, M., Brockmann, J., McLaren, A., and Friend, P., "Liver transplantation from non–heart-beating donors: Current status and future prospects," *Liver Transplantation*, vol. 10, no. 10, pp. 1223–1232, 2004.

[15] Guarrera, J., Henry, S., Samstein, B., Reznik, E., Musat, C., Lukose, T., Ratner, L., Brown Jr, R., Kato, T., and Emond, J., "Hypothermic machine preservation facilitates successful transplantation of "orphan" extended criteria donor livers," *American Journal of Transplantation*, vol. 15, no. 1, pp. 161–169, 2015.

[16] Dutkowski, P., Schlegel, A., Oliveira, M. de, Müllhaupt, B., Neff, F., and Clavien, P.-A., "Hope for human liver grafts obtained from donors after cardiac death," *Journal of hepatology*, vol. 60, no. 4, pp. 765–772, 2014.

[17] Linares, I., Selzner, N., and Selzner, M., "Machine preservation of the liver: What is the future holding?" *Current Transplantation Reports*, vol. 5, pp. 82–92, 2018.

[18] Eshmuminov, D., Leoni, F., Schneider, M. A., Becker, D., Muller, X., Onder, C., Hefti, M., Schuler, M. J., Dutkowski, P., Graf, R., *et al.*, "Perfusion settings and additives in liver normothermic machine perfusion with red blood cells as oxygen carrier. a systematic review of human and porcine perfusion protocols," *Transplant International*, vol. 31, no. 9, pp. 956–969, 2018.

[19] Michelotto, J., Gassner, J. M., Moosburner, S., Muth, V., Patel, M. S., Selzner, M., Pratschke, J., Sauer, I. M., and Raschzok, N., "Ex vivo machine perfusion: Current applications and future directions in liver transplantation," *Langenbeck's archives of surgery*, vol. 406, pp. 39–54, 2021.

[20] Lascaris, B., Meijer, V. E. de, and Porte, R. J., "Normothermic liver machine perfusion as a dynamic platform for regenerative purposes. what does the future have in store for us?" *Journal of Hepatology*, 2022.

[21] Widmer, J., Eden, J., Carvalho, M. F., Dutkowski, P., and Schlegel, A., "Machine perfusion for extended criteria donor livers: What challenges remain?" *Journal of Clinical Medicine*, vol. 11, no. 17, p. 5218, 2022.

[22] Watson, C. J., Kosmoliaptsis, V., Pley, C., Randle, L., Fear, C., Crick, K., Gimson, A. E., Allison, M., Upponi, S., Brais, R., *et al.*, "Observations on the ex situ perfusion of livers for transplantation," *American journal of transplantation*, vol. 18, no. 8, pp. 2005–2020, 2018.

[23] Ceresa, C. D., Nasralla, D., Coussios, C. C., and Friend, P. J., "The case for normothermic machine perfusion in liver transplantation," *Liver Transplantation*, vol. 24, no. 2, pp. 269–275, 2018.

[24] Jamieson, R. W., Zilvetti, M., Roy, D., Hughes, D., Morovat, A., Coussios, C. C., and Friend, P. J., "Hepatic steatosis and normothermic perfusion-preliminary experiments in a porcine model," *Transplantation*, vol. 92, no. 3, pp. 289–295, 2011.

[25] Schön, M. R., Kollmar, O., Wolf, S., Schrem, H., Matthes, M., Akkoc, N., Schnoy, N. C., Neuhaus, P., *et al.*, "Liver transplantation after organ preservation with normothermic extracorporeal perfusion," *Annals of surgery*, vol. 233, no. 1, pp. 114–123, 2001.

[26] St. Peter, S. D., Imber, C. J., De Cenarruzabeitia, I. L., Mcguire, J., James, T., Taylor, R., and Friend, P. J., "β-galactosidase as a marker of ischemic injury and a mechanism for viability assessment in porcine liver transplantation," *Liver transplantation*, vol. 8, no. 1, pp. 21–26, 2002.

[27] Fondevila, C., Hessheimer, A. J., Maathuis, M.-H. J., Muñoz, J., Taurá, P., Calatayud, D., Leuvenink, H., Rimola, A., Ploeg, R. J., and Garcıa-Valdecasas, J. C., "Superior preservation of dcd livers with continuous normothermic perfusion," *Annals of surgery*, vol. 254, no. 6, pp. 1000–1007, 2011.

[28] Ghinolfi, D., Melandro, F., Patrono, D., Lai, Q., De Carlis, R., Camagni, S., Gambella, A., Ruberto, F., and De Simone, P., "A new ex-situ machine perfusion device. a preliminary evaluation using a model of donors after circulatory death pig livers," *Artificial Organs*, vol. 46, no. 12, pp. 2493–2499, 2022.

[29] Goldaracena, N., Echeverri, J., Spetzler, V. N., Kaths, J. M., Barbas, A. S., Louis, K. S., Adeyi, O. A., Grant, D. R., Selzner, N., and Selzner, M., "Anti-inflammatory signaling during ex vivo liver perfusion improves the preservation of pig liver grafts before transplantation," *Liver Transplantation*, vol. 22, no. 11, pp. 1573–1583, 2016.

[30] Imber, C. J. *et al.*, "Advantages of normothermic perfusion over cold storage in liver preservation," *Transplantation*, vol. 73, no. 5, pp. 701–9, 2002.

[31] Liu, Q. *et al.*, "Sanguineous normothermic machine perfusion improves hemodynamics and biliary epithelial regeneration in donation after cardiac death porcine livers," *Liver Transplantation*, vol. 20, no. 8, pp. 987–999, 2014.

[32] Nassar, A. *et al.*, "Ex vivo normothermic machine perfusion is safe, simple, and reliable: Results from a large animal model," *Surgical Innovation*, vol. 22, no. 1, pp. 61–69, 2015.

[33] Tingle, S. J., Thompson, E. R., Bates, L., Ibrahim, I. K., Govaere, O., Shuttleworth, V., Wang, L., Figueiredo, R., Palmer, J., Bury, Y., *et al.*, "Pharmacological testing of therapeutics using normothermic machine perfusion: A pilot study of 2, 4-dinitrophenol delivery to steatotic human livers," *Artificial Organs*, vol. 46, no. 11, pp. 2201–2214, 2022.

[34] Boteon, Y. L., Attard, J., Boteon, A. P., Wallace, L., Reynolds, G., Hubscher, S., Mirza, D. F., Mergental, H., Bhogal, R. H., and Afford, S. C., "Manipulation of lipid metabolism during normothermic machine perfusion: Effect of defatting therapies on donor liver functional recovery," *Liver Transplantation*, vol. 25, no. 7, pp. 1007–1022, 2019.

[35] Bellomo, R. *et al.*, "Extended normothermic extracorporeal perfusion of isolated human liver after warm ischaemia: A preliminary report," *Critical Care and Resuscitation*, vol. 16, no. 3, pp. 197–201, 2014.

[36] Eshmuminov, D. *et al.*, "An integrated perfusion machine preserves injured human livers for 1 week," *Nature Biotechnology*, vol. 38, no. 2, pp. 189–198, 2020.

[37] Nadalin, S., Testa, G., Malagó, M., Beste, M., Frilling, A., Schroeder, T., Jochum, C., Gerken, G., and Broelsch, C. E., "Volumetric and functional recovery of the liver after right hepatectomy for living donation," *Liver transplantation*, vol. 10, no. 8, pp. 1024–1029, 2004.

[38] Neuhaus, P. and Blumhardt, G., "Extracorporeal liver perfusion: Applications of an improved model for experimental studies of the liver," *International Journal of Artificial Organs*, vol. 16, no. 10, pp. 729–739, 1993.

[39] Lauschke, V. M., Hendriks, D. F., Bell, C. C., Andersson, T. B., and Ingelman-Sundberg, M., "Novel 3d culture systems for studies of human liver function and assessments of the hepatotoxicity of drugs and drug candidates," *Chemical research in toxicology*, vol. 29, no. 12, pp. 1936–1955, 2016.

[40] Deng, J., Wei, W., Chen, Z., Lin, B., Zhao, W., Luo, Y., and Zhang, X., "Engineered liver-on-a-chip platform to mimic liver functions and its biomedical applications: A review," *Micromachines*, vol. 10, no. 10, p. 676, 2019.

[41] Beckwitt, C. H., Clark, A. M., Wheeler, S., Taylor, D. L., Stolz, D. B., Griffith, L., and Wells, A., "Liver 'organ on a chip'," *Experimental cell research*, vol. 363, no. 1, pp. 15–25, 2018.

[42] Stevens, L. J., Zhu, A. Z. X., Chothe, P. P., Chowdhury, S. K., Donkers, J. M., Vaes, W. H. J., Knibbe, C. A. J., Alwayn, I. P. J., and Steeg, E. van de, "Evaluation of normothermic machine perfusion of porcine livers as a novel preclinical model to predict biliary clearance and transporter-mediated drug-drug interactions using statins," *Drug Metabolism and Disposition*, vol. 49, no. 9, pp. 780–789, 2021.

[43] Watson, C. J., Kosmoliaptsis, V., Randle, L. V., Gimson, A. E., Brais, R., Klinck, J. R., Hamed, M., Tsyben, A., and Butler, A. J., "Normothermic perfusion in the assessment and preservation of declined livers before transplantation: Hyperoxia and vasoplegia—important lessons from the first 12 cases," *Transplantation*, vol. 101, no. 5, p. 1084, 2017.

[44] Grosse-Siestrup, C., Pfeffer, J., Unger, V., Nagel, S., Witt, C., Fischer, A., and Groneberg, D. A., "Isolated hemoperfused slaughterhouse livers as a valid model to study hepatotoxicity," *Toxicologic pathology*, vol. 30, no. 6, pp. 749–754, 2002.

[45] Krüger, M., Ruppelt, A., Kappler, B., Van Soest, E., Samsom, R. A., Grinwis, G. C., Geijsen, N., Helms, J. B., Stijnen, M., Kock, L. M., *et al.*, "Normothermic ex vivo liver platform using porcine slaughterhouse livers for disease modeling," *Bioengineering*, vol. 9, no. 9, p. 471, 2022.

[46] Helke, K. L. and Swindle, M. M., "Animal models of toxicology testing: The role of pigs," *Expert opinion on drug metabolism & toxicology*, vol. 9, no. 2, pp. 127–139, 2013.

[47] Mrus, J. M., Chao, R. Y. N., Chao, S. H. Y., Andrews, W. S., and Eberhart, R. C., "An extracorporeal perfusion system to bridge pediatric liver transplant candidates," *ASAIO Transactions*, vol. 36, no. 3, pp. M603–M607, 1990.

[48] Jablonski, P., Douglas, M. C., Gordon, E., Owen, J. A., and McK. Watts, J., "Studies on the isolated perfused pig liver," *British Journal of Surgery*, vol. 58, no. 2, pp. 129–137, 1971.

[49] Schön, M. R., Hunt, C. J., Pegg, D. E., and Wight, D. G., "The possibility of resuscitating livers after warm ischemic injury.," *Transplantation*, vol. 56, no. 1, pp. 24–31, 1993.

[50] Lee, W. Y., Lee, K. W., Heo, J. S., Choi, S. H., Kim, S. J., Joh, J. W., and Lee, S. K., "Prolongation of pig liver perfusion time by gabexate mesilate continuous infusion in extracorporeal perfusion system using biopump," *Transplantation Proceedings*, vol. 35, no. 1, pp. 128–129, 2003.

[51] Pascher, A., Poehlein, C., Stangl, M., Hoebel, G., Thiery, J., Mueller-Derlich, J., and Hammer, C., "Application of immunoapheresis for delaying hyperacute rejection during isolated xenogeneic pig liver perfusion," *Transplantation*, vol. 63, no. 6, pp. 867–875, 1997.

[52] Naruse, K., Sakai, Y., Guo, L., Natori, T., Shindoh, J., Karasawa, Y., Iida, Y., Kojima, K., Michishita, K., and Makuuchi, M., "Development of a new extracorporeal whole-liver perfusion system," *Journal of Artificial Organs*, vol. 6, no. 3, pp. 211–217, 2003.

[53] Grosse-Siestrup, C., Nagel, S., Unger, V., Meissler, M., Pfeffer, J., Fischer, A., and Groneberg, D. A., "The isolated perfused liver: A new model using autologous blood and porcine slaughterhouse organs," *Journal of Pharmacological and Toxicological Methods*, vol. 46, no. 3, pp. 163–168, 2002.

[54] Lau, N. S., Ly, M., Dennis, C., Liu, K., Kench, J., Crawford, M., and Pulitano, C., "Long-term normothermic perfusion of human livers for longer than 12days," *Artificial Organs*, vol. 46, no. 12, pp. 2504–2510, 2022.

[55] Nagel, S., Hegemann, O., Groneberg, D. A., and Grosse-Siestrup, C., "An improved model of isolated hemoperfused porcine livers using pneumatically driven pulsating blood pumps," *Toxicologic Pathology*, vol. 33, no. 4, pp. 434–440, 2005.

[56] Riveros, S., Marino, C., Ochoa, G., Morales, E., Soto, D., Alegría, L., Zenteno, M. J., Brañes, A., Achurra, P., and Rebolledo, R. A., "Implementation and design of customized ex vivo machine perfusion. analysis of its first results," *Artificial Organs*, vol. 46, no. 2, pp. 210–218, 2022.

[57] Schoening, W. N., Feige, I., Schubert, T., Olschewski, P., Buescher, N., Helbig, M., Schmitz, V., Neuhaus, P., Pratschke, J., and Puhl, G., "Iloprost donor treatment reduces ischemia-reperfusion injury in an isolated extracorporeal pig liver perfusion model.," *Experimental and Clinical Transplantation: Official Journal of the Middle East Society for Organ Transplantation*, vol. 13, no. 1, pp. 51–61, 2015.

[58] Butler, A. J., Rees, M. A., Wight, D. G., Casey, N. D., Alexander, G., White, D. J., and Friend, P. J., "Successful extracorporeal porcine liver perfusion for 72 hr," *Transplantation*, vol. 73, no. 8, pp. 1212–8, 2002.

[59] Ntonas, A., Katsourakis, A., Galanis, N., Filo, E., and Noussios, G., "Comparative anatomical study between the human and swine liver and its importance in xenotransplantation," *Cureus*, vol. 12, no. 7, 2020.

[60] Lascaris, B., Thorne, A. M., Lisman, T., Nijsten, M. W., Porte, R. J., and Meijer, V. E. de, "Long-term normothermic machine preservation of human livers: What is needed to succeed?" *American Journal of Physiology-Gastrointestinal and Liver Physiology*, vol. 322, no. 2, G183–G200, 2022.

[61] Chauhan, S. and Rh, A., "Physiological motion and registration of abnormalities in liver during focused ultrasound surgery," *Physics Procedia*, vol. 87, pp. 48–53, 2016.

[62] Clifford, M. A., Banovac, F., Levy, E., and Cleary, K., "Assessment of hepatic motion secondary to respiration for computer assisted interventions," *Computer Aided Surgery*, vol. 7, no. 5, pp. 291–299, 2002.

[63] Rohlfing, T., Maurer Jr, C. R., O'Dell, W. G., and Zhong, J., "Modeling liver motion and deformation during the respiratory cycle using intensity-based nonrigid registration of gated mr images," *Medical physics*, vol. 31, no. 3, pp. 427–432, 2004.

[64] Hickman, R., Saunders, S. J., Simson, E., and Terblanche, J., "Perfusion of the isolated pig liver functional assessment under control normothermic conditions," *British Journal of Surgery*, vol. 58, no. 1, pp. 33–38, 1971.

[65] Terajima, H., Shirakata, Y., Yagi, T., Mashima, S., Shinohara, H., Satoh, S., Arima, Y., Gomi, T., Hirose, T., Takahashi, R., *et al.*, "Successful long-term xenoperfusion of the pig liver: Continuous administration of prostaglandin e: 1: And insulin: 1," *Transplantation*, vol. 63, no. 4, pp. 507–512, 1997.

[66] Abouna, G. M., Ashcroft, T., Hull, C., Hodson, A., Kirkley, J., and Walder, D. N., "The assessment of function of the isolated perfused porcine liver," *The British Journal of Surgery*, vol. 56, no. 4, pp. 289–95, 1969.

[67] Müller, S., Maier-Hein, L., Mehrabi, A., Pianka, F., Rietdorf, U., Wolf, I., Grenacher, L., Richter, G., Gutt, C., Schmidt, J., *et al.*, "Creation and establishment of a respiratory liver motion simulator for liver interventions," *Medical physics*, vol. 34, no. 12, pp. 4605–4608, 2007.

[68] Naghibi, H., Dorp, J. van, and Abayazid, M., "Development of a soft robotics diaphragm to simulate respiratory motion," in *2020 8th IEEE RAS/EMBS International Conference for Biomedical Robotics and Biomechatronics (BioRob)*, IEEE, 2020, pp. 140–145.

[69] Jong, T. L. de, Moelker, A., Dankelman, J., and Dobbelsteen, J. J. van den, "Designing and validating a pva liver phantom with respiratory motion for needle-based interventions," *International journal of computer assisted radiology and surgery*, vol. 14, pp. 2177–2186, 2019.

[70] De Gasperi, A., Mazza, E., and Prosperi, M., "Indocyanine green kinetics to assess liver function: Ready for a clinical dynamic assessment in major liver surgery?" *World journal of hepatology*, vol. 8, no. 7, p. 355, 2016.

[71] Damiao, J. and Gentry, T., "A systematic review of the effectiveness of pressure relieving cushions in reducing pressure injury," *Assistive Technology*, pp. 1–5, 2021.

[72] Borie, D. C., Eyraud, D., Boleslawski, E., Lemoine, A., Sebagh, M., Cramer, D. V., Roussi, J., Imbert-Bismut, F., Germain, G., and Hannoun, L., "Functional metabolic characteristics of intact pig livers during prolonged extracorporeal perfusion: Potential, for a unique biological liver-assist device," *Transplantation*, vol. 72, no. 3, pp. 393–405, 2001.

[73] Rees, M. A., Butler, A. J., Chavez-Cartaya, G., Wight, D. G. D., Casey, N. D., Alexander, G., Khuder, S. A., White, D. J. G., and Friend, P. J., "Prolonged function of extracorporeal hdaf transgenic pig livers perfused with human blood," *Transplantation*, vol. 73, no. 8, pp. 1194–1202, 2002.

[74] Steffen, R., Ballmer, F., Luder, P., Mettler, D., and Barbier, P., "Extracorporeal isolated pig liver perfusion: Influence of various blood primes on liver function," *Research in experimental medicine*, vol. 187, pp. 265–274, 1987.

[75] Mets, B., Rose-Innes, C., Lotz, Z., Hickman, R., and Chalton, D., "Comparison of in vivo and ex vivo porcine liver function using the same liver," *Journal of hepatology*, vol. 17, no. 1, pp. 3–9, 1993.

[76] He, X., Ji, F., Zhang, Z., Tang, Y., Yang, L., Huang, S., Li, W., Su, Q., Xiong, W., Zhu, Z., *et al.*, "Combined liver-kidney perfusion enhances protective effects of normothermic perfusion on liver grafts from donation after cardiac death," *Liver Transplantation*, vol. 24, no. 1, pp. 67–79, 2018.

[77] Gilbo, N., Wylin, T., Heedfeld, V., Jochmans, I., Pirenne, J., Friend, P., and Monbaliu, D., "Porcine liver normothermic machine perfusion: Methodological framework and potential pitfalls," *Transplantation Direct*, vol. 8, no. 1, 2022.

[78] Brüggenwirth, I. M., Leeuwen, O. B. van, Porte, R. J., and Martins, P. N., "The emerging role of viability testing during liver machine perfusion," *Liver Transplantation*, vol. 28, no. 5, pp. 876–886, 2022.

[79] Matton, A. P. M. *et al.*, "Biliary bicarbonate, ph, and glucose are suitable biomarkers of biliary viability during ex situ normothermic machine perfusion of human donor livers," *Transplantation*, vol. 103, no. 7, pp. 1405–1413, 2019.

[80] Banan, B., Lin, Y. I., and Chapman, W., "Development of a normothermic extracorporeal liver perfusion system toward improving viability and function of human extended criteria donor livers reply," *Liver Transplantation*, vol. 22, no. 11, pp. 1617–1618, 2016.

[81] Brüggenwirth, I. M., Meijer, V. E. de, Porte, R. J., and Martins, P. N., "Viability criteria assessment during liver machine perfusion," *Nature Biotechnology*, vol. 38, no. 11, pp. 1260–1262, 2020.

[82] Adham, M. *et al.*, "The isolated perfused porcine liver: Assessment of viability during and after six hours of perfusion," *Transplant International*, vol. 10, no. 4, pp. 299–311, 1997.

[83] Janssen, M. W. W. *et al.*, "Indocyanine green r15 ratio depends directly on liver perfusion flow rate," *Journal of Hepato-Biliary-Pancreatic Sciences*, vol. 17, no. 2, pp. 180–185, 2010.

[84] Zinchuk, V., Khodosovsky, M., and Maslakov, D., "Influence of different oxygen modes on the blood oxygen transport and prooxidant-antioxidant status during hepatic ischemia/reperfusion," 2003.

[85] Nui, A., Katsuramaki, T., Kikuchi, H., Kukita, K., Kimura, H., Meguro, M., Nagayama, M., Isobe, M., and Hirata, K., "The functional integrity of a normothermic perfusion system using artificial blood in pig liver," *Journal of Surgical Research*, vol. 131, no. 2, pp. 189–198, 2006.

[86] Bell, R., Shiel, A. G. R., Dolan, P., Mears, D. c., and Woodman, K., "The evaluation of the isolated perfused liver as a model for the assessment of liver preservation," *Australian and New Zealand Journal of Surgery*, vol. 63, no. 1, pp. 44–52, 1993.

[87] Merle, U., Sieg, O., Stremmel, W., Encke, J., and Eisenbach, C., "Sensitivity and specificity of plasma disappearance rate of indocyanine green as a prognostic indicator in acute liver failure," *BMC gastroenterology*, vol. 9, pp. 1–7, 2009.

[88] Lautt, W. W., "Hepatic circulation: Physiology and pathophysiology," 2010.

[89] Pesce, A., Piccolo, G., Lecchi, F., Fabbri, N., Diana, M., and Feo, C. V., "Fluorescent cholangiography: An up-to-date overview twelve years after the first clinical application," *World Journal of Gastroenterology*, vol. 27, no. 36, p. 5989, 2021.

[90] Boni, L., David, G., Mangano, A., Dionigi, G., Rausei, S., Spampatti, S., Cassinotti, E., and Fingerhut, A., "Clinical applications of indocyanine green (icg) enhanced fluorescence in laparoscopic surgery," *Surgical endoscopy*, vol. 29, pp. 2046–2055, 2015.

[91] Leber, B., Schlechter, S., Weber, J., Rohrhofer, L., Niedrist, T., Aigelsreiter, A., Stiegler, P., and Schemmer, P., "Experimental long-term sub-normothermic machine perfusion for non-allocable human liver grafts: First data towards feasibility," *European Surgery*, vol. 54, no. 3, pp. 150–155, 2022.

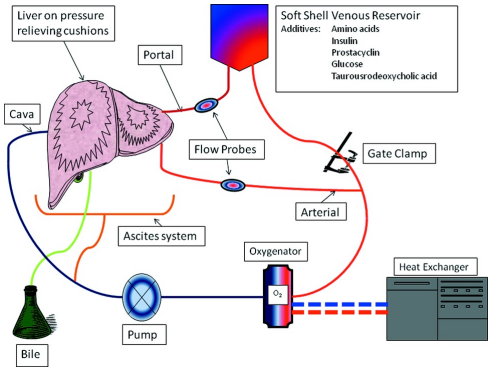
[92] Thorne, A. M., Ubbink, R., Brüggenwirth, I. M., Nijsten, M. W., Porte, R. J., and Meijer, V. E. de, "Hyperthermia-induced changes in liver physiology and metabolism: A rationale for hyperthermic machine perfusion," *American Journal of Physiology-Gastrointestinal and Liver Physiology*, vol. 319, no. 1, G43–G50, 2020.

[93] Dimitrakakis, N., Waterhouse, A., Lightbown, S., Leslie, D. C., Jiang, A., Bolgen, D. E., Lightbown, K., Cascio, K., Aviles, G., Pollack, E., *et al.*, "Biochemical and hematologic reference intervals for anesthetized, female, juvenile yorkshire swine," *Journal of the American Association for Laboratory Animal Science*, vol. 61, no. 1, pp. 21–30, 2022.

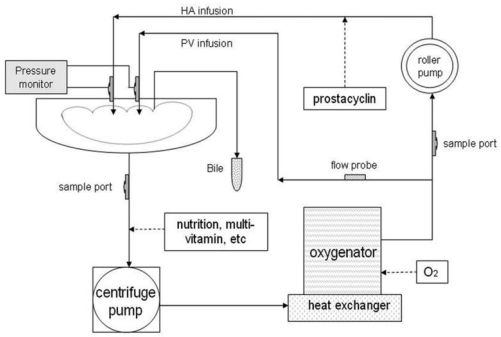
Appendix
A. Perfusion machine setups used in previous porcine NMP experiments

Table A1: Schematic representations and pictures of NMP setups described by porcine NMP studies with their main principle.

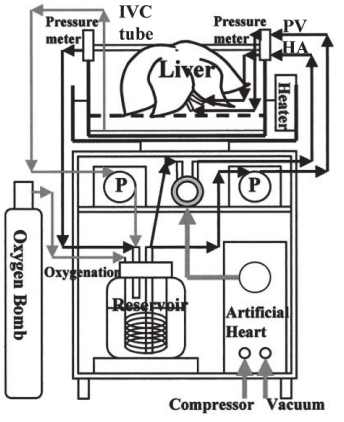
Principle	Setup
Soft surface	Liver placed on water-filled balloons [24], on a biocompatible mattress [31], or on a polyester non-woven fabric sheet in a chamber placed in a water bath [52].

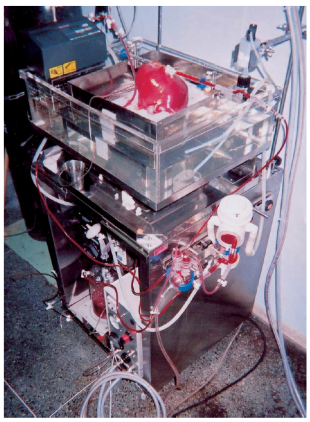


Jamieson, 2011 [24]



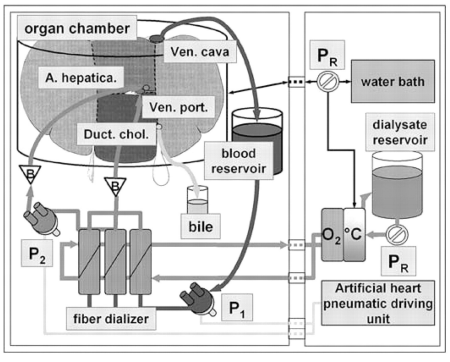
Liu, 2010 [31]



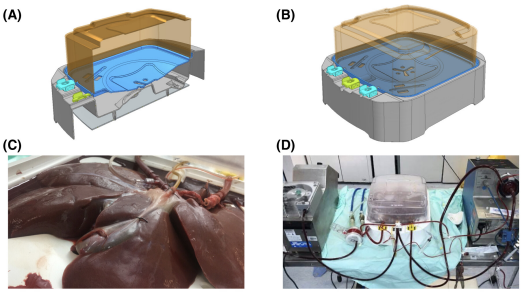


Naruse, 2003 [52]

Hard surface	Liver placed in bags on a PMMA shell mimicking the diaphragm [55] or in a concave fenestrated 3D printed level [56].



Nagel, 2005 [55]

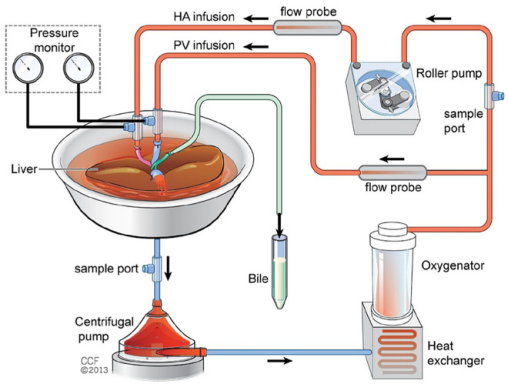


Riveros, 2022 [56]

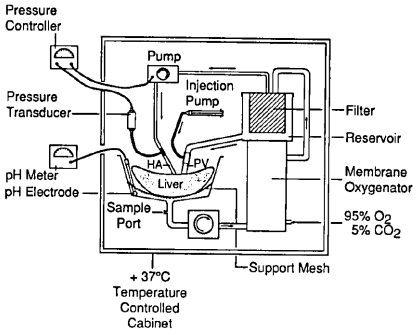
Continued on next page

Table A1: – continued from previous page

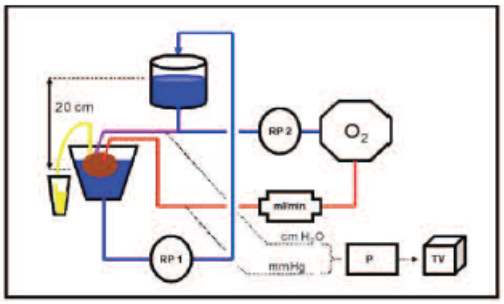
Principle	Setup
Humid and soft	Liver floating freely in fluid [32, 49, 57].



Nassar, 2015 [32]

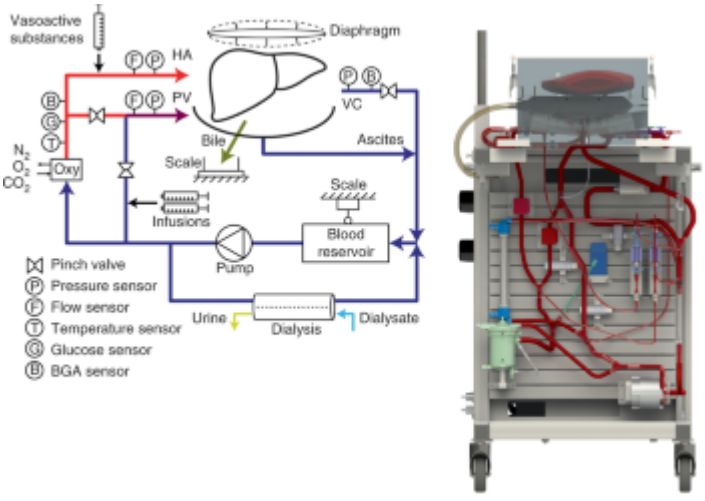


Schon, 1993 [49]



Schoening, 2015 [57]

Movement	Liver placed on an inflatable balloon [36].

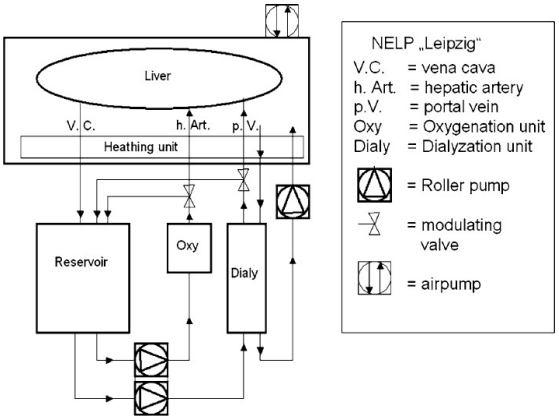


Eshmuminov, 2020 [36]

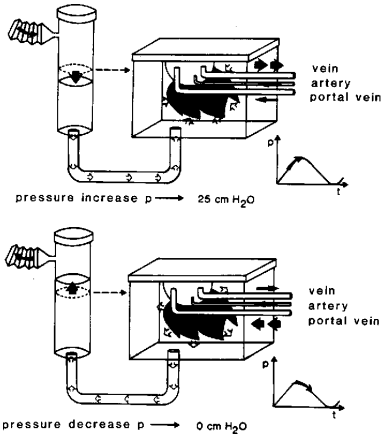
Continued on next page

Table A1: – continued from previous page

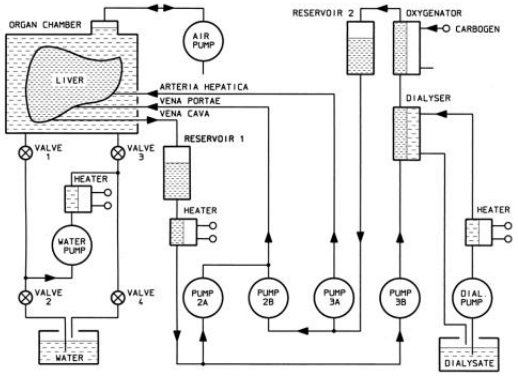
Principle	Setup
Pressure difference	Liver placed in fluid in a chamber subjected to oscillations [25, 38, 74, 83].



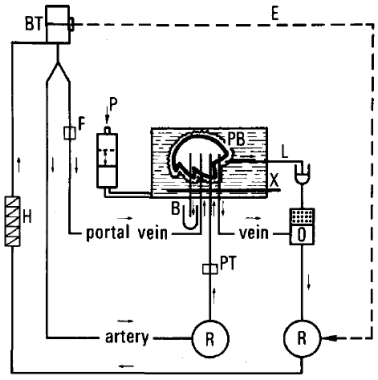
Janssen, 2010 [83]



Neuhaus, 1993 [38]

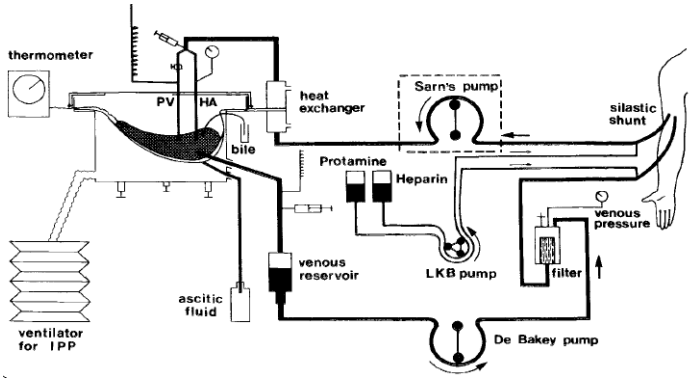


Schon, 2001 [25]



Steffen, 1987 [74]

Pressure difference	Liver placed in a sling in a chamber subjected to oscillations [66].



Abouna, 1969 [66]

B. Arduino code

Code in Arduino language send to the Arduino microcontroller to alternatively inflate and deflate two balloons:

```
1 //Alternative inflate and deflate 2 balloons with 4 pumps
2 #include <Servo.h>
3
4 Servo myservo8;
5 Servo myservo9;
6 Servo myservo10;
7 Servo myservo4;
8 Servo myservo5;
9 Servo myservo6;
10
11 void setup() {
12   //setup balloon 1
13   myservo8.attach(8);  //pin 8 is connected to air pump no. 1 for
        inflation (trachea is connected to the head of the air pump)
14   myservo9.attach(9);  //pin 9 is connected to the three-way electronic
        valve 1 (inflation and suction are respectively connected to 2 heads
        and middle is connected to the balloon. Metal end to pump no. 1 and
        plastic end to pump no.2)
15   myservo10.attach(10); //pin 10 is connected to air pump no. 2 for
        deflation (trachea is connected to the middle interface of the air
        pump)
16
17   //setup balloon 2
18   myservo4.attach(4);  //pin 4 is connected to air pump no. 3 for
        inflation (trachea is connected to the head of the air pump)
19   myservo5.attach(5);  //pin 5 is connected to the three way electronic
        valve 2 (inflation and suction are respectively connected to 2 heads
        and middle is connected to the balloon. Metal end to pump no. 3 and
        plastic end to pump no.4)
20   myservo6.attach(6); //pin 6 is connected to air pump no. 4 for deflation
         (trachea is connected to the middle interface of the air pump)
21
22   //initialise balloons, inflate for certain time for total starting
        volume of balloons
23   myservo8.write(180); //inflate balloon 1
24   myservo9.write(0);
25   myservo10.write(0);
26   myservo4.write(180); //inflate balloon 2
27   myservo5.write(0);
28   myservo6.write(0);
29
30   delay(120000); //initial volume balloon 1
31
32   myservo8.write(0);
33   myservo9.write(0);
34   myservo10.write(0);
35   myservo4.write(180); //inflate balloon 2
36   myservo5.write(0);
37   myservo6.write(0);
38
39   delay(8000); //additional initial volume balloon 2
40 }
```

```
41
42 void loop() {
43   //repeatedly run following code for alternative inflation and deflation
        of two balloons:
44
45   //open valve 2 prepare for deflation balloon 2
46   myservo8.write(0);
47   myservo9.write(0);
48   myservo10.write(0);
49   myservo4.write(0);
50   myservo5.write(180); //open valve 2
51   myservo6.write(0);
52
53   delay(100);
54
55   myservo8.write(180); //inflate balloon 1
56   myservo9.write(0);
57   myservo10.write(0);
58   myservo4.write(0);
59   myservo5.write(180);
60   myservo6.write(180); //deflate balloon 2
61
62   delay(8000); //adjust ms to change rythm or range of movement, less
        degree of tilting less ms, more degree of tilting more ms
63
64   //if necessary extra inflate balloon 1 and deflate balloon 2
65   //myservo8.write(0);
66   //myservo9.write(0);
67   //myservo10.write(0);
68   //myservo4.write(0);
69   //myservo5.write(180); //keep valve 2 open to prepare for additional
        deflation of balloon 1
70   //myservo6.write(0);
71
72   //delay(100);
73
74   //extra inflate balloon 1 and deflate balloon 2
75   //myservo8.write(180); //extra inflate balloon 1 if necessary to
        maintain a contant total volume
76   //myservo9.write(0);
77   //myservo10.write(0);
78   //myservo4.write(0);
79   //myservo5.write(180);
80   //myservo6.write(180); //extra deflate balloon 2 if necessary to
        maintain a contant total volume
81
82   //delay(ms); //adjust depending on the power of the pump and the
        difference between air out/in of the pump
83
84   //open valve 1 prepare for deflation balloon 1
85   myservo8.write(0);
86   myservo9.write(180); //open valve 1
87   myservo10.write(0);
88   myservo4.write(0);
89   myservo5.write(0);
90   myservo6.write(0);
```

```
91
92    delay(100);
93
94    myservo8.write(0);
95    myservo9.write(180);
96    myservo10.write(180); //deflate balloon 1
97    myservo4.write(180); //inflate balloon 2
98    myservo5.write(0);
99    myservo6.write(0);
100
101   delay(8000); //adjust ms to change rythm or range of movement, less
          degree of tilting less ms, more degree of tilting more ms
102
103   //if necessary extra deflate balloon 1 and inflate balloon 2
104   //myservo8.write(0);
105   //myservo9.write(180); //keep valve 1 open to prepare for additional
          deflation of balloon 1
106   //myservo10.write(0);
107   //myservo4.write(0);
108   //myservo5.write(0);
109   //myservo6.write(0);
110
111   //delay(100);
112
113   //myservo8.write(0);
114   //myservo9.write(180);
115   //myservo10.write(180); //extra deflate balloon 1 if necessary to
          maintain a contant total volume
116   //myservo4.write(180); //extra inflate balloon 2 if necessary to
          maintain a contant total volume
117   //myservo5.write(0);
118   //myservo6.write(0);
119
120   //delay(ms); //adjust depending on the power of the pump and the
          difference between air out/in of the pump
121 }
```

C. Validation Experiments

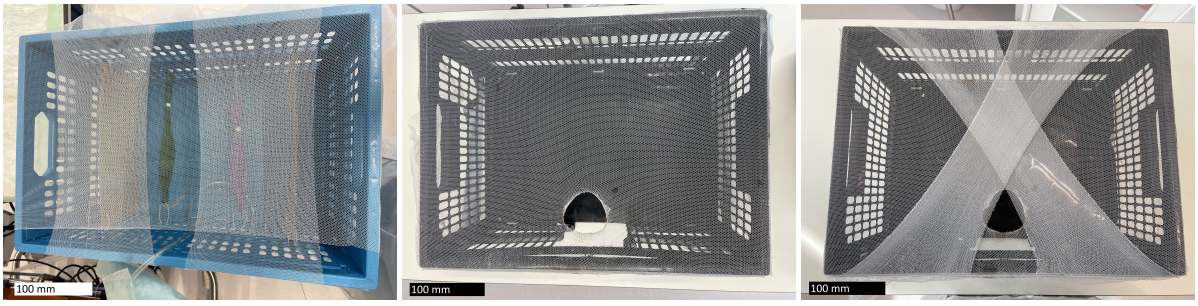
C.1. Setup HMP Validation experiments



(a) **(b)**

Figure C1: The setup of the HMP validation experiments. **(a)** From left to right the Liver Assist device, the liver reservoir, and the electronic system with the laptop. **(b)** Measurement of inferior vena cava (IVC) flow. During these experiments, the perfusate reservoir of the Liver Assist device was used, which is depicted in the lower right corner.

C.2. Additional Results Validation Experiments



(a) **(b)** **(c)**

Figure C2: The different net configurations used. **(a)** The configuration during the validation experiments. **(b)** The configuration after the validation experiments, during Experiment 1. **(c)** The configuration of the net during Experiments 2, 3, and 4. Scale bars 50 mm.

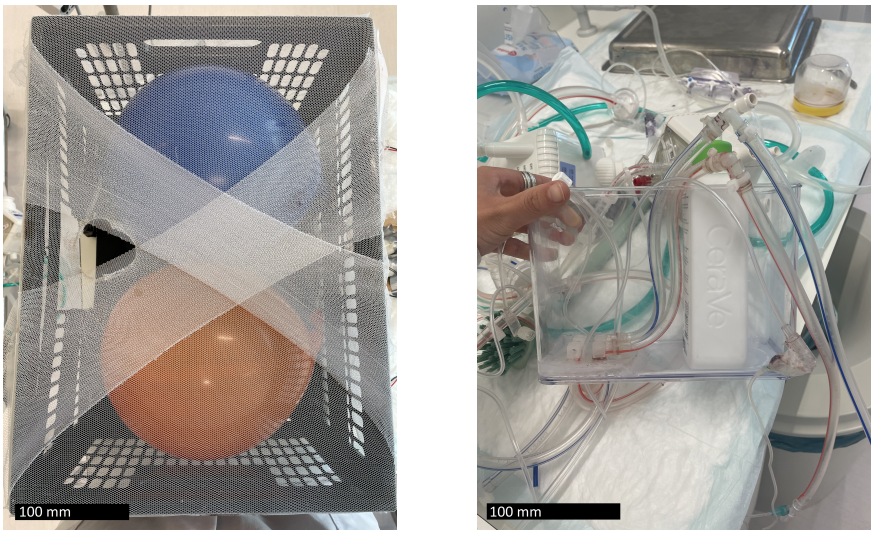
D. Reference Values Blood Gas Analysis

Table D1: Reference values blood gas analysis used during the NMP experiments. Based on physiological human and porcine arterial blood gas analysis [93].

Measurement	Reference Value	Unit	Comment
pH	7.35-7.45		
pCO_2	35-45	mmHg	
pO_2	80-110	mmHg	
HCO_3	20-28	mmol L^{-1}	Calculated
BE	-3 - 3	mmol L^{-1}	Calculated, dependent on pH
SO_2	100	%	Calculated
TCO_2	N/A	mmol L^{-1}	Calculated, dependent on pH and carbogen
Lactate	Decrease after t = 1 h	mmol L^{-1}	
Sodium (N)	130-160	mmol L^{-1}	
Potassium (K)	4-7	mmol L^{-1}	
Chloride (Cl)	100-105	mmol L^{-1}	
Urea nitrogen (BUN)	Increases from baseline around 3	mg dL^{-1}	
Creatinine	1-2	mg dL^{-1}	Not relevant for liver, dependent on plasma concentration pig
Glucose (Glu)	t = 0 low, t = 1-2 h peak, decreases during perfusion	mmol L^{-1}	
Ionized calcium (iCa)	0.5-1	mmol L^{-1}	
Anion gap	N/A	mmol L^{-1}	Calculated, dependent on pH and carbogen
Hematocrit (Hct)	t = 0 >25	%PCV	For example a PCV of 30% means 30 ml of cells in 100 ml perfusate)
Hemoglobin (Hgb)	t = 0 > 5	g dL^{-1}	

E. Additional Results NMP Experiments

E.1. Setup Alterations



(a) **(b)**

Figure E1: Setup alterations after the first NMP experiment under the established movement condition. **(a)** The net configuration was changed and the distance between the balloons was reduced, to give the liver more support between the balloons. **(b)** The volume of the perfusate reservoir was reduced. Scale bars 100 mm.

E.2. Additional Graphs of Perfusate Temperature and Hemodynamics

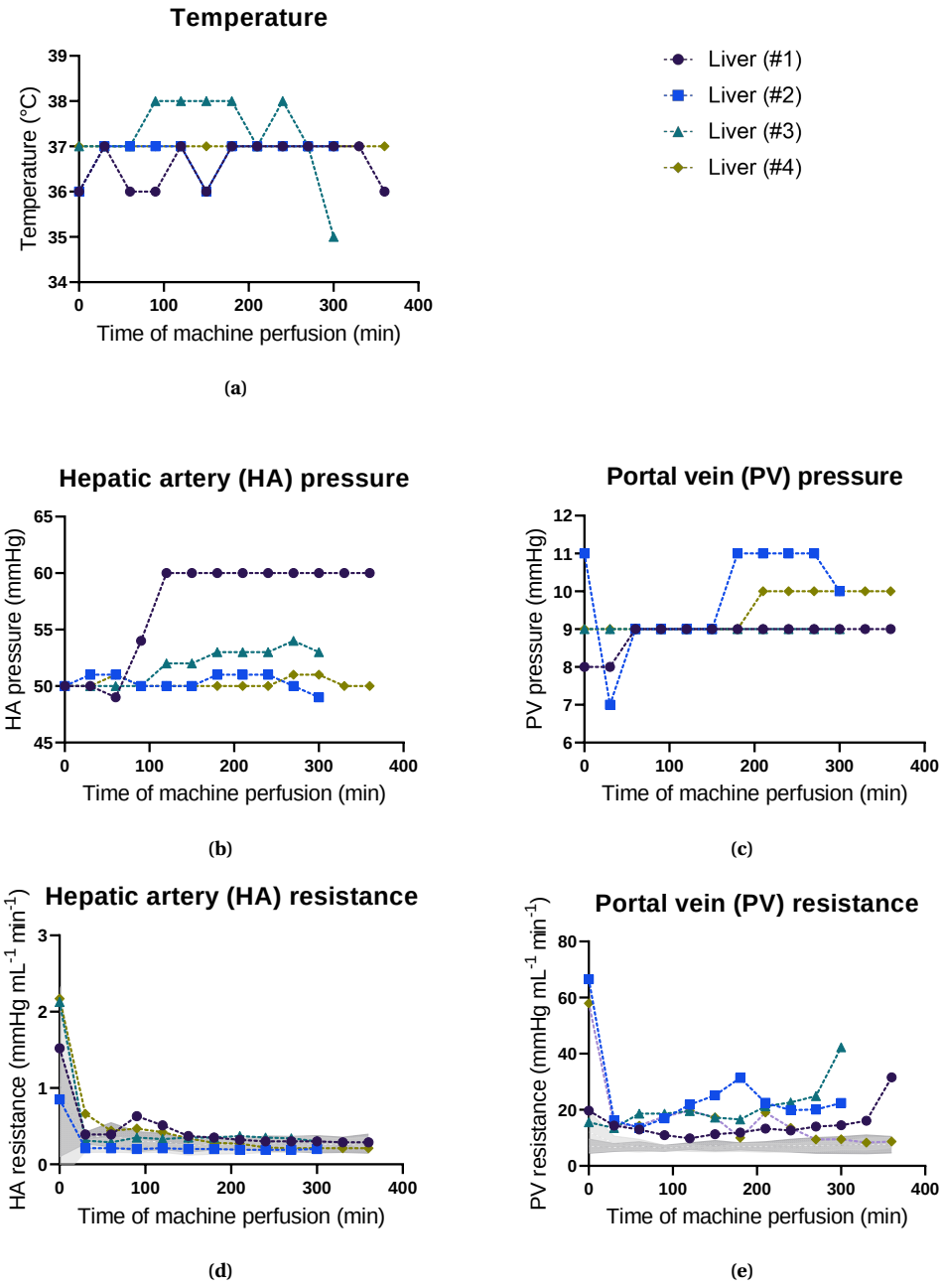


Figure E2: Perfusate temperature and hemodynamics to assess the stability of the NMP experiments under the established movement condition. **(a)** Perfusate temperature. **(b)** Hepatic artery (HA) and **(c)** portal vein (PV) pressure. Each of the four NMP experiments under the movement condition is depicted individually. **(d)** HA and **(e)** PV resistance. Additionally, the data from the control NMP experiments performed in Zeist (n = 3) and Leiden (n = 3) are presented as the means of the three experiments, accompanied by their respective standard deviations.

E.3. Additional Graphs of Blood Gas Analysis

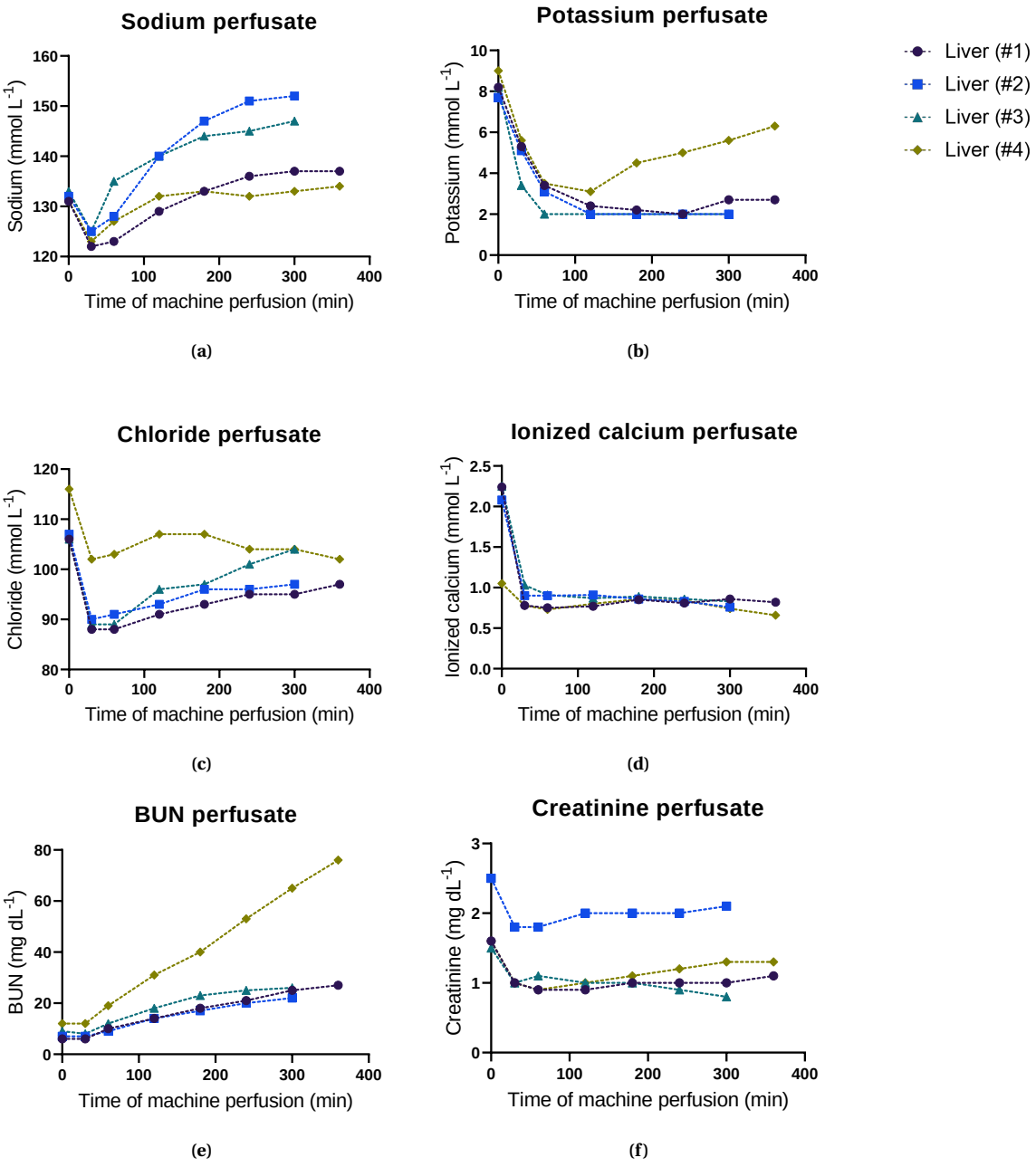


Figure E3: Measurement of electrolytes in the perfusate to assess the overall performance of the NMP experiments under the established movement condition. **(a)** Sodium, **(b)** potassium (2 = < 2, 9 = > 9, out of measurable range), **(c)** chloride, **(d)** ionized calcium, **(e)** urea nitrogen (BUN), and **(f)** creatinine perfusate concentrations. Each of the four NMP experiments under the movement condition is depicted individually.

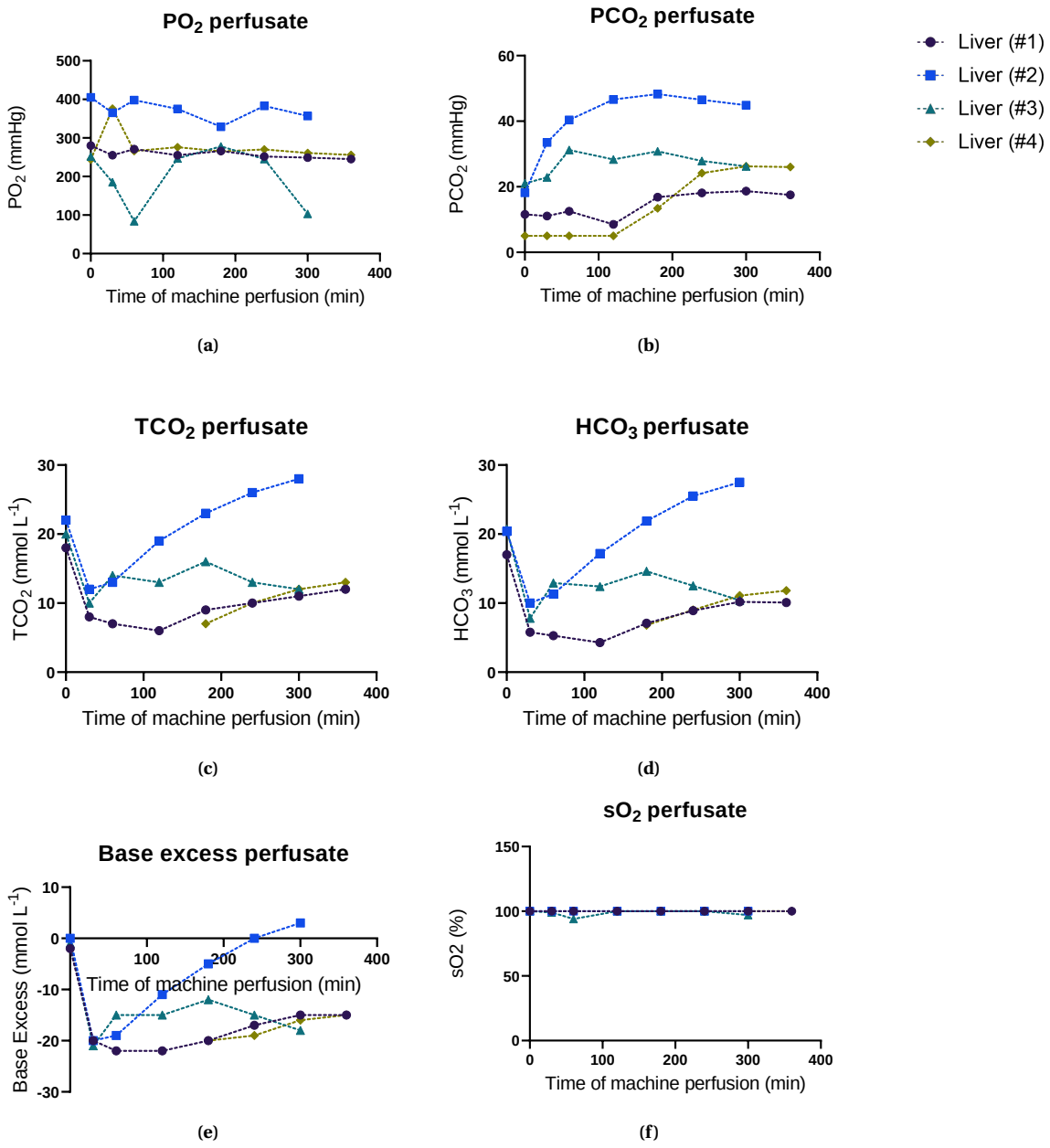
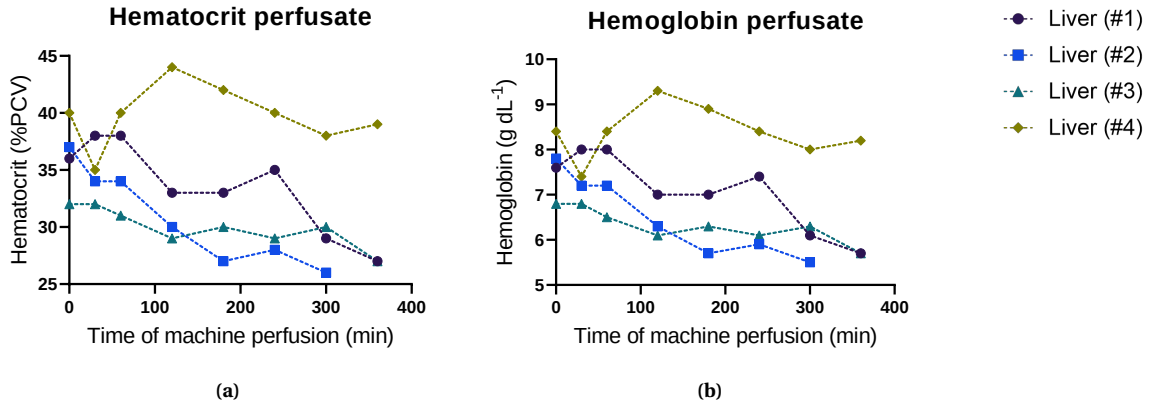


Figure E4: Measurements of blood gasses in the perfusate to assess the overall performance of the NMP experiments under the established movement condition. **(a)** PO_2, **(b)** PCO_2 (5 = < 5, out of measurable range), **(c)** TCO_2, **(d)** HCO_3, **(e)** base excess, and **(f)** sO_2. Each of the four NMP experiments under the movement condition is depicted individually.

Table E1: Sodium bicarbonate (HCO_3) administration in mL at different time points during NMP under the established movement condition to keep the pH in the physiological range (7.35−7.45).

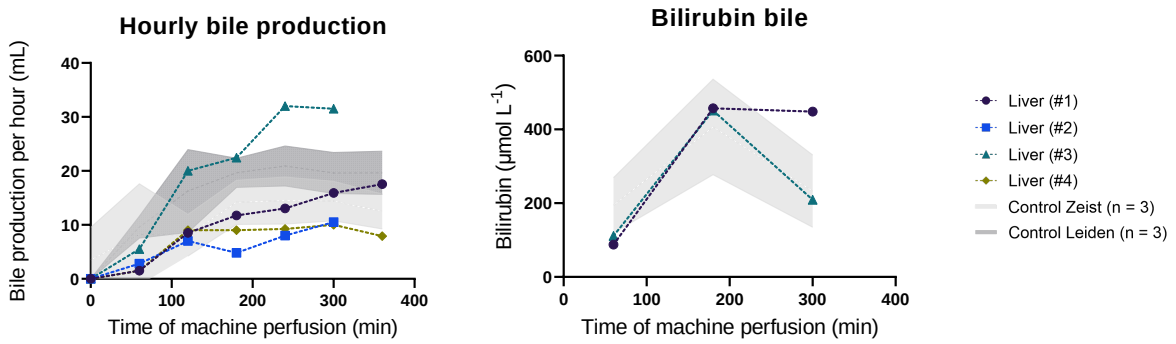
	Time (min)					
	30	60	120	180	240	300
Liver 1	-	10 mL	10 mL	-	-	-
Liver 2	-	30 mL	30 mL	15 mL	-	10 mL
Liver 3	30 mL	15 mL	-	30 mL	-	-
Liver 4	-	-	-	-	15 mL	10 mL



(a) **(b)**

Figure E5: Measurement of **(a)** Hematocrit and **(b)** hemoglobin concentrations in the perfusate during NMP under the established movement condition. Each of the four NMP experiments under the movement condition is depicted individually.

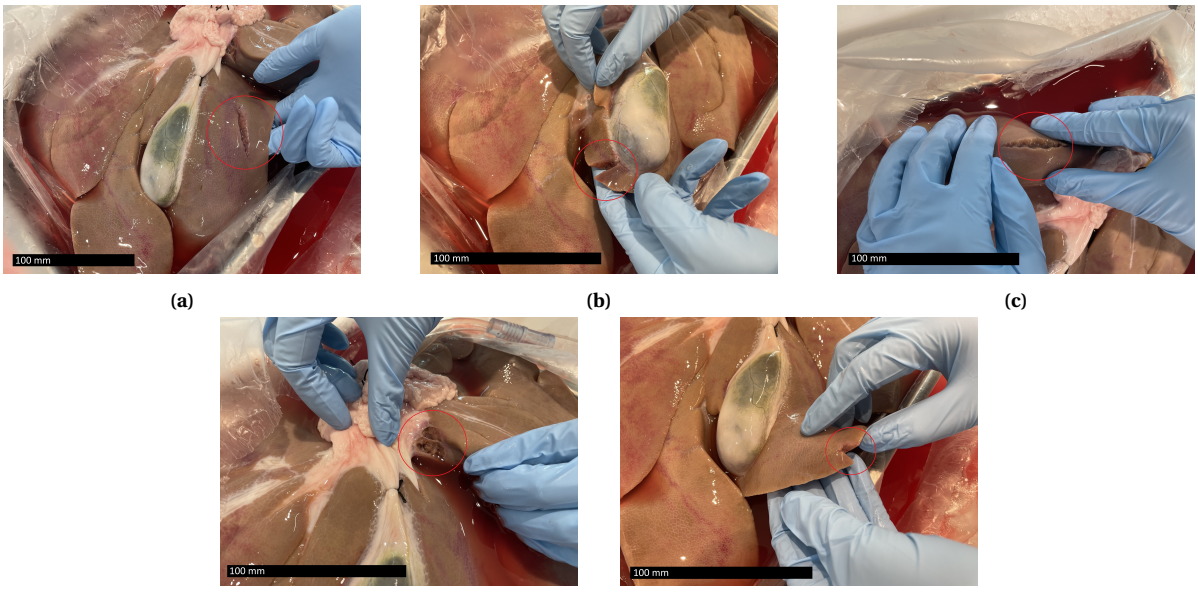
E.4. Additional Graphs of Bile production



(a) **(b)**

Figure E6: (a) Hourly bile production and **(b)** bile bilirubin concentration during NMP under the established movement condition. With these measurements the bilirubin concentration in the bile corrected by the hourly bile production was calculated. Each of the four NMP experiments under the movement condition is depicted individually. The data from the control NMP experiments performed in Zeist (n = 3) and Leiden (n = 3) are presented as the means of the three experiments, accompanied by their respective standard deviations. Bilirubin in the bile was only measured for Experiments 1 and 3, and control NMP experiments performed in Zeist.

E.5. Additional Pictures of Appearance



(a) **(b)** **(c)**

(d) **(e)**

Figure E7: The damaged liver before the start of NMP for which the experiment was terminated. The liver had multiple cuts and tears in different areas **(a-e)**. Scale bars 100 mm.

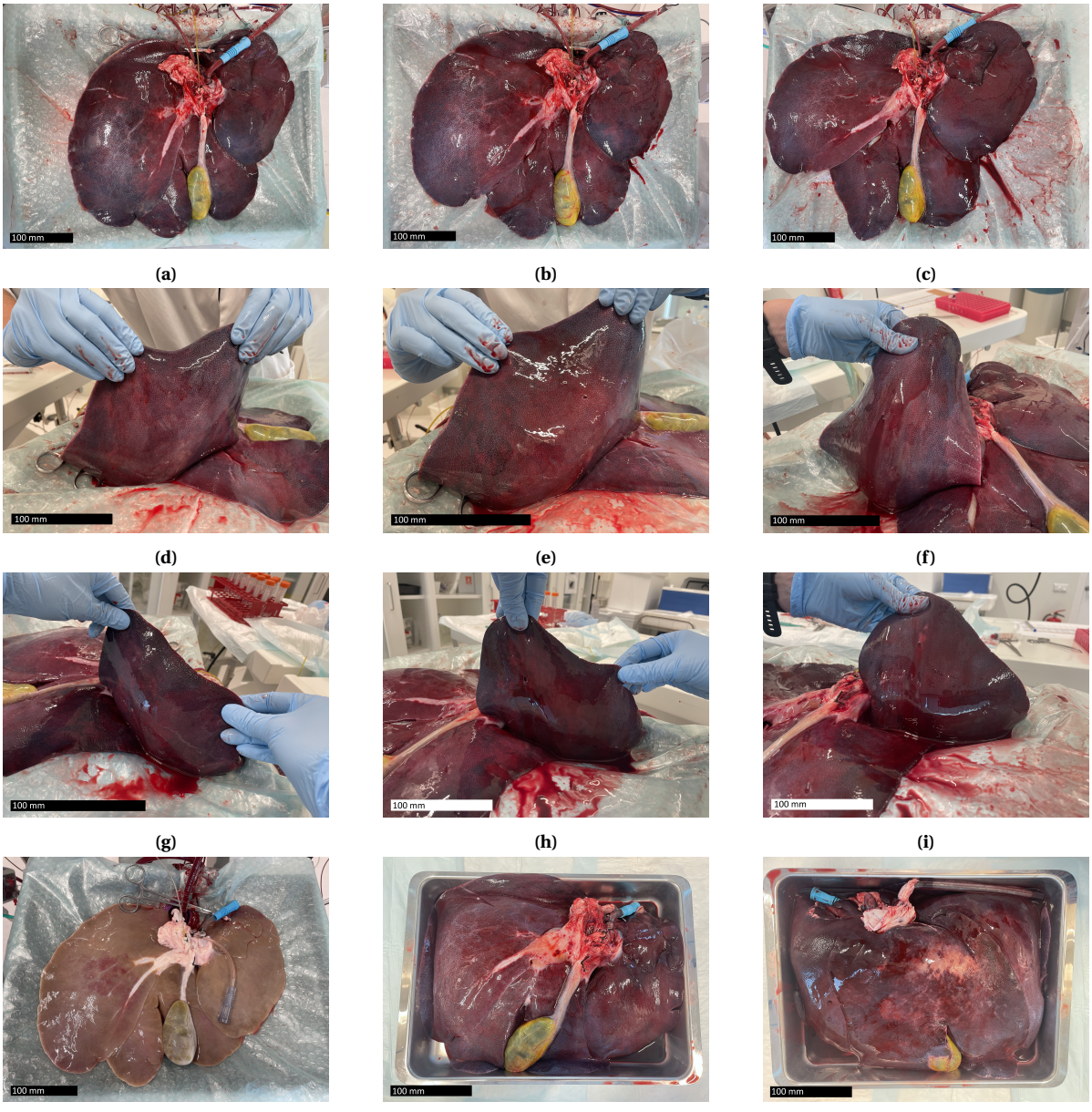


Figure E8: Appearance of the liver during NMP Experiment 1 under the established movement condition. The top of the liver at **(a)** t = 120 min, **(b)** 240 min, and **(c)** 360 min. The bottom of lobe 1 at **(d)** t = 120 min, **(e)** 240 min, and **(f)** 360 min. The bottom of lobe 4 at **(g)** t = 120 min, **(h)** 240 min, and **(i)** 360 min. The top of the liver at **(j)** t = 0 and **(k)** the top and **(l)** bottom of the liver at t = 360 min. Scale bars 100 mm.

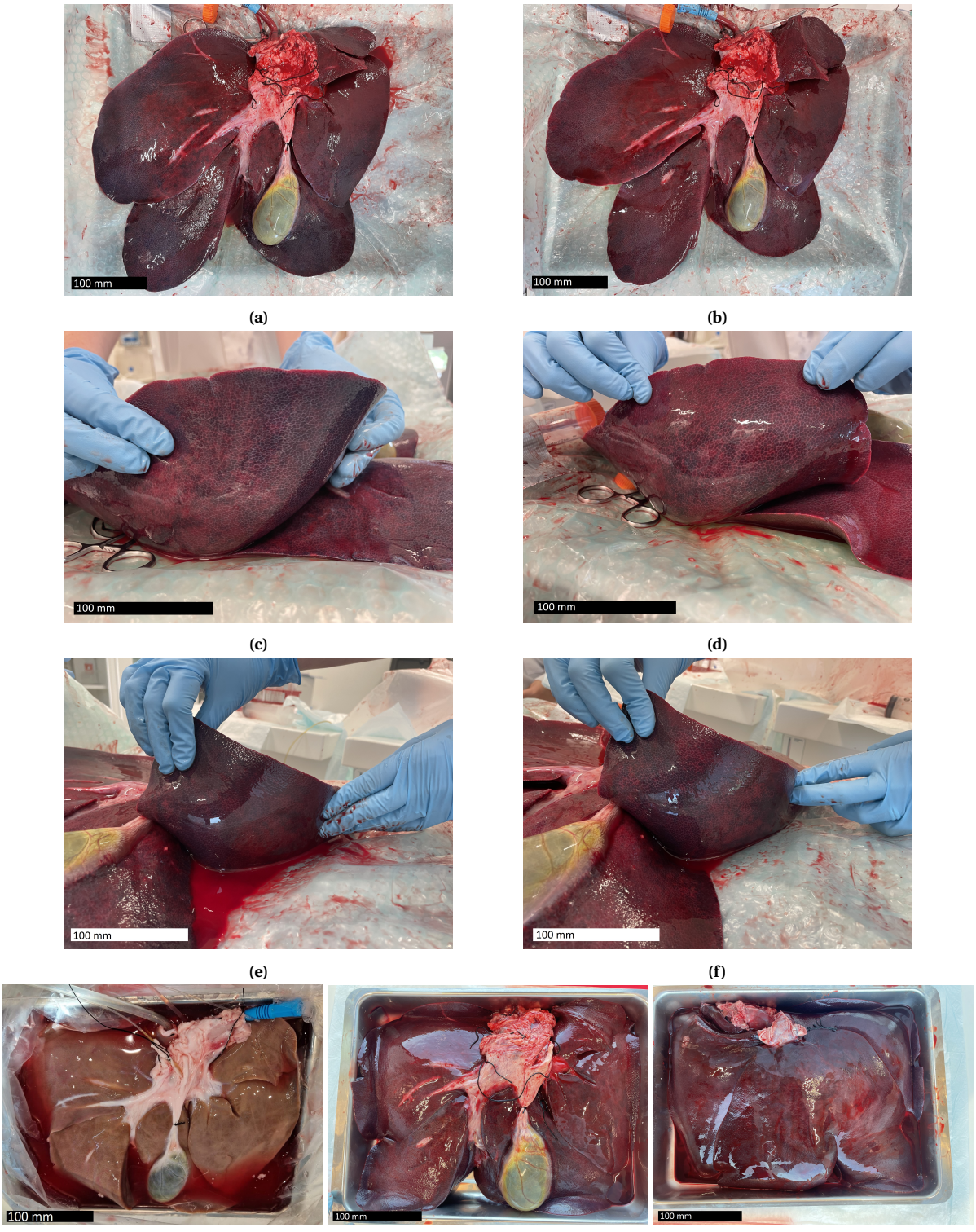


Figure E9: Appearance of the liver during NMP Experiment 2 under the established movement condition. The top of the liver at **(a)** t = 120 min and **(b)** 240 min. The bottom of lobe 1 at **(c)** t = 120 min and **(d)** 240 min. The bottom of lobe 4 at **(e)** t = 120 min and **(f)** 240 min. The top of the liver at **(g)** t = 0 and **(h)** the top and **(i)** bottom of the liver at t = 300 min. Scale bars 100 mm.

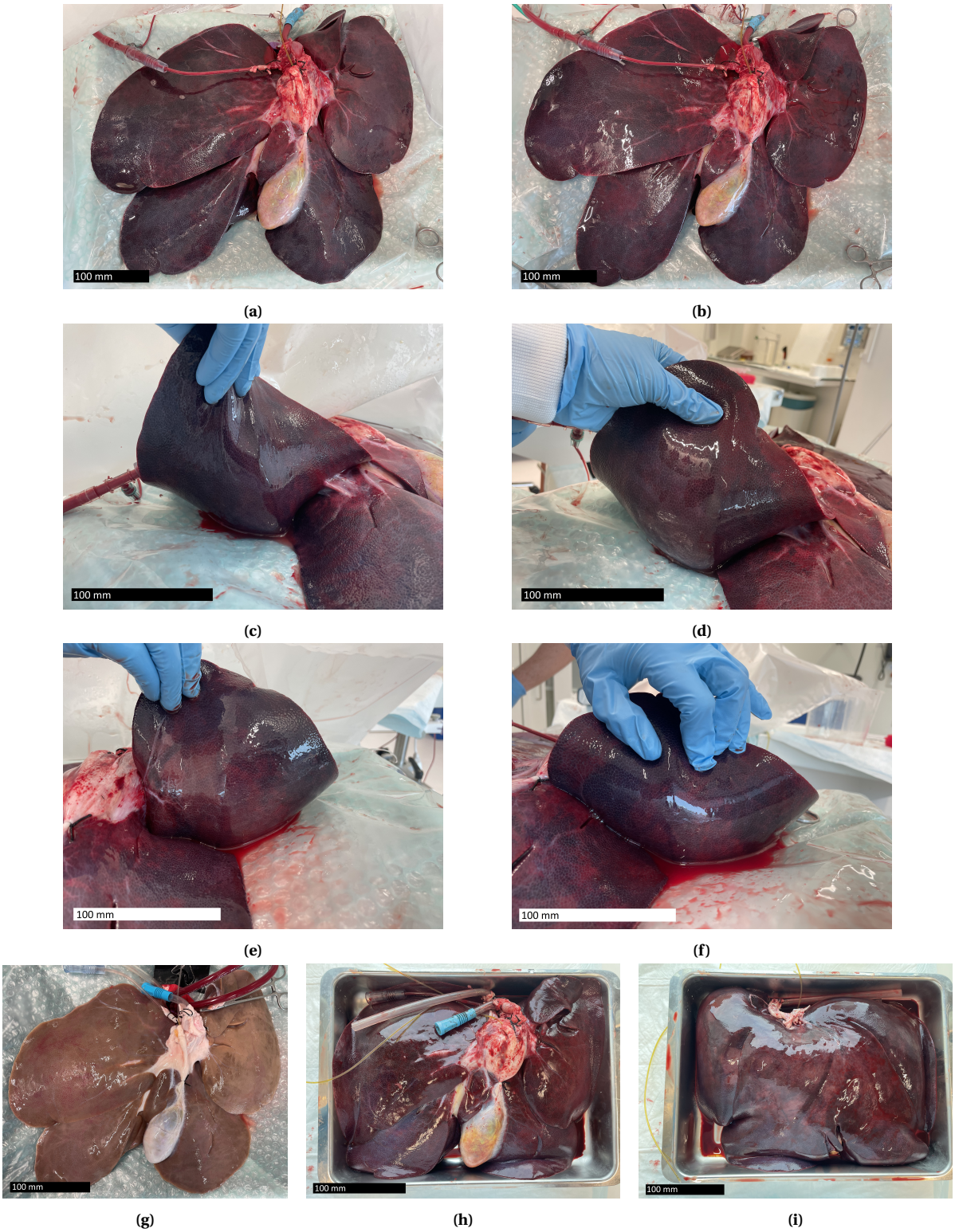
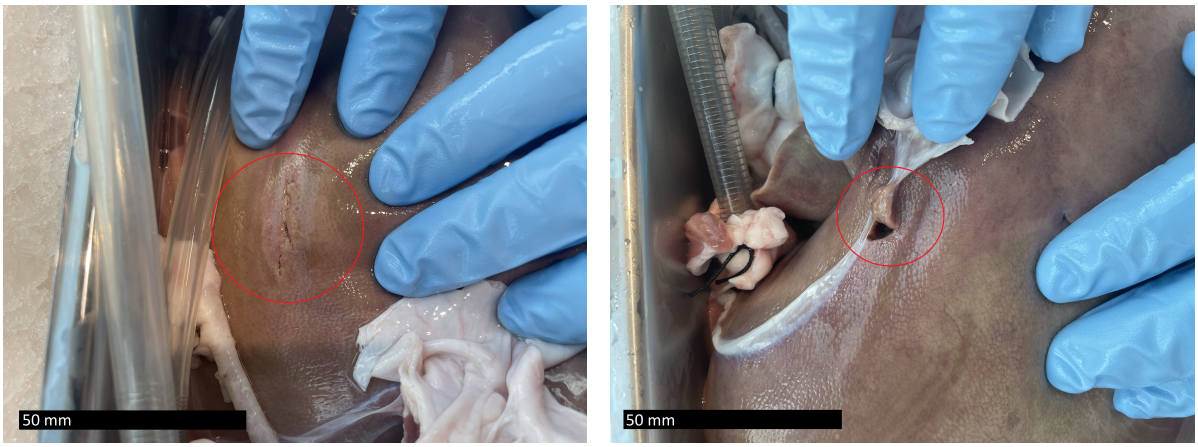
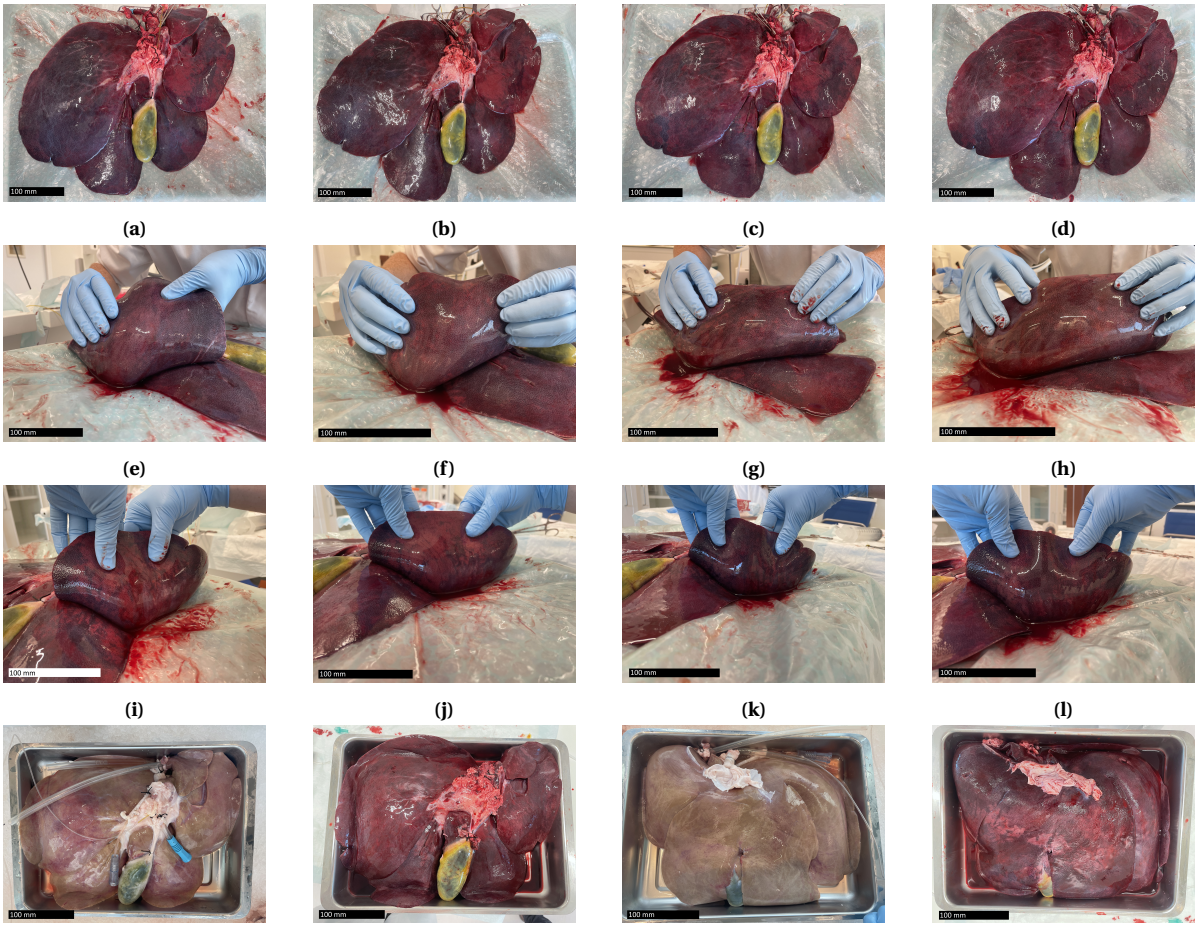


Figure E10: Appearance of the liver during NMP Experiment 3 under the established movement condition. The top of the liver at **(a)** t = 120 min and **(b)** 240 min. The bottom of lobe 1 at **(c)** t = 120 min and **(d)** 240 min. The bottom of lobe 4 at **(e)** t = 120 min and **(f)** 240 min. The top of the liver at **(g)** t = 0 and the **(h)** top and **(i)** bottom of the liver at t = 300 min. Scale bars 100 mm.



(a) (b)

Figure E11: Injuries of Liver 4 before the start of NMP Experiment 4. Torn tissue at the bottom of **(a)** lobe 1 and **(b)** lobe 4. Scale bars 50 mm.



(a) **(b)** **(c)** **(d)**

(e) **(f)** **(g)** **(h)**

(i) **(j)** **(k)** **(l)**

(m) **(n)** **(o)** **(p)**

Figure E12: Appearance of the liver during NMP Experiment 4 under the established movement condition. The top of the liver at **(a)** t = 120 min, **(b)** 240 min, **(c)** 360 min, and **(d)** 420 min. The bottom of lobe 1 at **(e)** t = 120 min, **(f)** 240 min, **(g)** 360 min, and **(h)** 420 min. The bottom of lobe 4 at **(i)** t = 120 min, **(j)** 240 min, **(k)** 360 min, and **(l)** 420 min. The top of the liver at **(m)** t = 0 min and **(n)** t = 420 min. The bottom of the liver at **(o)** t = 0 min and **(p)** t = 420 min. Scale bars 100 mm.

E.6. Additional Results Histological Analysis

Table E2: Observations and scores of the H&E stained liver sections from the biopsies obtained during and after NMP under the established movement condition. According to the observations done, a blinded pathologist scored the liver sections from good tissue quality (dark green) to poor tissue quality (red).

Experiment	Time (min)	Biopsy	Observation	Score
Liver 1	180	1	Minimal focal hypertrophy	
	180	2	Minimal focal hypertrophy, mild multifocal vacuolation	
	360	1	Minimal focal single cell necrosis	
	360	2	Minimal focal single cell necrosis, mild hypertrophy	
Liver 2	180	1	Minimal focal single cell necrosis associated with hemorrhages	
	180	2	Minimal multifocal single cell necrosis	
	300	1	Minimal multifocal single cell necrosis associated with hemorrhages	
	300	2	Minimal focal single cell necrosis associated with hemorrhages	
Liver 3	300	1	Minimal focal single cell necrosis, mild multifocal vacuolation	
	300	2	Mild focal single cell necrosis, characterized by hypertrophy, rounding of cells and karyolysis	
Liver 4	360	1	Minimal focal single cell necrosis associated with minimal hemorrhages, mild hypertrophy	
	360	2	Minimal focal single cell necrosis, mild hypertrophy, minimal focal vacuolation	
	420	1	Mild multifocal single cell necrosis, associated with mild hemorrhages, mild hypertrophy, mild multifocal vacuolation	
	420	2	Minimal multifocal single cell necrosis, associated with mild hemorrhages	



Good Quality Poor Quality

F. Additional Results Statistical Analysis

Table F1: Descriptive statistics and *t* test results comparing the mean of various measurements between the NMP experiments under the established movement condition (n = 4) and the control NMP experiments performed in Zeist (n =3), without liver movement. Two-sided unpaired *t* tests were performed. No test was performed when there was only one data point for the group, there was no data for one group, or data was idential between groups. Mean (M), standard deviation (SD), t(df)= *t* statistic, *p* value, and significance at a 0.05 level are reported.

	NMP movement n = 4		NMP control Zeist n = 3					
Measure	M	SD	M	SD	df	*t* statistic	*p* value	Sign. < 0.05
Glucose perfusate								
t = 0	3.875	0.6397	4.000	0.1732	5	0.3225	0.7601	no
t = 60	34.53	8.750	30.33	14.84	5	0.4741	0.6554	no
t = 120	34.55	8.700	29.20	16.80	5	0.5567	0.6017	no
t = 180	31.25	9.947	24.00	15.23	5	0.7695	0.4764	no
t = 240	26.25	8.310	17.20	12.70	5	1.151	0.3017	no
t = 300	20.70	5.683	13.47	9.421	5	1.278	0.2572	no
t = 360	14.65[2]	3.041	6.567	6.974	3	1.486	0.2340	no
Lactate perfusate								
t = 0	6.825	1.580	5.600	2.921	5	0.7237	0.5017	no
t = 60	5.933	3.210	3.667	0.2155	5	1.192	0.2869	no
t = 120	6.388	3.427	3.500	1.135	5	1.375	0.2276	no
t = 180	6.843	4.302	2.907	1.036	5	1.518	0.1896	no
t = 240	6.505	4.237	2.623	1.609	5	1.479	0.1992	no
t = 300	6.350	4.413	2.390	1.965	5	1.426	0.2133	no
t = 360	3.350[2]	3.309	2.423	2.072	3	0.3978	0.7174	no
Bilirubin perfusate								
t = 0	10.65[3]	1.886	17.38[2]	12.48	3	0.9998	0.3911	no
t = 60	8.550[3]	0	10.23	2.916	4	1.000	0.3739	no
t = 120	8.550[3]	0	11.60	5.283	4	1.000	0.3739	no
t = 180	10.43[3]	3.262	12.73	2.065	4	1.032	0.3604	no
t = 240	11.59[3]	4.778	9.967	2.454	4	0.5246	0.6276	no
t = 300	10.23[3]	2.916	12.90	5.465	4	0.7447	0.4978	no
t = 360	8.550[1]	0	15.50	8.107				
ALT								
t = 0	51.58	19.70	29.60[2]	1.970	4	1.482	0.2125	no
t = 60	157.5	29.83	149.7	53.61	5	0.2489	0.8133	no
t = 120	157.3	27.54	169.3	54.86	5	0.3885	0.7137	no
t = 180	174.0	50.39	160.0	50.32	5	0.3640	0.7308	no
t = 240	183.8	55.40	177.0	65.28	5	0.1484	0.8878	no
t = 300	176.8	73.95	177.0	59.09	5	0.004786	0.9964	no
t = 360	219.5[2]	118.1	172.0	53.03	3	0.6443	0.5653	no
AST								
t = 0	43.35	12.59	148.9[2]	140.1	4	1.719	0.1608	no
t = 60	5280	627.2	4620	2070	5	0.6188	0.5631	no
t = 120	5175	980.5	5033	2326	5	0.1120	0.9152	no
t = 180	6105	1008	5167	1813	5	0.8855	0.4164	no
t = 240	5125	747.9	5787	2279	5	0.5578	0.6011	no
t = 300	5835	623.8	6127	2438	5	0.2363	0.8226	no
t = 360	6755[2]	1266	6017	1190	3	0.4409	0.6891	no

Continued on next page

[1] only n = 1; [2] only n = 2; [3] only n = 3; *no* no data; *id* identical data

Table F1: – continued from previous page

	NMP movement n = 4		NMP control Zeist n = 3					
Measure	M	SD	M	SD	df	*t* statistic	*p* value	Sign. < 0.05
HA flow	176.6	52.17	206.7	45.95	24	1.559	0.1320	no
PV flow	597.7	119.6	1593	293.5	24	11.33	<0.0001	yes
Cumulative bile production								
t = 300	58.50	36.05	62.90	23.09	5	0.1828	0.8621	no
t = 360	57.45[2]	15.27	75.39	25.87	3	0.8584	0.4538	no
Bilirubin bile								
t = 60	99.35[2]	16.48	194.0	75.19	3	1.669	0.1937	no
t = 180	454.0[2]	4.243	406.7	129.7	3	0.4896	0.6580	no
t = 300	328.5[2]	169.0	232.9	97.98	3	0.8303	0.4673	no
Bilirubin bile corrected for bile flow								
t = 60	0.3710[2]	0.3387	1.881	2.567	3	0.7857	0.4894	no
t = 180	1.021[2]	0.1510	0.9152	0.3190	3	0.4211	0.7021	no
t = 300	3.494[2]	0.06413	0.5355	0.2877	3	13.63	0.0009	yes
PDR_{ICG} 2h	24.09	14.47	11.01	3.343	5	1.502	0.1935	no
PDR_{ICG} 5h	30.68[2]	11.74	11.01	3.343	3	2.949	0.0601	no
% ICG cleared 2h	88.29	5.187	93.87	5.807	5	1.341	0.2377	no
% ICG cleared 5h	88.04[2]	4.676	93.87	5.80	3	1.169	0.3267	no

[1] only n = 1; [2] only n = 2; [3] only n = 3; ^{no} no data; ^{id} identical data

Table F2: Descriptive statistics and *t* test results comparing the mean of various measurements between the NMP experiments under the established movement condition (n = 4) and the control NMP experiments performed in Leiden (n =3), without liver movement. Two-sided unpaired *t* tests were performed. No test was performed when there was only one data point for the group, there was no data for one group, or data was idential between groups. Mean (M), standard deviation (SD), t(df)= *t* statistic, *p* value, and significance at a 0.05 level are reported.

	NMP movement n = 4		NMP control Leiden n = 3					
Measure	M	SD	M	SD	df	*t* statistic	*p* value	Sign. < 0.05
Glucose perfusate								
t = 0	3.875	0.6397	4.100	0.7000	5	0.44434	0.6760	no
t = 60	34.53	8.750	33.93	8.603	5	0.08913	0.9324	no
t = 120	34.55	8.700	28.67	13.70	5	0.7017	0.5142	no
t = 180	31.25	9.947	20.77	13.78	5	1.180	0.2911	no
t = 240	26.25	8.310	15.43	10.68	5	1.518	0.1894	no
t = 300	20.70	5.683	12.07	8.403	5	1.638	0.1623	no
t = 360	14.65[2]	3.041	9.733	9.361	3	0.6868	0.5415	no
Lactate perfusate								
t = 0	6.825	1.580	6.427	2.778	5	0.2436	0.8172	no
t = 60	5.933	3.210	3.027	2.022	5	1.361	0.2317	no
t = 120	6.388	3.427	4.243	3.411	5	0.8208	0.4491	no
t = 180	6.843	4.302	2.543	1.903	5	1.589	0.1730	no
t = 240	6.505	4.237	2.000	1.253	5	1.747	0.1410	no
t = 300	6.350	4.413	1.907	0.9752	5	1.675	0.1548	no
t = 360	3.350[2]	3.309	1.733	1.365	3	0.8006	0.4819	no
Bilirubin perfusate								
t = 0	10.65[3]	1.886	9.035[2]	0.4031	3	0.3385	0.3385	no
t = 60	8.550[3]	0	8.550[2]	0				*id*
t = 120	8.550[3]	0	8.550[2]	0				*id*
t = 180	10.43[3]	3.262	*no*					
t = 240	11.59[3]	4.778	10.43[2]	2.652	3	0.3054	0.7800	no
t = 300	10.23[3]	2.916	*no*					
t = 360	8.55[1]	0	10.68[2]	3.005				
ALT								
t = 0	51.58	19.70	34.93	2.804	5	1.418	0.2153	no
t = 60	157.5	29.83	105.3	15.67	5	2.720	0.0418	yes
t = 120	157.3	27.54	99.07	12.05	5	3.363	0.0200	yes
t = 180	174.0	50.39	86.8[1]	0				
t = 240	183.8	55.40	111.6	11.48	5	2.170	0.0821	no
t = 300	176.8	73.95	88.9[1]	0				
t = 360	219.5[2]	118.1	112.6	15.37	3	1.689	0.1899	no
AST								
t = 0	43.35	12.59	83.87	27.94	5	2.628	0.0466	yes
t = 60	5280	627.2	3320	1123	5	2.982	0.307	yes
t = 120	5175	980.5	3167	161.7	5	3.431	0.0186	yes
t = 180	6105	1008	3040[1]	0				
t = 240	5125	747.9	3347	250.1	5	3.877	0.0117	yes
t = 300	5835	623.8	3480[1]	0				
t = 360	6755[2]	1266	3480	423.3	3	4.438	0.0213	yes

Continued on next page

[1] only n = 1; [2] only n = 2; [3] only n = 3; *no* no data; *id* identical data

Table F2: – continued from previous page

	NMP movement n = 4		NMP control Leiden n = 3					
Measure	M	SD	M	SD	df	*t* statistic	*p* value	Sign. < 0.05
HA flow	176.6	52.17	202.3	43.17	24	1.369	0.1837	no
PV flow	597.7	119.6	1447	64.69	24	22.53	<0.0001	yes
Cumulative bile production								
t = 300	58.50	36.05	86.02	16.04	5	1.213	0.2795	no
t = 360	57.45[2]	15.27	105.7	18.41	3	3.031	0.0563	no
PDR_{ICG} 2h	24.09	14.47	21.92	13.81	5	0.1999	0.8494	no
PDR_{ICG} 5h	30.68[2]	11.74	21.92	13.81	3	0.7294	0.5186	no
% ICG cleared 2h	88.29	5.187	95.20	1.277	5	2.205	0.0785	no
% ICG cleared 5h	88.04[2]	4.676	95.20	1.277	3	2.707	0.0733	no

[1] only n = 1; [2] only n = 2; [3] only n = 3; *no* no data; *id* identical data

Table F3: Descriptive statistics and *t* test results comparing the mean PDR_{ICG} and % of ICG cleared from the perfusate after 60 minutes between the t = 120 min (n = 2) and t = 300 min (n = 2) administration of ICG during NMP under the established movement condition. Two-sided unpaired *t* tests were performed. Mean (M), standard deviation (SD), t(df)= *t* statistic, *p* value, and significance at a 0.05 level are reported.

	t = 120 min n = 2		t = 300 min n = 2					
Measure	M	SD	M	SD	df	*t* statistic	*p* value	Sign. < 0.05
PDR_{ICG}	13.56	0.7071	30.68	11.74	2	2.059	0.1757	no
% ICG cleared 2h	86.61	2.234	88.05	4.674	2	0.3917	0.7331	no